



THE AMERICAN UNIVERSITY IN CAIRO

Modified Force/Displacement-based Procedure for Performance-based Seismic Design of Regular RC Frames

A Thesis submitted in partial fulfillment of the requirements for the degree of

Doctor of Philosophy

in Engineering

by

Soha Hassan Elkassas, BSc, MSc

Under the supervision of

Dr. Ezzat Fahmy, Professor

Dr. Ezzeldin Yazeed, Professor

Dr. Mohamed AbdelMooty, Professor

Department of Construction Engineering

School of Sciences and Engineering

The American University in Cairo

May 2019

DEDICATION

To the Memory of Professor Medhat Haroun

Your foreknowledge and belief in me have made this journey possible

ACKNOWLEDGEMENTS

I am eager to take this opportunity to express my appreciation to all those who helped me during my research journey.

First, I would like to thank my advisor and mentor Dr. Ezzat Fahmy for his motivation and valuable advice through two decades, both at the academic and personal levels, and for all the structural engineering knowledge he gave to me during my undergraduate and postgraduate studies. This work would not have been possible without his constant guidance. I would also like to offer my gratitude and my sincerest appreciation to Dr. Ezzeldin Yazeed for being my advisor and for his great support and patience in helping create a joyful ending to a long journey. It was a privilege to work with him and benefit from his great expertise. Moreover, I would like to thank Dr. Mohamed Abdel-Mooty for being an advisor in a transient and difficult time, and for the valuable insights at the beginning of this research. Last but foremost, I would like to thank the late Dr. Medhat Haroun whose inspiration is the basis for my work. He has always believed in me and encouraged me to follow my dreams. I will always remember and cherish the reassurance and unparalleled support he has given me.

I would additionally like to express my gratitude to all those who have supported me through my academic journey at the American University in Cairo, especially everyone in the department of Construction Engineering. I would notably like to thank Engineer Jasmin Osama for her great help in bringing the design office experience to this research.

While it is a monumental task in itself to undertake a Doctor of Philosophy, it is an even greater task being a mother of three, and for that I want to thank my three children, Laila, Hassan and Alia for their paramount sacrifices and support. I would further like to thank my husband Amr for experiencing this long journey with me through all its ups and downs. It is his understanding and constant motivation that has helped me to conclude this work.

I am eternally grateful to my parents, not just for this work, but for shaping me into the person I am today. While offering utmost support and encouragement, it is their absolute and unequivocal love that is my backbone. I owe to them every success I have in my life. I would also like to thank my sisters Samar, Heba and Fatma for their perpetual love.

Thanks are due to the Youssef Jameel scholarship foundation for providing a fellowship grant for my graduate studies. I would also like to acknowledge the Mid-America earthquake Center and the National Science Foundation (Award Number EEC-9701785) for the use of their analysis platform ZEUS-NL in my study.

Finally, it is a privilege to be a timeless grain of sand in the infinite universe of the evolution of Science and Engineering. A grain of sand that can help future generations build monuments that make today's impossible, tomorrow's possible.

ABSTRACT

Performance-based seismic design has been the thrust of international research on earthquake engineering for the past 20 years. The major decisive factor for the success of its most recent framework is the development of efficient “preliminary design” methodologies that follow common design formats in order to maintain the process at an affordable level of complexity for practitioners. Using the traditional force-based seismic design method for this purpose, though simple and easy, will be inefficient because it designs structures to only one performance objective (which is life safety), and any other performance objective would be part of the drift check that follows the design, which will result in a highly iterative process. Therefore, in order to use the standard seismic design method in the context of the performance-based framework, there is a need for its adjustment to match the multi-level performance concept, by incorporating the performance measures at the beginning.

The potential of a hybrid force/displacement design format in this respect has been well recognized and developed over a decade for steel structures. The method is characterized by the establishment of a direct analytical link between the performance requirements and the reduction of elastic forces to the design force level, in a format that mixes the advantages of both force-based and displacement-based methods. Using the same analytical architecture, this thesis, titled “*Modified Force/Displacement-based Procedure for Performance-based Seismic Design of Regular RC Frames*,” proposes a “tool” for preliminary design of RC framed structures that can be suitable for the design office environment. The methodology uses displacement demand as input parameter, which more rationally represent actual earthquake response and eliminates the iterative steps required to satisfy the acceptable performance limits in the traditional code design procedure. The research serves to develop the displacement estimate relations for RC structures for use at the beginning of design, which lie at the heart of this design method.

For development of these displacement prediction relations, prototype structures with various geometrical characteristics are selected for study. A rigorous modelling approach and validated analytical tool are utilized to perform nonlinear time-history analysis as the closest approximation of actual earthquake loading. Incremental dynamic analysis is performed, employing a diverse range of synthetically developed ground motion records, in order to identify the ground motion intensity at which three preselected damage levels are reached, as defined by the inter-story drift ratio (the chosen damage metric). Time-history analysis is conducted at those determined loading levels and the displacement response values are analyzed. Adopting nonlinear regression, equations are developed for estimating the roof displacement as a factor of the performance target (in terms of the inter-story drift ratio) and some structural attributes such as the number of floors and bays. This estimate can be used together with the roof yield displacement to derive a performance-dependent force-reduction factor, and design can then proceed in the conventional way. A design case study helps to prove the efficiency and higher reliability of the proposed modification in achieving targeted performance and thus its suitability for application in performance-based design, provided elimination of its limitations and broadening its scope of application.

Keywords: Performance-based seismic design, Hybrid force/displacement design method, Reinforced Concrete structures, Moment-resisting frames, Maximum displacement estimates, Drift

TABLE OF CONTENTS

ACKNOWLEDGEMENTS	i
ABSTRACT	ii
LIST OF ABBREVIATIONS	v
LIST OF SYMBOLS	vi
LIST OF TABLES	vii
LIST OF FIGURES	viii

Chapter 1

INTRODUCTION

1.1	PREAMBLE	1
1.2	PROBLEM STATEMENT	4
1.3	RESEARCH OBJECTIVES	5
1.4	SCOPE AND WORK PLAN.....	6
1.5	ORGANIZATION OF THE THESIS	8

Chapter 2

PERFORMANCE-BASED SEISMIC DESIGN: STATE-OF-THE-ART REVIEW

2.1	INTRODUCTION	10
2.2	A PERSPECTIVE OF PERFORMANCE-BASED EARTHQUAKE ENGINEERING.....	10
2.2.1	Definition and Advantages	10
2.2.2	Applications of Performance-Based Seismic Design.....	12
2.2.3	Evolution of Performance-Based Design.....	13
2.2.3.1	History of performance criteria in major seismic source codes	13
2.2.3.2	Development of official guidelines for Performance-based seismic design	17
2.3	PROSPECT APPROACHES FOR PRELIMINARY BUILDING DESIGN	28
2.3.1	Codes and Guidelines Methods	29
2.3.1.1	Force-based design (FBD) approaches	29
2.3.1.2	Displacement-based design (DBD) approaches	31
2.3.2	Non-iterative Methods Developed by Other Researchers.....	36
2.3.2.1	Yield point spectra method	36
2.3.2.2	Performance-based Plastic Design	38
2.3.2.3	Hybrid force/displacement method.....	40
2.4	RELATIONSHIP BETWEEN PERFORMANCE AND DISPLACEMENT DEMAND	43
2.4.1	Relations Valid Only in the Elastic Range of Behavior.....	43
2.4.2	Relations Valid Up to the Inelastic Range of Behavior	46

Chapter 3

PROPOSED FORCE/DISPLACEMENT-BASED DESIGN

3.1	INTRODUCTION	49
3.2	MODIFICATION ENVISAGED	49
3.3	THEORETICAL BASIS.....	51
3.4	PROCEDURAL STEPS OF THE PROPOSED HFD METHOD.....	54
3.5	DEVELOPMENT METHODOLOGY	56

Chapter 4

NONLINEAR TIME HISTORY ANALYSIS

4.1	INTRODUCTION	58
4.2	DESCRIPTION OF PROTOTYPE BUILDINGS	58
4.2.1	General Description and Geometrical Configuration.....	58

4.2.2	Design Details and Assumptions	60
4.3	NONLINEAR TIME-HISTORY ANALYSIS	63
4.3.1	Theoretical Basis	63
4.3.2	Analysis Program.....	64
4.3.2.1	Pertinent features and advantages.....	64
4.3.2.2	Nonlinear modeling approach	65
4.3.2.3	The solver	67
4.3.2.4	Limitations.....	68
4.3.3	Modeling Assumptions	69
4.3.4	Description of Nonlinear Model Input	70
4.3.4.1	Material models.....	71
4.3.4.2	Cross-sections	75
4.3.4.3	Element formulations	76
4.3.4.4	Nodes and mesh configuration	79
4.3.5	Eigenvalue Analysis	81
4.3.6	Seismic Input and Selection of Ground Motion Records.....	84
4.4	INCREMENTAL DYNAMIC ANALYSIS	87
4.4.1	Intensity Measure and Scaling	87
4.4.2	Engineering Demand Parameter	88
4.4.3	Definition of Seismic Performance Levels	89
4.4.4	IDA Analysis Procedure and Results.....	90

Chapter 5

PERFORMANCE-BASED DISPLACEMENT ESTIMATE

5.1	INTRODUCTION	95
5.2	DISPLACEMENT PROFILES AT THE STUDIED PERFORMANCE LEVELS	95
5.3	ROOF DISPLACEMENT RESULTS.....	99
5.4	FACTORS AFFECTING ROOF DISPLACEMENT.....	102
5.4.1	Effect of the Number of Floors on Roof Displacement Response	103
5.4.2	Effect of the Number of Bays on Roof Displacement Response	105
5.4.3	Effect of Damage Level on Roof Displacement Response.....	107
5.5	PREDICTION OF DISPLACEMENT DEMAND	110
5.5.1	Definition of the Expected Relation	110
5.5.2	Regression Analysis.....	112
5.5.3	Proposed Prediction Equation.....	112
5.5.4	Incorporation of Displacement Prediction into the HFD Design	116

Chapter 6

DESIGN CASE STUDY

6.1	INTRODUCTION	118
6.2	DESCRIPTION OF BUILDING AND DESIGN ASSUMPTIONS.....	118
6.3	PERFORMANCE LEVELS CONSIDERED.....	119
6.4	COMPARISON BETWEEN CODE DESIGN AND MODIFIED DESIGN	121
6.4.1	Efficiency and Iterations	121
6.4.2	Performance of the Designed Frames	125

Chapter 7

CONCLUSIONS AND RECOMMENDATIONS

7.1	INTRODUCTION	132
7.2	SUMMARY	132
7.3	CONCLUSIONS AND CONTRIBUTIONS.....	133
7.4	LIMITATIONS AND RECOMMENDATIONS FOR FUTURE STUDY	136

REFERENCES	138
-------------------------	-----

LIST OF ABBREVIATIONS

AISC	The American Institute of Steel Construction
ATC	Applied Technology Council
CP	Collapse Prevention
DAF	Displacement Amplification Factor
DBD	Displacement-Based Design
DBE	Design Basis Earthquake
DDBD	Direct Displacement-Based Design
EDBD	Equal Displacement-Based Design
EDP	Engineering Demand Parameter
ESLM	Equivalent Static Load Method
FBD	Force-Based Design
FEMA	Federal Emergency Management Agency
FOE	Frequently Occurring Earthquake
HFD	Hybrid Force/Displacement-Based
IDA	Incremental Dynamic Analysis
IDR	Inter-story Drift Ratio
IM	Intensity Measure
IO	Immediate Occupancy
LS	Life Safety
MAE	Mid-America Earthquake (later: Multi-hazard Approach to Engineering)
MAPE	Mean Absolute Percentage Error
MCE	Maximum Considered Earthquake
MDOF	Multi-Degree-Of-Freedom
MRF	Moment-Resisting Frames
NEHRP	National Earthquake Hazards Reduction Program
NIST	National Institute of Standards and Technology
PBEE	Performance-Based Earthquake Engineering
PBSD	Performance-Based Seismic Design
PEER	Pacific Earthquake Engineering Research (Center)
PGA	Peak Ground Acceleration
RC	Reinforced Concrete
SDOF	Single -Degree-Of-Freedom
SEAOC	Seismology Committee of the Structural Engineers Association of California
SF	Scale Factor
SRD	Statistical Reference Datasets (Project)
THA	Time History Analysis
YFS	Yield Frequency Spectra

LIST OF SYMBOLS

a_g	Peak ground acceleration as a ratio to the acceleration due to gravity
D	Dead load
Δ_d	Design displacement
Δ_e	Elastic displacement
Δ_r	Maximum roof displacement demand
$\Delta_{r,max}$	Maximum roof displacement
$\Delta_{r,y}$	Global yield displacement
$\Delta_{r,in}$	Instantaneous roof displacement
Δ_u	Inelastic displacement
Δ_y	Yield displacement
E	Young's modulus
ϵ_{CO}	Strain at peak stress
f_t	Tensile strength
f'_l	Effective lateral confining stress
f_{yh}	Yield stress of the stirrups
f_{cc}	Confined concrete compressive strength
f_c	Unconfined concrete compressive strength
K	Confinement factor
k_e	Confinement effectiveness coefficient
L	Live load
μ	Strain hardening parameter
n_B	Number of bays
n_F	Number of floors
q	Behaviour factor in Eurocode
R	Force reduction factor/ Response reduction factor in US codes
R_{CP}	Force reduction factor to be applied to the MCE to satisfy the CP performance level
R_{CR}	Most critical force reduction factor to be applied to the DBE
R_{IO}	Force reduction to be applied to the FOE to satisfy the IO performance level
R_{LS}	Force reduction factor to be applied to the DBE to satisfy the LS performance level
ρ_x	Effective ratio of transverse reinforcement
S	Seismic load
S_a	Spectral Acceleration
σ_y	Yield strength
SDR_{in}	Instantaneous story drift ratio
SDR_{max}	Maximum story drift ratio
T_p	Earthquake predominant period
U	Ultimate load
V_d	Design base shear
V_e	Elastic base shear
V_y	Yield base shear

LIST OF TABLES

Table 1-1	Damage Control and Building Performance Levels (FEMA 356, 2000).....	22
Table 2-2	Structural Performance Levels and Damage, Concrete Frames (FEMA 356, 2000).....	22
Table 4-1	Prototype Buildings' description and notation.....	59
Table 4-2	Properties of materials employed in design and time-history analysis.....	61
Table 4-3	Member dimensions and reinforcement of the prototype frames.....	62
Table 4-4	Input parameters for concrete uniaxial constant confinement model.....	72
Table 4-5	Calculations of confinement factors of columns for model input.....	74
Table 4-6	Input parameters for uniaxial bilinear steel model with kinematic strain hardening	75
Table 4-7	Stiffness-proportional damping coefficients used in the prototype buildings...	79
Table 4-8	Modal Analysis Results.....	83
Table 4-9	Characteristics of selected artificial ground motion records.....	86
Table 5-1	Summary of conditional mean $E[\Delta_{r,max} IDR]$ and conditional dispersion $[\sigma_{\Delta_{r,max}} IDR]$ of displacement results for all frames.....	99
Table 5-2	Maximum roof displacement values ($\Delta_{r,max}$) for all structure-accelerogram pairs at the three study performance levels, and the floor at which the associated limiting value of Inter-storey drift ratio (IDR) first occurred.....	101
Table 5-3	Percentage change in displacement per one-floor increase for the different combinations of number of bays and interstorey drift ratio.....	103
Table 5-4	Percentage change in displacement per one-bay increase for the different combinations of number of floors and interstorey drift ratio.....	105
Table 5-5	Percentage change in displacement per unit increase of IDR for the different combinations of number of floors and bays.....	108
Table 6-1	Definition of the performance levels used in the design case study.....	120
Table 6-2	Baseline-frame's member dimensions and reinforcement for the strength design step.....	121
Table 6-3	Baseline-frame's member dimensions and reinforcement, final after all iterations.....	122
Table 6-4	Calculation of performance level-dependent force reduction factors(R).....	124
Table 6-5	Modified design-frame's member dimensions and reinforcement.....	124
Table 6-6	IDR response at the different hazards corresponding to the performance levels.	127
Table 6-7	THA results for the roof displacement at IDR=2%.....	127
Table 6-8	Probability of exceedance of the three performance levels given an earthquake intensity, for the BL-frame.....	129
Table 6-9	Probability of exceedance of the three performance levels given an earthquake intensity, for the MD-frame.....	129

LIST OF FIGURES

Figure 1-1	Performance-based seismic design approach, reproduced from FEMA-445 (2006).....	3
Figure 2-1	Building performance level for a basic function building (FEMA, 1997a)...	19
Figure 2-2	Performance objectives for buildings, recommended in SEAOC (1995)....	20
Figure 2-3	Global displacement capacities for various performance levels (Rai, 2000)	21
Figure 2-4	Probabilistic framework of the PEER methodology (after Moehle, 2003)...	26
Figure 2-5	Yield Point Spectra of the 1940 El-Centro record (after Aschheim, 2000)...	37
Figure 2-6	(a)Selected yield mechanism for desirable response in a typical moment frame (b)Energy equating concept for deriving design base shear of PBPD method (after Liao and Goel, 2014).....	40
Figure 3-1	Sequence of code force-based method and proposed modification.....	50
Figure 3-2	Design concept of the traditional force-based method.....	52
Figure 3-3	Typical performance levels of an RC structure with associated damage states (after Ghobarah, A., 2004).....	53
Figure 3-4	Flowchart for the methodology of development of displacement prediction equations for RC MRFs to be used in the context of the HFD design method.....	57
Figure 4-1	Elevations of the prototype frames.....	59
Figure 4-2	Fiber-element modeling of a reinforced concrete frame (after ATC, 2016)...	67
Figure 4-3	Equivalent point loads applied on beams.....	69
Figure 4-4	Uni-axial constant-confinement concrete material model.....	71
Figure 4-5	Unconfined and confined concrete monotonic stress-strain behavior (after Mander et al, 1989).....	72
Figure 4-6	Uniaxial elasto-plastic steel model with kinematic strain-hardening.....	75
Figure 4-7	Cross sections used in modeling beams and columns.....	76
Figure 4-8	Forces and displacements of the cubic formulation for the beam-column element.....	77
Figure 4-9	Locations of the two Gaussian sections.....	77
Figure 4-10	Meshing of the elements.....	80
Figure 4-11	Elastic model cross sections and materials for (a)beams ;(b) columns.....	82
Figure 4-12	5% damped spectra of the selected artificial ground motion (GM) records compared with the target spectrum.....	86
Figure 4-13	Incremental dynamic analysis results for the 4-storey frames relating the maximum IDR (damage level) with the scale factor (SF) of each earthquake record.....	92
Figure 4-14	Incremental dynamic analysis results for the 7-storey frames relating the maximum IDR (damage level) with the scale factor (SF) of each earthquake record.....	93
Figure 4-15	Incremental dynamic analysis results for the 10-storey frames relating the maximum IDR (damage level) with the scale factor (SF) of each earthquake record.....	94
Figure 5-1	Displacement profiles of the 4-storey prototype frames.....	96
Figure 5-2	Displacement profiles of the 7-storey prototype frames.....	97
Figure 5-3	Displacement profiles of the 10-storey prototype frames.....	98
Figure 5-4	Relationship between maximum roof displacement ($\Delta_{r,max}$) and number of floors for different number of bays at fixed values of IDR (based on the average of the results given the acceptance criteria of the three studied performance levels).....	102
Figure 5-5	Change of the roof displacement with the number of floors.....	103
Figure 5-6	Change of the roof displacement with the number of bays.....	105

Figure 6-1	A representative layout of the design example frame, together with the notation used for numbering the columns and beam reinforcement.....	119
Figure 6-2	Elastic Pseudo-acceleration design spectrum associated with the three study performance levels.....	120
Figure 6-3	Fragility curves for the BL-frame and the MD-frame showing conditional probability of exceeding the IO performance level target IDR of 1%.....	130
Figure 6-4	Fragility curves for the BL-frame and the MD-frame showing conditional probability of exceeding the LS performance level target IDR of 2%.....	130
Figure 6-5	Fragility curves for the BL-frame and the MD-frame showing conditional probability of exceeding the CP performance level target IDR of 3%.....	131

Chapter 1

INTRODUCTION

1.1 PREAMBLE

Through history, seismic design techniques have been in a continuing process of evolution – much more than design for any other load cases such as gravity, wind and snow. Because it is difficult to replicate the complex geological nature of an earthquake in an experiment, some missing links remain unsolved, while nature stays the principal laboratory. Observations of the performance of buildings during damaging earthquakes have always revealed deficiencies in design and construction practices and have triggered a need for change. Advances in the state of knowledge about earthquake occurrence and ground motion characteristics have also allowed replacing empirical rules with scientifically-based relations. Moreover, the development of computer-aided design tools and analytical techniques, for example finite element analysis and dynamic analysis, has effected a paradigm shift in the design practice.

Although earthquakes impose deformations on structures rather than forces, seismic design have always followed a force-based design (FBD) procedure, as an extension to traditional gravity and wind load design schemes. The first seismic design procedures in the early twentieth century called for designing structures to have sufficient resistance to withstand the inertia forces resulting from the base displacement and perceived as simple mass-proportional lateral forces, based on an elastic analysis. New extensive research and empirical evidence in the 1960's led to the awareness that due to the great uncertainty surrounding the estimation of seismic loading, it is not economical and may still be unreliable to design a structure to respond in the elastic range to a ground motion representative of the maximum intensity earthquake with low probability of occurrence. Therefore, relying on the structure's capacity to dissipate a substantial portion of the energy imparted to it through ductile behavior of its elements, seismic design started to deliberately allow inelastic response, while still performing an elastic analysis based on reduced design force levels. The reduction is achieved using a stipulated force reduction factor (R) (response modification factor R in US codes and behavior factor q in Eurocode), that were derived empirically as an estimate of assumed

system ductility. This approach, which in its simplest form is referred to as the equivalent static load method (ESLM), remains a mainstream in seismic design practice until present.

A major shift in seismic design philosophy occurred in response to the ensuing losses of the 1995 Kobe Earthquake and the 1994 Northridge earthquake which are considered among the costliest earthquakes in history. Code-compliant buildings at that time suffered significant levels of structural and nonstructural damage that were deemed far from acceptable by the public, despite satisfying the design objective of life-safety. For the first time a lesson was learnt that challenged the design objective in the first place rather than the design approach. There were increased demands from stakeholders for better accountability of new and existing designs which they needed to make reliable economic and life-safety decisions. This led to a new perception of life-cycle cost as an added key design variable, and thus research practice has moved towards predictive methods for assessing different levels of seismic performance. At this point, the requisite to switch to performance-based design – a design whose objectives are in terms of multiple performance levels – became imperative.

Along with the growing interest in development of performance-based codes to replace common prescriptive codes came the realization that seismic vulnerability of structures to various types of risks (for example loss of usage, repair and collapse) is directly related to their damage potential, which is better represented by displacement than force parameters. This brought emphasis on displacement as a governing design parameter and highlighted the limitations of the well-established FBD procedures in representing seismic demand and capacity in strength terms. Consequently, new design approaches, based on deformation parameters, were developed, that are generally termed displacement-based design (DBD) methods. In the DBD design process, the demand – as represented by the displacement of the structure in response to the design level earthquake – is compared to target displacement values based on the structure's displacement capacity. Since this is a more realistic approximation of the actual response of structures, DBD is considered a promising approach for performance-based seismic design provided proper implementation in the standards.

The current and future approach for performance-based seismic design (PBSD) was first liberally described in the FEMA-445 document published by the Federal Emergency Management Agency of the United States (FEMA, 2006). The document presents a comprehensive approach for performance-based design that converts probabilities of exceeding values of performance metrics, whether displacements or forces, to real-world losses such as casualties, time lost without operation, repair and replacement costs. The procedure is illustrated in Figure 1-1. It starts with description of the selected performance objectives that form input design criteria for performing a preliminary design, then the designed structure's performance is assessed and evaluated in terms of achieving the predefined objectives and the process is repeated iteratively, if required, till the desired design objectives are satisfied. The methodology for the third step which is the performance assessment has been already presented in the P-58 report (ATC, 2012), while progress in the second step of performing preliminary building design has been slow where it is expected to be developed as part of the second phase of the FEMA project.

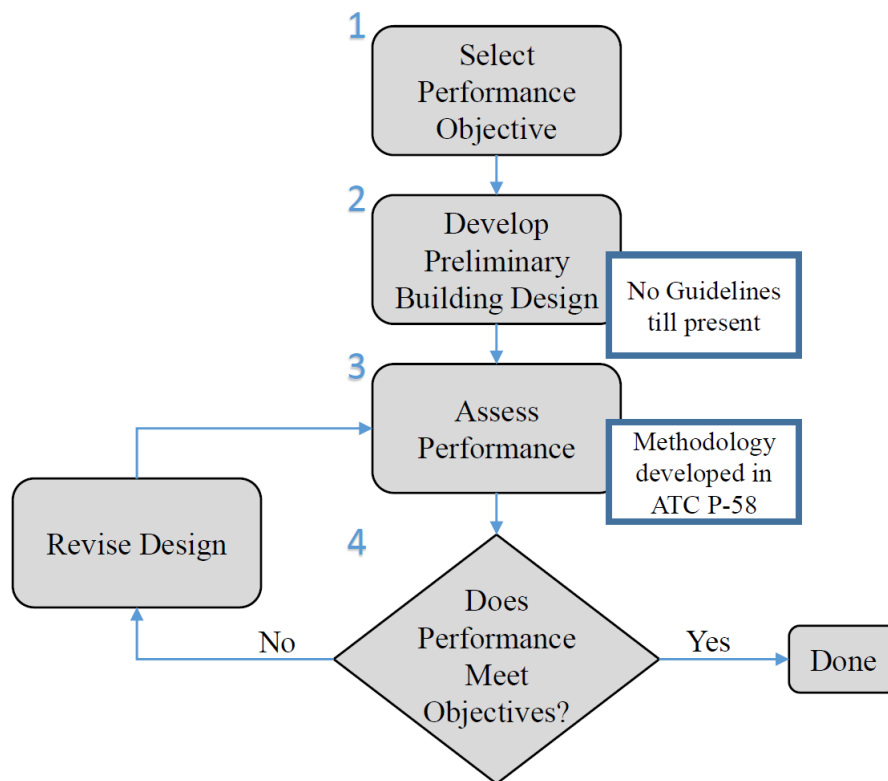


Figure 1-1 Performance-based seismic design approach, reproduced from FEMA-445 (2006)

1.2 PROBLEM STATEMENT

In the context of the latest approach for performance-based design as presented in the FEMA-445 report and summarized in Figure 1-1, the performance assessment methodology (step 3) is a relatively long process that involves advanced structural analysis techniques and complex probabilistic approaches, therefore an efficient preliminary building design (step 2) is of paramount importance to avoid the time consuming iterations of performance assessment. The FEMA-445 report itself acknowledges the challenge of developing efficient preliminary designs capable of meeting the desired objectives without extensive iterations and defines this challenge as the major decisive factor of the success of the whole framework of performance-based design, because otherwise the implementation process will be inefficient and uneconomical. The key requirement is that this design needs to address the system geometrical attributes as well as proportioning it in a manner consistent with the defined performance objectives (FEMA, 2006).

The current state of knowledge renders two options for preliminary design, either building code provisions for force-based design (FBD) or the aforementioned displacement-based design (DBD) methods developed specifically for performance-based application. In modern seismic codes, FBD incorporates displacement control as a final design check, rather than a design criterion – which can result in re-design in an iterative process to fulfill the target displacement limits. Also, FBD has several other drawbacks like relying on empirically-derived force reduction factors as well as displacement modification factors used to estimate inelastic displacement from its elastic counterpart (Elnashai and Mwafy, 2002). On the other side, limitations of present DBD techniques have been identified by several researchers (Sullivan et al., 2003). Firstly, a predesigned structure is needed to get a starting estimate for the displacement demand, which renders these DBD methods more applicable to performance evaluation of existing structures for rehabilitation, rather than new designs. Besides, these procedures have many approximations especially regarding adoption of an equivalent single-degree-of-freedom (SDOF) representation of the structure and not recognizing basic differences in response due to different lateral load resisting systems. More importantly, existing DBD process is relatively complex and

lack practicality and acceptance in the design community when compared to conventional methods, as evidenced by results of a recent survey of practicing engineers in North America about their current seismic design practice (Kramer, 2011).

Accordingly, FBD is likely to remain the principal method of seismic design for some time. Therefore, for performance-based seismic design to be a viable practice in the design office, there is a need to bridge the gap between conventional FBD seismic design methods (that have always been in accordance with common education of practitioners) and the FEMA performance-based design framework (that requires a preliminary design methodology directly based on, and capable of achieving the intended performance targets, so as to minimize subsequent performance assessment).

1.3 RESEARCH OBJECTIVES

The general aim of this research is to propose an efficient seismic design approach for reinforced concrete (RC) structures that can serve to meet the rising call for performance-based engineering design without sacrificing practicality of traditional practice. To fit into the context of performance-based seismic design, the procedure should treat damage and displacements as a target design condition, rather than an outcome of analysis, while in order to maintain simplicity, the well-known FBD method should be employed. In a sense, the objective is to develop a method that mixes the advantages of the force-based and displacement-based method, where the design starts with a displacement variable that is converted into a force parameter, so that design can proceed in the conventional way. The vision of the proposed design process is that the designer can perform a design of optimum performance control, based on elastic analysis and using traditional code formats for earthquake representation, with minimum amount of iterations after the initial design. On the long run, the application of the recommended design scheme can be validated for a wider range of structural systems and materials, for implementation in design codes and textbooks.

The basis of the designated methodology has been first proposed for steel moment resisting frame structures by Bazeos and Beskos (2003), later developed in detail (Karavasilis et al, 2006-2010; Stamatopoulos and Bazeos, 2011; Skalomenos et al., 2015; Tzimas et al., 2013, 2017), and is still under refinement till present. This

group of researchers have termed it the hybrid force/displacement (HFD) based method. The present work is an additional effort along the same frontier of employing a HFD design method for preliminary performance-based seismic design but through application on RC framed structures, which does not only represent a gap in the literature but also requires extensive study due to the complex hysteretic behavior of RC as a composite nonlinear material.

Within this framework, the key objectives of this thesis are

1. Study and present the application of the HFD design method to reinforced concrete framed structures with limited ductility, as a modification to the traditional force-based seismic design method to satisfy various performance objectives.
2. Develop prediction equations and design charts for estimating the maximum roof displacement of the building corresponding to various target performance levels, based on extensive nonlinear incremental dynamic time-history analyses. The developed relationships can be used to map the HFD design procedure to RC structures, where they are used for calculation of the force reduction factor at the initiation of design, and thus should be independent of the section properties.
3. Validate the enhancement achieved by the modified design in realizing performance objectives based on a case study, where results from the developed HFD design are compared to those from conventional force-based design method.

1.4 SCOPE AND WORK PLAN

The use of the proposed modified FBD method or HFD design method can be especially promoted in low-to-moderate seismic zones where the frequency and intensity of seismic events do not merit more complicated and costly seismic design procedures. Due to its low cost, RC construction is prevalent in many developing countries that meet this seismicity criteria for example Turkey, Pakistan, Colombia, Algeria and Egypt. Moment-resisting frame buildings with limited ductility are chosen as the scope of study which are prominent lateral load-resisting systems in these areas, where all RC frames are inherently moment-resisting because building codes requires continuity of the reinforcing bars that compose the main structural framing system.

The research is applied in Egypt, employing seismic zones, material properties and design factors of the Egyptian seismic design code. ECP- 201 “The Egyptian Code for calculation of Loads and forces on Structural and masonry works” (ECP-201, 2012) which is largely in line with the Eurocode 8 (EN1998-1, 2004) – a widely used and well-established source code for the European Union. Therefore, results of this study can be extended for application in other countries, and furthermore the approach can be adapted to other codes around the world.

Low to moderate height frames with number of stories 4, 7 and 10 and number of bays 3, 5 and 7 are chosen for study, representing a variety of buildings commonly constructed in Egypt, where for example, RC frame buildings represent 55% of the new trend of low-density construction of gated communities in Greater Cairo (Dorra, 2011). The buildings are assumed to be for office use and to be located on soft soils. Still, the outcomes and findings of the study may be useful for seismic design of mid-rise building stock, not just in Egypt but also in other earthquake prone regions with similar seismic activity and construction practice.

In order to formulate the HFD design method for RC frame structures, the relationship between the maximum roof displacement, building geometrical attributes and damage metrics at various performance levels is developed in order to be able to estimate a realistic R values, based on performance objectives, to be later used following the common guidelines of FBD. For this end, nonlinear time-history analysis is employed, as the closest representative of real structural behavior under seismic action, to study and establish the objective relation, under the suite of seven artificial ground motion records, generated and selected to match the design spectrum. Inter-story drift ratio (IDR) is chosen as the Engineering Demand Parameter (EDP) that indicates the level of structural performance. Nonlinear models of the study frames having different geometrical properties are run with progressively increasing scale of accelerograms, scaled based on the Peak Ground Acceleration (PGA) as an intensity measure, and the values of IDR versus accelerogram scale factors are recorded. Scale factors corresponding to three specifically defined performance levels: Immediate Occupancy (IDR = 1%), Life Safety (IDR = 2%), and Collapse Prevention (IDR = 3%) are identified for studying the drift response at those specific performance levels. Employing nonlinear multi-variable regression analysis of the response values, a

relationship is developed between the maximum roof displacement and the maximum IDR along the height of the building for the different prototype structures, and consequently prediction charts are created that can be integrated into the HFD design method. Finally, a case study is presented to validate the reliability of the proposed modification in achieving the targeted performance.

1.5 ORGANIZATION OF THE THESIS

The research comprises five chapters, as follows:

Chapter (1) briefly introduces the evolving nature of seismic design with performance-based design as the ultimate target. The limitations of the available methods for performance-based design are briefly outlined that signifies the need for the current research, leading to the study objectives with definition of its scope and work plan.

Chapter (2) covers a detailed appraisal of the philosophy of performance-based earthquake engineering, as well as the history and evolution of performance-based seismic design procedures. Also, it explains the different methods for performance-based design while conducting a detailed categorized review of the available literature on similar studies.

Chapter (3) presents the proposed hybrid force/displacement design method for performance-based design of RC moment-resisting frames. The targeted modification of the force-based method is described along with the expected advantages and procedural steps. The methodology for extension of the HFD design method to RC frames with its associated required analytical study is defined.

Chapter (4) discusses in detail the numerical analysis and the nonlinear modeling technique. It explains the prototype models employed, the case study scenarios chosen, the stages of analysis with the corresponding assumptions, the modeling methods of members and earthquakes, the software used, the assessment criteria for the damage potential, and the parameters identified for developing the numerical relationships.

Chapter (5) presents the results of the numerical study and their regression analysis for developing the displacement prediction equations and charts that can be incorporated in the modified HFD design method.

Chapter (6) sets forth a design case study for validation of the reliability of the proposed method as compared to traditional force-based method in achieving performance objectives.

Chapter (7) enumerates the main conclusions from this study identifying any limitations and proposing recommendations for future work.

Chapter 2

PERFORMANCE-BASED SEISMIC DESIGN: STATE-OF-THE-ART REVIEW

2.1 INTRODUCTION

Extensive research effort has been conducted in the past to develop performance-based seismic design procedures. This chapter reviews the background information related to the philosophy of performance-based earthquake engineering, particularly concerning the evolution of standardized procedures for performance-based seismic design. It provides insight into the sequential generations of performance-based frameworks with emphasis on the future “next-generation” procedures and the principal requirements for their success. The suitability of modern seismic code methods and various other simple approaches suggested in the literature for application in the stage of preliminary building design of the next-generation performance-based framework is covered briefly. The objective is not to give a comprehensive review of the approaches, but rather to summarize their concept. A detailed literature review is provided for the hybrid force/displacement method and the available relations for estimating displacement demands of RC frames as associated with variable performance, which provides the basis of the methodology applied in the subsequent chapters of this thesis.

2.2 A PERSPECTIVE OF PERFORMANCE-BASED EARTHQUAKE ENGINEERING

2.2.1 Definition and Advantages

Performance based earthquake engineering (PBEE) can be defined as design, construction and maintenance of engineered structures, whose performance under various anticipated earthquake loading levels, meet the diverse expectations and objectives of their owners, users and society, with a quantifiable degree of confidence. It promises to produce structures with performance predictable enough to allow the different stakeholders to make informed decisions based on life-cycle considerations (in terms of casualties, cost of repair or replacement, disruption of use, etc.), rather than

initial costs alone (Krawinkler and Miranda, 2004). In a Performance-based approach, all decisions are directed towards the required performance-in-use. The term performance refers to the system ability to fulfil its intended purpose and stakeholders' targets pertaining to its functionality, safety, or costs.

Implementation of PBEE necessitates radical changes in seismic design codes to incorporate more scientifically oriented methodologies, based on realistic prediction of structural behavior, rather than prescriptive rules. This is what is termed Performance-based Seismic Design (PBSD). In PBSD the focus of all design steps is on demand requirements with required performance placed at the forefront, unlike traditional practice that highly depends on heuristic and experience-based conventions. The literature has different interpretations of the meaning of PBSD (ATC 1996, 1997; SEAOC, 1995). The most applicable definition is that PBSD is a design philosophy in which the design criteria are reliably defined in terms of performance targets at various levels of seismic hazard.

Comparing PBSD to conventional design codes, the main differences and advantages lies in the vocabulary, the reliability of the intended performance, and the range of design events, as follows:

- While PBSD terminology focuses on the ends which is the performance of the designed building taking into account the consequence of its failure to meet its objectives, design codes focus on the design process and the minimum acceptable consensus standards that have been developed over time as a convenient means to achieve safe economical designs (Fardis, 2010). Ideally, PBSD would have the desired performance characteristics stated in terms of rational and measurable quantitative indicators, thus providing a meaningful basis understandable by both the designer and the client, which can improve interaction for reaching an optimum design option.
- Although the prescriptive criteria in design codes include a performance objective which is life-safety at the design event, other performance levels at other levels of ground shaking cannot be reliably ensured. Deficiencies in the prescriptive provisions in terms of accomplishing other performance objectives have been identified following past earthquakes even those not exceeding the design level

earthquake. Despite realization of the life-safety objective, some structures sustained much more extensive structural and nonstructural damage than anticipated by the design. On the other side, PBSB ensures higher reliability in attaining performance objectives by having a performance assessment step embedded in the design process at presumably all levels of expected hazards. The design is adjusted in an iterative process until the assessment results renders a risk of loss, in terms of safety and cost, that is considered acceptable by the various stakeholders and decision makers based on the specific needs of a project.

In that sense, PBSB offers society the promise of higher quality of building designs that is more efficient and effective in avoiding future earthquake losses. PBSB is considered the paramount goal available for seismic design evolution, however its implementation still faces many challenges. The high level of uncertainty inherent in the seismic loading and structural capacity makes it impossible to reach perfect confidence in the reliability of the design performance. Extensive research is required to arrive at appropriate analysis procedures for accurate performance assessment that encompasses all possible risk factors. Furthermore, robust implementation of the performance-based methodology requires coordination efforts between professionals from all disciplines involved in the life cycle of the building.

2.2.2 Applications of Performance-Based Seismic Design

Performance-based seismic design can be used for the following purposes:

- To design buildings with a higher level of confidence in achieving the performance intended by present building codes, so it serves like a sort of guarantee.
- To design buildings with standard performance equivalent to that intended by the building codes, but with lower construction costs, thus attracting sharp developers.
- To design buildings to achieve higher performance (with more reliability) than that provided by present building codes, which is an essential requirement for critical facilities.
- To develop innovative designs employing the latest development in technology and structural materials that do not fall in the scope of code prescriptions, therefore encouraging design creativity.

- To select design options based on anticipated performance by identifying better performing design alternatives.
- To assess the seismic performance of existing structures and estimate potential losses in case of a seismic event, thus supporting decisions of upgrading and repair.
- To conduct research on the performance of new designs resulting from current prescriptive code requirements and identifying areas of improvements for better reliability of the code criteria.

2.2.3 Evolution of Performance-based Design

Although performance-based concepts have been applied in many areas of engineering like the automotive and nuclear industry, its application to seismic design of structures is still more complicated, due to the high variability of the built product in general, and due to the increased uncertainty in earthquake engineering in particular. Therefore, to-date PBSB has not been a practical substitute to conventional prescriptive design codes. With advances in seismic hazard assessment, loss analysis methodologies, experimental facilities, and computer applications, it is expected that PBEE can become the standard method for design and delivery of earthquake resistant structures.

2.2.3.1 History of performance criteria in major seismic source codes

In a broad sense, all past seismic codes can be considered partially performance oriented, in that they attempt to relate the design criteria to a required performance goal usually that of collapse prevention. However, the design criteria themselves are prescriptive measures based on empirical rules, and there is lack of quantification of the limits of engineering parameters as related to the stated performance objectives. The following section summarizes how major source documents, that form the basis for seismic codes, first approached performance requirements.

i. SEAOC Blue Book editions

The first document to prescribe design guidelines was the Blue Book issued by the Seismology Committee of the Structural Engineers Association of California

(SEAOC) in 1959, alternatively named SEAOC Recommended Lateral Force Requirements and Commentary (SEAOC, 1959). It was later the source of seismic provisions in the US Uniform building code (UBC) until 1997 (Krawinkler and Miranda, 2004). Its first edition stated some generic performance goals; yet without any corresponding quantitative criteria, wherein the design objective is to produce structures that should be able to resist

- A minor level of earthquake ground motion without damage
- A moderate level of ground motion without structural damage but possibly experience some nonstructural damage
- A major level of ground motion having an intensity equal to the strongest, either experienced or forecast for the building site, without collapse, but possibly with some structural as well as nonstructural damage.

The Blue book prescribed empirical approaches for calculation of the seismic load for example the well-known base shear equation (SEAOC, 1980) that included various coefficients empirically quantified to be used at the allowable stress design level with an elastic drift criterion. The ground motions related to the design earthquakes were estimated deterministically, initially by heuristic specification of ground acceleration, and subsequently using median values from early attenuation relationships (Kramer, 2014). This method ignored the uncertainty inherent in ground motion estimation, and therefore produced designs with variable margins of safety against collapse (Osteraas and Krawinkler, 1990). The design was also force-based and disregarded inelastic behavior that reflects the actual performance of the structures.

ii. ATC-3-06

The Tentative Provisions for the Development of Seismic Regulations for Buildings, published by the Applied Technology Council (ATC) has contributed to the most drastic improvement in seismic design practice (ATC-3-06, 1978). The major outcome was the probabilistic description of the seismic input using principles of seismic hazard analysis and response spectra. In terms of seismic action design levels, ATC-3-06 recommended that design be based on a single level of ground shaking 10/50 (a 10 percent probability of exceedance in a 50-years period, 475 years return period). Design remained force-based but using component strength approach rather than

allowable stress design, and introduced the concept of the response modification factor yet still empirically defined and with the problem of being period independent. The provisions also included a deflection amplification factor that allowed estimation of drifts to be compared to allowable story drifts, as a basis for performance measure. The allowable drifts were empirically presented for three seismic hazard exposure groups differentiated by the building importance to post-earthquake recovery and by the number of occupants. The seismic hazard exposure groups were in turn related to four seismic performance categories, depending on a seismicity index. Thus, although highly generic in nature, ATC-03-06 laid the foundation for performance-based earthquake engineering by introducing the use of deformation-based response as metrics of performance, and the idea of adjusting the design to affect the likely performance of critical structures through boosting its required strength. Nevertheless, the importance factors used to adjust the required strength were still arbitrary, and there was no mention of direct procedures for predicting the performance of a particular building design.

iii. NEHRP 2000

The National Earthquake Hazards Reduction Program (NEHRP) was created and funded by the Federal Emergency Management Agency (FEMA) to develop seismic provisions that serve as a resource for all US standards and design professionals. A major update came in the NEHRP 1997 and NEHRP 2000 Recommended Provisions (FEMA 368, 2001), which presented a new hazard level 2/50 (2475 years return period) representative of the maximum considered earthquake (MCE) with elaborate hazard mapping for the US. The design earthquake can be derived from MCE by dividing by 1.5, thus ensuring uniform design requirement and risk of collapse using the same measure of ground motion. Also, in this update there were changes in the terms “seismic hazard exposure group” and “seismic performance category” of ATC-3-06 to be “seismic use group” and “seismic design category”, yet still signifying the same thing. The adoption of the MCE maps is one of the tools required for advancement of PBEE as it improves the reliability of the predicted performance of buildings being designed under a uniform hazard. Most current US codes, for example ASCE 7, use the seismic loading criteria recommended by NEHRP.

iv. **Eurocode**

The Eurocode 8 (EN1998-1, 2004) was issued as a result of much research and collaboration between countries in the European Union. The design philosophy is similar to US code documents; however, there are still some distinctions. Eurocode-8 explicitly specifies two-level seismic design with the two following performance requirements:

- No-collapse requirement

The structure shall be designed and constructed to withstand the design seismic action without local or global collapse, thus retaining its structural integrity and a residual load bearing capacity after the seismic event.

- Damage limitation requirement

The structure shall be designed and constructed to withstand a seismic action having a larger probability of occurrence than the design seismic action, without the occurrence of damage and the associated limitations of use, the costs of which would be disproportionately high in comparison with the costs of the structure itself.

In accordance with the Eurocode framework of limit states, the stipulated “no-collapse” and “damage limitation” performance requirements are associated with the “ultimate” limit state and the “serviceability” limit state, respectively, to be in their turn checked against two different hazard levels related to the seismicity of the region, and recommended as a 10/50 hazard (475 years return period) for collapse prevention and a 10/10 hazard (95 years return period) for damage limitation. The design is performed at only one level which is the 10/50 hazard, while a modification factor “ ν ” is applied to the deformation results as an approximation to arriving at the 10/10 hazard for checking the compliance criteria at the serviceability limit state. Both these levels of the seismic action are defined for ordinary structures (as a reference seismic action) and should be modified by an “importance factor” to differentiate the target reliabilities of the performance requirements for different classes of buildings, depending on their importance for public safety and the social and economic consequences of collapse. “Importance classes” term is used in lieu of “seismic use group” of US codes of practice. The hazard level 2/50 (2475 years return period) representative of the MCE, is not included.

In the strength design process, the Eurocode uses the “behavior factor q ” with prescribed ductility detailing to reflect inelastic behavior, which is similar to the “ R -factor” employed in US codes of practice; however, it incorporates the overstrength into the q factor by explicitly including the ratio of the strength of the structure at mechanism to that at first plastic hinge formation. Otherwise, both Eurocode and US codes have similar design provisions, which have an essence of performance-based design in its objectives and deformation checks. It should be noted that the Egyptian seismic code of practice (ECP-201, 2012), used in the current study is largely based on the Eurocode and follows the same limit states.

2.2.3.2 Development of official guidelines for Performance-based seismic design

Large economic losses from the 1994 M6.7 Northridge earthquake in Los Angeles and the 1995 M7.2 Hanshin-Awaji (Kobe) earthquake in Japan, amounting to 40 and 80 billion dollars, respectively were the main triggers for development of a formal process for PBSD (Hamburger and Moehle, 2010). Although these earthquakes did not cause collapse of many structures designed to modern codes, thus demonstrating the success of building code procedures in achieving their primary objective of life safety, they also evidently demonstrated the shortcomings of code provisions in permitting much higher than anticipated damage and economic losses due to loss of use and cost of repair. Therefore, these earthquakes prompted the alert of owners and tenants, especially of buildings having critical functions, to the importance of upgrading their existing buildings to achieve better performance during earthquakes. Governments were also concerned with performance assessment of their building inventory for proper mitigation of earthquake risks. However, engineers could not practically apply code-based strength and ductility requirements to the evaluation and upgrade of existing buildings, thus performance-based seismic design procedures were developed as an answer to this need.

Ideally PBSD should have considered all possible future earthquake events with their annual probability of occurrence and their corresponding consequences during the structure life-cycle, however, this could have been too complex for practical applications. Therefore, PBSD started by replacing the traditional single-tier design against collapse, with a multi-tier seismic design, meeting several performance

objectives at their corresponding design event in a deterministic approach (first- and second -generation procedures). Later, the next-generation of procedures integrated all possible design events with their corresponding weighted average based on their likelihood of occurrence (probabilistic approach) in order to arrive at a single estimation of the performance in terms of total loss as an integral of all possible risks.

i. First-Generation Procedures

Three documents are credited for laying the foundation for robust performance-based seismic design procedures, namely

1. Vision 2000 Report, *Performance-Based Seismic Engineering of Buildings* (SEAOC, 1995), which describes a performance-based seismic design framework for design of new buildings.
2. The Applied Technology Council report, ATC-40, *Seismic Evaluation and Retrofit of Concrete Buildings* (ATC, 1996), and
3. FEMA 273 Report, *NEHRP Guidelines for the Seismic Rehabilitation of Buildings* (1997a), and its companion document FEMA 274 *NEHRP Commentary on the Guidelines for the Seismic Rehabilitation of Buildings* (1997b), which addressed seismic upgrade of existing buildings. Although they were not intended for use in design of new buildings, they can be adapted for checking performance of code designed buildings as a final check design step.

These documents marked a major milestone in the evolution of PBSB by introducing several key concepts essential for performance-based engineering practice. Some of these concepts are

1. The concept of *performance levels* to represent performance with names intended to connote the expected/permisible level of post-earthquake damage condition, for example: Collapse Prevention, Life Safety, Immediate Occupancy and Operational Performance. These levels relate to qualitative measures of the damage of structural and nonstructural components, as well as measures of casualties and expected property and operational losses. While Vision 2000 included discretely-defined building performance levels, the FEMA-273 document defines separate structural and nonstructural performance levels as well as a *Performance Range* to encompass a band of performance between two levels. The three Structural

Performance Levels and two Structural Performance Ranges consist of: S-1: Immediate Occupancy Performance Level, S-2: Damage Control Performance Range (extends between S1 and S3), S-3: Life Safety Performance Level, S-4: Limited Safety Performance Range (extends between S3 and S5), S-5: Collapse Prevention Performance Level and S-6: structural performance not considered. The four Nonstructural Performance Levels are: N-A: Operational Performance Level, N-B: Immediate Occupancy Performance Level, N-C: Life Safety Performance Level, N-D: Hazards Reduced Performance Level and N-E: nonstructural performance not considered. The structural and nonstructural performance levels are coupled to form the building performance level as presented for a basic function building in Figure 2-1.

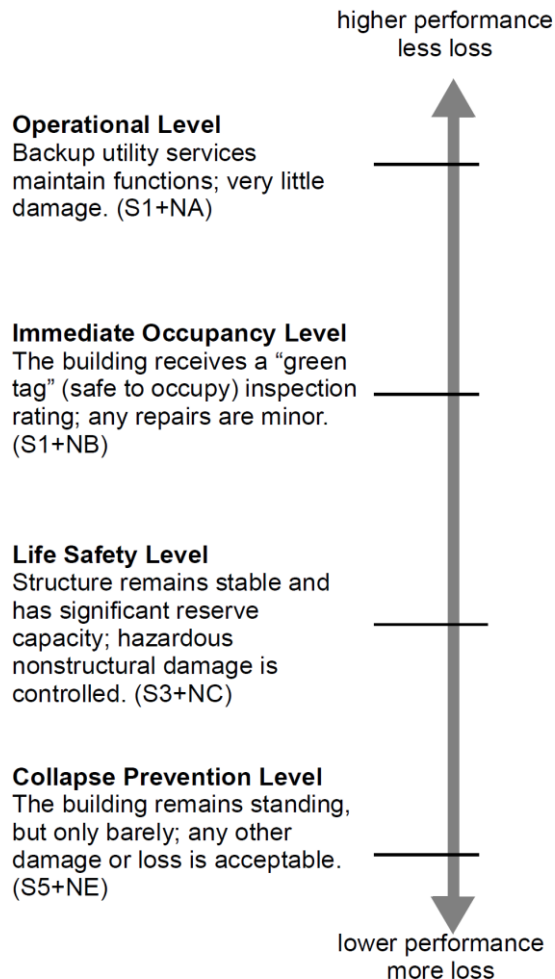


Figure 2-1 Building performance level for a basic function building (FEMA, 1997a)

2. More probabilistic earthquake hazard levels are introduced: the frequent 50%-in-50-years earthquake event (73 years mean return period), the occasional 30%-in-

50-years earthquake event (225 years mean return period), the rare 10%-in-50-years earthquake event (474 years mean return period), and the very rare 2%-in-50-years earthquake event (2,475 years mean return period).

3. A *Performance objective* is defined as a combination of one performance level and one defined earthquake hazard level (design event) for a particular category of building importance. Figure 2-2 illustrates the performance objectives defined by Vision 2000. The building importance is expressed as “basic”, “essential” such as hospitals and fire stations, “hazardous” containing confined hazardous materials, and “safety critical” such as nuclear stations and buildings containing explosives. According to Vision 2000 description, a basic function building would be expected to suffer more damage if it were subjected to a more severe, less likely earthquake, and a safety critical building would be expected to have less damage for the same earthquake design level. ATC-40 and FEMA 273 define performance levels a little differently but using the same concepts (Krawinkler and Miranda, 2004).

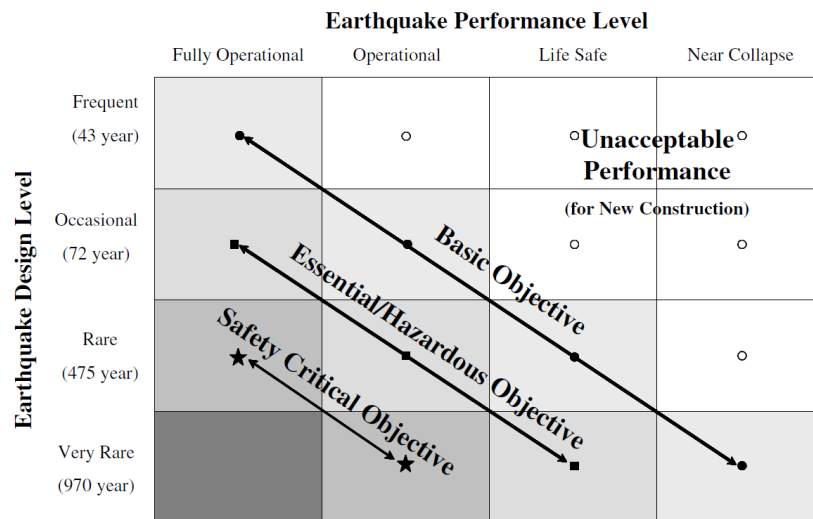


Figure 2-2 Performance objectives for buildings, recommended in SEAOC (1995).

4. Expression of damage state in terms of engineering limit states (for example drift values) corresponding to the various performance level for a particular component, for the sake of definition of quantitative performance *acceptance criteria*. The previously defined qualitative performance levels with their corresponding levels of damage of FEMA 273/274 are shown in Figure 2-3 superimposed on a global force-displacement relationship for a sample building to clarify the various displacement limit states.

5. The use of nonlinear analysis methods as a design tool rather than just research is introduced.

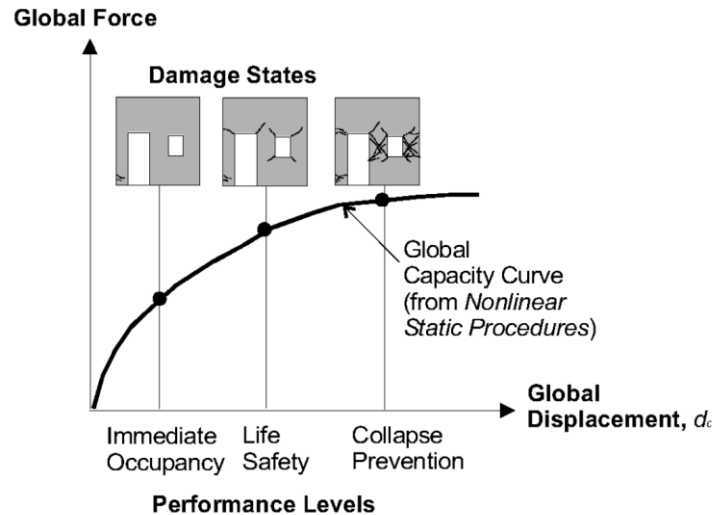


Figure 2-3 Global displacement capacities for various performance levels (Rai, D., 2000)

ii. Second-Generation Procedures (present procedures)

1. FEMA 356 and ASCE 41-06

Based on the information gained from applying the first-generation procedures in engineering practice, the FEMA produced an updated series, FEMA 356: *Prestandard and Commentary for the Seismic Rehabilitation of Buildings* (FEMA, 2000), with just an incremental improvement to include a mandatory language as a basis for future standards that can be incorporated into mainstream design. The performance levels and descriptions of corresponding physical damage are shown in Table Error! No text of specified style in document.-1. The standard includes many tables for specific structural components (e.g., for concrete frames, braced steel frames, metal deck diaphragms, etc.) and nonstructural components (e.g., for glazing, piping, cladding, etc.) with some engineering limit states (e.g., drift values) that correspond to the various performance levels for a particular component. Table 2-2 is one sample for concrete frames. The FEMA-356 document was later revised and standardized as the ACSE 41-06 *Standard for Seismic Rehabilitation of Existing Buildings* (ASCE/SEI, 2006) for adoption in building codes.

Table Error! No text of specified style in document.-1 Damage Control and Building Performance Levels (FEMA 356, 2000)

	Target Building Performance Levels			
	Collapse Prevention Level (5-E)	Life Safety Level (3-C)	Immediate Occupancy Level (1-B)	Operational Level (1-A)
Overall Damage	Severe	Moderate	Light	Very Light
General	Little residual stiffness and strength, but load-bearing columns and walls function. Large permanent drifts. Some exits blocked. Infills and unbraced parapets failed or at incipient failure. Building is near collapse.	Some residual strength and stiffness left in all stories. Gravity-load-bearing elements function. No out-of-plane failure of walls or tipping of parapets. Some permanent drift. Damage to partitions. Building may be beyond economical repair.	No permanent drift. Structure substantially retains original strength and stiffness. Minor cracking of facades, partitions, and ceilings as well as structural elements. Elevators can be restarted. Fire protection operable.	No permanent drift. Structure substantially retains original strength and stiffness. Minor cracking of facades, partitions, and ceilings as well as structural elements. All systems important to normal operation are functional.
Nonstructural components	Extensive damage.	Falling hazards mitigated but many architectural, mechanical, and electrical systems are damaged.	Equipment and contents are generally secure, but may not operate due to mechanical failure or lack of utilities.	Negligible damage occurs. Power and other utilities are available, possibly from standby sources.
Comparison with performance intended for buildings designed under the <i>NEHRP Provisions</i> , for the Design Earthquake	Significantly more damage and greater risk.	Somewhat more damage and slightly higher risk.	Less damage and lower risk.	Much less damage and lower risk.

Table Error! No text of specified style in document.-2 Structural Performance Levels and Damage, Concrete Frames. (FEMA 356, 2000)

Elements	Type	Structural Performance Levels		
		Collapse Prevention S-5	Life Safety S-3	Immediate Occupancy S-1
Concrete Frames	Primary	Extensive cracking and hinge formation in ductile elements. Limited cracking and/or splice failure in some nonductile columns. Severe damage in short columns.	Extensive damage to beams. Spalling of cover and shear cracking (<1/8" width) for ductile columns. Minor spalling in nonductile columns. Joint cracks <1/8" wide.	Minor hairline cracking. Limited yielding possible at a few locations. No crushing (strains below 0.003).
	Secondary	Extensive spalling in columns (limited shortening) and beams. Severe joint damage. Some reinforcing buckled.	Extensive cracking and hinge formation in ductile elements. Limited cracking and/or splice failure in some nonductile columns. Severe damage in short columns.	Minor spalling in a few places in ductile columns and beams. Flexural cracking in beams and columns. Shear cracking in joints <1/16" width.
	Drift	4% transient or permanent	2% transient; 1% permanent	1% transient; negligible permanent

2. FEMA 350 and the SAC joint venture guidelines.

Recognizing the main limitation of the FEMA-356 procedure in the absence of reliability measures of achieving the performance objectives and the disregard of uncertainty and randomness in demand and capacity, a partnership was enacted between FEMA, SEAOC, ATC and California Universities for Research in Earthquake Engineering (CUREe), referred to as SAC joint venture, to develop guidelines for

seismic design of steel structures employing performance-based procedures. The resulting report, FEMA 350, Recommended Seismic Design Criteria for New Steel Moment-Frame Buildings (SAC, 2000) was issued almost concurrently with FEMA 356 and had a basic Limit State Design Format applicable only to steel moment frames. Up till present, this is the only FEMA guidelines that specifies a performance-based procedure explicitly for new design. Its framework is based on the definition of a performance objective as an acceptable probability of exceeding a specified performance level with quantitative confidence statements. The performance levels in their turn are quantified based on expressions relating generic structural variables “demand” and “capacity” with their associated randomness and uncertainty characteristics as derived from separate probabilistic analysis. A safety-check following the conventional “load and resistance factor Design LRFD” format is developed with “load” and “resistance” terms being replaced by the terms “demand” and “capacity,” respectively. Based on these assessments, the engineer is provided with a tool to assess the confidence with respect to the likelihood of unacceptable behavior (Cornell et al, 2002). The validity of this procedure is limited to steel design concepts.

3. ASCE 7-10 revisions to chapter 1

The 2010 edition of the ACSE 7 standard for Minimum Design Loads for Buildings and Other Structures (SEI, 2010) marked a major step in its evolution as a comprehensive design standard, by inclusion of performance-based design procedures as one of three approaches for design, the other two being the allowable stress and strength design methods. Under the performance-based approach, both structural and nonstructural components and their connections must be designed and proven to meet a target reliability equivalent to that expected when designed using the strength procedures. ACSE 7-10 also presents the acceptable procedures used to demonstrate compliance, which can be testing, analysis or a combination of these. The Uniform-hazard ground motion is replaced by risk-targeted ground motion by switching from a 2% in 50-year hazard level to a 1% in 50-year collapse risk target. The risk-targeted maximum considered earthquake (MCE) ground motion is designated MCE_R ground motion (Hamburger, 2011). The performance-based design process, however, is still inherently an evaluation stage added at the end of the already developed design. And

despite its pioneering efforts in quantification of performance, the criteria of ASCE 7-10 still remain insufficient, since it addresses only those risks associated with structural failure and collapse, without reference to maintaining operability and function, and minimization of repair and replacement costs, which are key considerations in the seismic performance of structures. The standard also recognizes that it is economically impractical for seismic design to achieve reliability levels comparable with those resulting from design procedures for other load types, due to the high uncertainty associated with prediction of seismic loading.

iii. Next-Generation Procedures

A drive for initiating a new generation of PBSD procedures came from two major concerns: 1) the need to express performance in terms that can better relate to the decision-making needs of stakeholders and thus encompass economic, social and operational impacts, and 2) the necessity of accounting and adequately communicating the uncertainty in the whole performance process (Hamburger, 2014). The perception of building performance varies for the different entities involved in the building process, for example developers, owners, insurance companies, government decision makers and engineers. Performance can be characterized as response (for example force, displacement, acceleration, etc.), physical damage (structural or nonstructural) or losses (economic and social) (Kramer, 2014), where realistically a response results in physical damage which results in losses. While first- and second- generation PBSD principles define a performance objective as a statement of the acceptable risk of incurring specific levels of damages (as related to a structural response) at a specified level of seismic hazard, the next-generation principles realize consequential losses, such as casualties, direct economic costs (repair or replacement), and downtime (time to restore functionality) as more meaningful performance measures directly related to the decision-making process. As described in Section 1.1, a comprehensive assessment process is at the heart of the next-generation PBSD guidelines which were first described in the FEMA-445 document (FEMA, 2006). This assessment process requires a preliminary building design that can be subsequently evaluated in an iterative manner. The following discuss the basis of this assessment methodology and its associated source documents.

1. PEER framework

The foundation for the assessment stage of the next-generation OBSD was first proposed by the Pacific Earthquake Engineering Research Center (PEER) in the form of a probabilistic comprehensive framework that has been documented by several researchers like Cornell and Krawinkler (2000), Moehle (2003), Moehle and Deierlein (2003), Miranda and Aslani (2003), among others. The framework expresses performance as the probability of incurring particular values of key performance measures including casualties, repair costs and downtime, calculated using a complex multi-level integral that integrates the probability of incurring earthquake effects of differing intensity, over all intensities; the probability of experiencing structural response (drifts, accelerations) of different levels, given an intensity of earthquake; the probability of incurring damage of different types, given response; and the probability of incurring specific loss consequences given that damage occurs. The integral used for expressing the probable value of earthquake loss can be simplified for convenience as the following equation (Hamburger, 2014):

$$Performance = \iiint \{PM/DS\}\{DS/EDP\}\{EDP/I\} dz \dots\dots\dots(2.1)$$

where, *PM* is the value of a performance measure, e.g. repair cost, given the occurrence of a particular damage state *DS*, *EDP* (engineering demand parameter) is the value of a response quantity given an intensity of ground motion *I* and the integration occurs over the range of seismic hazards, considering uncertainty in hazard, response, damage and consequence loss using statistical definitions for each. In that sense the seismic design problem is de-constructed into four interim probabilistic models (namely seismic hazard, demand, capacity and loss models) as portrayed in Figure 2-4, which are combined by integration (based on the total probability theorem) over all levels of ground motion, response, and damage with the contributions of each variable weighted according to its relative likelihood of occurrence to estimate the probable losses in a given event or over the building's lifetime. The loss estimation, being a weighted average of all possible ground motion, response, damage, and loss scenarios, has a uniform and consistent probability (Kramer, 2014).

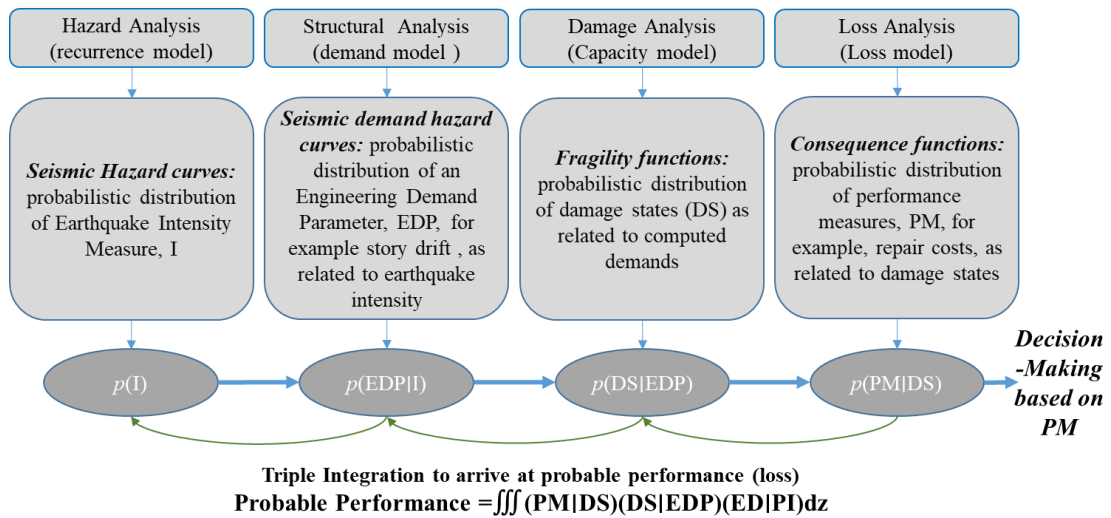


Figure Error! No text of specified style in document.-4 Probabilistic framework of the PEER methodology (after Moehle, 2003)

2. ATC P-58 (FEMA P-58)

The new probabilistic assessment philosophy behind the PEER framework, has also stirred FEMA to enter into a cooperative agreement with ATC in 2001 to develop next-generation performance-based seismic design guidelines, employing a mega multi-year research plan that closely coordinates with the three national earthquake engineering research centers in the US as well as with concurrent efforts in the blast and fire engineering field in order to facilitate the exchange of knowledge and to ensure compatibility with design and assessment methodologies used for other hazards than earthquakes (Hamburger et al., 2004). The project is divided into two phases, that were initially planned to last for 5 years but took longer than expected. The first phase was completed in 2012 with the publication of FEMA P-58: *Seismic Performance Assessment of Buildings, Methodology and Implementation* series of tools (ATC, 2012a, 2012b and 2012c) which provide a methodology to enable engineers to perform the tedious calculations necessary to compute a building's probable earthquake performance, employing a modified Monte Carlo analysis approach developed by Tony Yang, Jack Moehle, Craig Comartin, and Armen Der Kiureghian (Yang et al., 2009) for solution of the framework equation (2.1) which was first presented by Moehle and Deierlein (2004). The methodology implements the multi-level integration using inferred statistical distributions of building response (demand) obtained from a limited set of suites of analyses. These demand sets, together with fragility and consequence

functions, are used to determine a damage state and compute the associated losses. The work also included the development of a companion electronic calculation tool, referred to as the Performance Assessment Calculation Tool, or PACT (ATC, 2012c), that performs the probabilistic calculations and accumulation of losses described in the methodology, with a repository of fragility and consequence data.

The second and ongoing phase, which was initiated in 2013 and initially planned as a 5-year work, has a general goal of practical implementation of the FEMA P-58 performance assessment methodology developed in the first phase by developing design and stakeholder guidelines. Phase two is envisioned to result in products that (Heintz et. al, 2014):

- Assist stakeholders in selecting appropriate performance objectives based on the different occupancies of buildings.
- Assist design professionals in identifying appropriate structural design methods to accomplish specific decision-making needs of stakeholders.
- Assist design professionals in developing efficient preliminary designs that require minimum iteration during the design process.
- Quantify the performance capability of typical code-conforming buildings utilizing next-generation performance metrics.
- Assist design professionals in developing simplified design of buildings to achieve different performance objectives.
- Augment the assessment methodology by estimates of environmental impacts associated with earthquake damage.

The second phase is approaching completion with major improvements including: improving the fragility library; calibration of the P-58 methodology results against actual building performance in earthquakes; development of simplified design tools for example ATC-114 (2016, 2017) and FEMA P-1091 (2017); employment of a module for environmental consequences, improvement of available application software; and, development of technical assistance tools for stakeholders to understand how to utilize the powerful new tools (Hamburger, 2017). However, as acknowledged by FEMA (ATC-58, 2012a), the biggest challenge to the success of the next-generation framework still remains which is developing simple and relatively non-iterative

preliminary design procedures that have the necessary performance characteristics (Hamburger et al., 2004), which are not issued yet. The precision of the results of the performance assessment due to the cumulative uncertainties in the different components of the process (modelling, hazard, damage and losses) is also expected to remain a challenge (Heintz et al., 2014).

2.3 PROSPECT APPROACHES FOR PRELIMINARY BUILDING DESIGN

Most existing PBSO approaches and research tend to provide tools for the evaluation of the seismic performance of structures that have already been designed or even constructed. Much research work is still needed to develop methods for initial designs that can be later used in the PBSO assessment stage. In order to provide an initial design that is well suited for PBSO, key performance criteria need to be built into the design process from the start, and the design should reliably achieve the intended performance with minimum iterations possible so that the whole PBSO process can be relatively efficient and practical.

The input criteria for seismic design is normally a response parameter which can be force, displacement or acceleration. In the inelastic time history analysis method, seismic action is input in their most realistic form which is acceleration, therefore it provides the highest reliability in modeling actual structural behavior and performance. As a counterpart, this method requires complex computational effort for nonlinear modeling as well as special expertise for careful selection of appropriate ground motion records. These limitations render this method only suitable for research application rather than in the design office, and strength and displacement remain the fundamental criteria in seismic design. Energy-based seismic design methods have also been advocated – in which a structure is designed by ensuring that its total energy dissipation capacity is greater than the input energy of expected ground motions; however, they are usually supplementary to other design methods and are likewise still limited to research work.

The following section provides a literature review on the available seismic design methods that can be deemed appropriate as an initial design for application in PBEE. The methods reviewed are the major approaches adopted by modern codes and

some methods developed by other researchers that can fit in the framework of next-generation PBS. These procedures are analyzed based on their complexity, amount of iterations required, the matching of the seismic demand representation to familiar code methods, their incorporation of various performance levels and their reliability in achieving the presumed performance.

2.3.1 Codes and Guidelines Methods

Notwithstanding the recently increased appreciation of the significant role of deformation in describing seismic structural behavior, force-based design remains the most practical and primary method adopted by major modern seismic codes, because other alternatives are still in the development phase and not highly in accord with the norms of design procedures. With respect to code applications, displacement-based design is merely prescribed in rehabilitation guidelines for existing structures. Energy concepts are also applied in modern codes just in the form of capacity design rules which are an indispensable supplement to both force- and displacement-based procedures. The various force and displacement-based methods adopted in different codes are presented in the following sections.

2.3.1.1 Force-based design (FBD) approaches

i. Multi-modal Response Spectrum Method

The main method of design in modern seismic codes, including US codes, Eurocode and similarly the Egyptian code, is the response spectrum method. This is a linear dynamic procedure that permits taking multiple modes of response of a structure into account, and uses the elastic acceleration response spectrum modified through division of its ordinates by the formerly mentioned force reduction factor (R) to account for inelastic actions. The reduction using R is based on the “equal displacement rule”, the keystone of most seismic design methods, which was first presented by Veletsos and Newmark (1960), and further developed to the well-known Newmark and Hall (1973, 1982) design response spectrum. The equal displacement rule states that the displacement demand of an inelastic and elastic system undergoing dynamic action are approximately equal for long-period SDOF systems. This equivalence permits

reduction of the response spectrum and consequently the lateral forces by the force reduction factor “R” on the basis that the extra cost resulting from designing for a higher force, is not justified from a deformation demand point of view. In other words, it is uneconomical to design to resist the complete load due to the design earthquake, when a reduction in load would result in the same displacement and thus same damage of the system. This reduction also results in dragging the response of the structure into the inelastic region which allows favorable energy dissipation and ensures a more predictable mode of failure by ductile action. The R chosen depends on the assumed ductility of the system, which is in its turn related to the expected maximum displacement.

ii. Equivalent Static Load Method

The simplest form of response spectrum analysis is that one combined with the Equivalent Static Load Method (ESLM) which considers only the fundamental first mode of response, and involves a linear static analysis. ESLM is a central concept in seismic design and is still the most widely used in all seismic codes and standards, due to its efficiency and simplicity. In this method, the earthquake effects are merely represented by an equivalent static lateral load distribution all-over the building height. The loads applied are defined by the design response spectrum at the fundamental period of the building which the method assumes the building to be predominantly vibrating with. For this to be true, this simple design method is restricted to buildings of relatively low-rise and with no irregularities to avoid rotational modes.

With respect to damage considerations, the current force-based design procedures (response spectrum and ESLM) include displacement criteria as a final check after detailing of the structure by checking some drift requirements and comparing them to code-specified displacement limits. A displacement amplification factor (DAF) is used to convert the displacement resulting from the elastic analysis to its inelastic counterpart, which in most codes is set equal to “R” value following the equal displacement rule, or may include another multiplied factor that accounts for the ratio between inelastic and elastic displacement in case of inequality. If the calculated displacements exceed the code limits, redesign is required usually by increasing member sizes, until the displacement criteria are met. Therefore, encompassing

displacement verification in the force-based method results in adding multiple iterations to the design process.

As for incorporation of various performance criteria, as previously discussed in Section 2.2.3.1 (iv), most modern codes state multiple performance objectives of life safety, collapse prevention and damage limitation, however the design is only performed at a single level of seismic action (the design level earthquake) which is chosen in general to have a 10 % probability of being exceeded in 50 years, i.e. a mean return period of 475 years, and represents the ultimate limit state in case of a major earthquake. The requirement to satisfy the serviceability limit state in case of a more frequent minor earthquake is achieved indirectly by employing evaluation checks on the displacement response resulting from the ultimate limit state design after its reduction using conversion factors such as the “v” factors specified in the Eurocode 8 (EN1998-, 2004) and the Egyptian seismic code (ECP-201, 2012) as an approximation of the serviceability limit state response. Similarly to account for higher performance objectives for more important structures, seismic codes employ importance factors “I” that are either used to scale the design response spectrum, as in U.S. codes, in order to provide added strength response on the expense of ductility (and hence less damage), or to scale the hazard level and ground motion acceleration itself, as in EC8 and Egyptian code, in order to design a structure that can withstand a stronger earthquake with a higher return period. Therefore, the design itself is done at one performance level (life-safety), and other levels are assessed using approximate conversion factors which are usually based on consensus, hence the reliability of the design in achieving these other performance levels is usually non-uniform. Also, using FBD as preliminary building design tool when targeting several performance levels will result in a long iterative process involving the complex PBSB assessment method. FBD is only recommended by the FEMA P-1091 (2017) for seismic design of buildings in low seismic hazard regions for simplification of the process.

2.3.1.2 Displacement-based design (DBD) approaches

Because displacement parameters are better indicators of damage performance, different design approaches have been proposed to increase the emphasis on displacement as a means of easier implementation of PBSB. In DBD methods,

deformation of the structure is the starting point of the design rather than the end result as in traditional FBD methods. Despite their competitive edge of adopting the real direct effects of an earthquake which is deformation and displacement, better reflecting the nature of seismic action as well as achieving more control on damage and performance, DBD methods do not fail to have several limitations, as discussed hereinafter. Some DBD methods that have been able to find their ways to major seismic guidelines are briefly discussed, where they are categorized into: nonlinear analysis and linear analysis DBD methods.

i. Nonlinear Static Analysis DBD methods

These group of methods have a common basic principle which is combining two types of analysis: first, nonlinear static analysis, referred to as pushover analysis, that pushes the multi-degree-of-freedom (MDOF) structure to increasing loading levels until reaching a predefined target maximum displacement where the resulting pushover curve is bilinearly approximated; and second, response spectrum analysis of an equivalent single-degree-of-freedom (SDOF) for representation of earthquake demand using spectra with different ordinates. The use of the nonlinear static analysis is the main disadvantage of these methods where it is cumbersome and time-consuming, and involves a lot of approximations that challenge its accuracy in the first place, like using a time-independent displacement shape that doesn't consider the effect of higher modes and material degradation. Other limitations individually related to the most common methods that fall under this category are discussed herein.

1. Capacity Spectrum method

It was first proposed by Freeman (1978, 1998) as a rapid tool for evaluation of the seismic vulnerability of buildings. It is the basis of the method used in the ATC-40 document for seismic evaluation and retrofit of concrete buildings (1996), and is proposed as one of the seismic analysis procedures by the FEMA-440 document (2005). The method uses a simple graphical manner where the capacity diagram of the structure (pushover curve) is superimposed over the earthquake demand spectrum plotted with different levels of effective viscous damping, and both diagrams are converted to their acceleration-displacement format. The equivalent linear SDOF system used to

determine the target displacement is assumed to have larger effective period and damping than the original building to account for inelasticity. Despite its rational, the capacity spectrum method usually requires a lot of iterations to find the exact point where the capacity spectrum intersects the response spectrum having the correct level of damping, and therefore is more appropriate for evaluation and retrofit purposes than for designing new structures. The method is also subject to several problems, such as lack of convergence and multiple solutions (Lin and Miranda, 2004).

2. N2-method

The N2-method (Fajfar, 1996) (N stands for nonlinear analysis and 2 for two mathematical models), which is advocated by the EC8 code (EN1998- 2004), uses the same principle of the capacity spectrum method with a rather more straightforward approach in the demand side to minimize iterations. The capacity diagram is the same, while inelastic demand spectra (rather than various elastic spectrum with equivalent damping and period) are used by reducing elastic spectra using reduction factors obtained from statistical analysis, or directly by time-history analyses of inelastic SDOF systems. The acceleration-displacement format is still used, and the target displacement is estimated from the elastic-displacement of an equivalent SDOF system defined by the bilinear idealization of the pushover curve imposing that the yield strength is equal to the strength of the target point. Less iterations are used because there is no need to reach a certain effective damping and effective period like the capacity spectrum method, however there are major approximations in developing the inelastic spectra themselves. Evaluations of the accuracy of this method has shown that it can lead to significant underestimation of inelastic deformation demands in the case of near-fault ground motions, for systems with low strength and for soft soil conditions (Bento et al, 2004)

3. Displacement Coefficient method

The displacement coefficient method again uses nonlinear static analysis to derive the MDOF structure capacity curve, while it uses displacement versus period elastic response spectrum for the demand representation. For computing the target displacement, the displacement of a linearly-elastic SDOF system, having the same

period and damping as the fundamental mode of the original building, is extracted from the response spectrum, and then modified by a series of empirical coefficients to arrive at its MDOF equivalence, without any iteration. The methods implemented in FEMA-273 (1997a), FEMA-356 (2000), and FEMA-440 (2005) documents belong to this type of displacement coefficient method. Because the seismic hazard is essentially measured in acceleration terms, converting the acceleration spectrum into displacement ordinates involves a lot of approximations, which, in addition to the empirical coefficients, represent the main source of limitation in this method.

ii. Linear Analysis DBD methods

To overcome the limitation of using complex and not highly accurate nonlinear analysis methods, several linear methods that uses displacement as the starting point were also developed. Out of these methods, the direct-displacement-based design (DDBD) method and the equal displacement-based design (EDBD) have achieved some acceptance by the design community, being advocated by the SEAOC for the 1999 “Blue book” for performance-based design of new structures (SEAOC, 1999), and as an alternative seismic design procedure for the New Zealand seismic design code (NZS, 1995).

1. Direct-displacement based design (DDBD)

The direct displacement-based design (DDBD) method proposed by Priestley and Kowalsky (2000) is one of the promising DBD methods that had been well promoted for its suitability for application in PBS. In addition to its proved superiority in achieving targeted performance as concluded by Varughese et al. (2012) compared to other DBD methods, it has the advantage of requiring only static linear analysis with minimum iterations to go directly from target displacement to required strength. The displacement parameters are used as a design input in a direct manner that can be applied for new designs where the displacement demand is estimated without any assumption about the member stiffness. A design displacement profile is first established using the code drift limits and the drift corresponding to the system’s inelastic rotation capacity. Using this displaced shape, the effective mass and target displacement of an equivalent single degree of freedom (SDOF) system are determined.

The displacement ductility demand is calculated by dividing the target displacement by the yield displacement of the structure (based on section dimensions but not strength) and is used to calculate an equivalent damping value according to the assumed level of energy dissipation capability. A displacement spectrum is then developed at this equivalent damping level, and the effective period corresponding to the target displacement is read off the displacement spectrum. Using the effective period and effective mass, the required effective (or tangent) stiffness is obtained and multiplied by the target design displacement to determine the design base shear. The base shear is distributed along the building height and members are designed according to the corresponding straining forces, as typical of other FBD procedures. Compared to FBD procedures, DDBD ensures more consistent designs that achieve, rather than be bound by performance criteria, however it still has some limitations: it is rather complex and not familiar to engineers; iterations may still be required if the check for the assumed level of damping fails, it employs the displacement response design spectrum which lacks acceptance by the profession as well as involves many approximations; and there is inaccuracy associated with the equivalent linear SDOF representation of the real structure.

2. Equal-displacement-based design (EDBD)

This method is based on the familiar equal displacement approximation by Newmark and Hall (1982), and is considered just an adaptation of the traditional force-based design (FBD) procedure by using acceleration-displacement response spectrum or displacement spectrum rather than the acceleration-period spectrum, thus focusing on displacement rather than forces. It differs from the DDBD by using initial stiffness and traditional viscous damping value of 5% rather than the secant stiffness and equivalent viscous damping at target displacement which is used in DDBD. The target displacement is similarly obtained based on the estimated displaced shape of an equivalent SDOF system. The main disadvantage of this method lies in its use of displacement spectrum which do not have a well-balanced catalogue same as the acceleration spectrum. Also, the ordinates of the displacement spectra are much more sensitive to the effects of processing and filtering applied on accelerograms than those of acceleration spectra (Bommer et al., 2000). Additionally, it was proven that this

method can lead to unconservative results for short-period structures due to the equal displacement approximation (Calvi et al.,1998).

2.3.2 Non-iterative Methods Developed by Other Researchers

In addition to the methods employed by standards and guidelines as discussed before, there are many other individual researchers that developed design approaches which emphasize displacement as a design factor so that it can fit in the context of performance-based engineering. Nevertheless, the majority of available approaches are merely intended to develop a preliminary design, coupled with an assessment stage for design verification, or require an existing structure or an already designed structure and thus is more applicable to performance evaluation (Franchin et. al, 2018). There is limited research suggesting direct design methods for new structures that start with a displacement criterion associated with a performance objective to arrive at the structural properties with minimum amount of iterations, and therefore can be used as an initial design tool in the framework of performance-based design. The following section presents a brief literature review about the most influential of these methods which have been studied for a considerable period of time by several researchers and are still under development till present. These are the Yield Point Spectra method, Performance-based plastic design and the Hybrid force/displacement-based design method, with the latter being the focus of the current study. It should be noted that all these approaches are still under improvement and development for practical applications.

2.3.2.1 Yield point spectra method

In typical seismic design, changes in strengths of components of the lateral force resisting system to satisfy lateral force requirements are assumed to have a negligible effect on the stiffness and period of the structure, while for displacement control it is usually required to adjust the period and stiffness of the structure and thus revise member dimensions. Several researchers have observed that it is the yield displacement of structures rather than the fundamental period of vibration which is invariant with changes in component strengths and stiffness, and hence seismic design could be better approached from the perspective of constant yield displacement rather than constant period, so that member dimensions can be more accurately estimated early in the design

process minimizing the need for iterations (Priestley and Kowalsky, 1998). Based on this presumption, Ascheim (1999, 2000) proposed a displacement-based design method that utilizes a graphical representation of the inelastic seismic demands as constant ductility curves plotted with the yield strength coefficient, C_y (ratio of the yield strength of a system to its weight) as a function of the system's yield displacement. These curves are termed “Yield Point Spectra” where they represent the yield points of oscillators having constant displacement ductility for a range of oscillator periods (Aschheim, 1999). It was further developed by Aschheim and Black (2000). This method is considered a variant of the capacity spectrum method in the acceleration-displacement format at the yield rather than the ultimate state, as shown in Figure 2-5. It was later enhanced to take the form of ‘yield frequency spectra’ (YFS) that offer a direct probabilistic solution space for the entire range of a system performance in terms of the mean annual frequency of exceeding global ductility levels versus the base shear strength (Vamatsikos and Aschheim, 2016; Katsanos and Vamvatsikos, 2017).

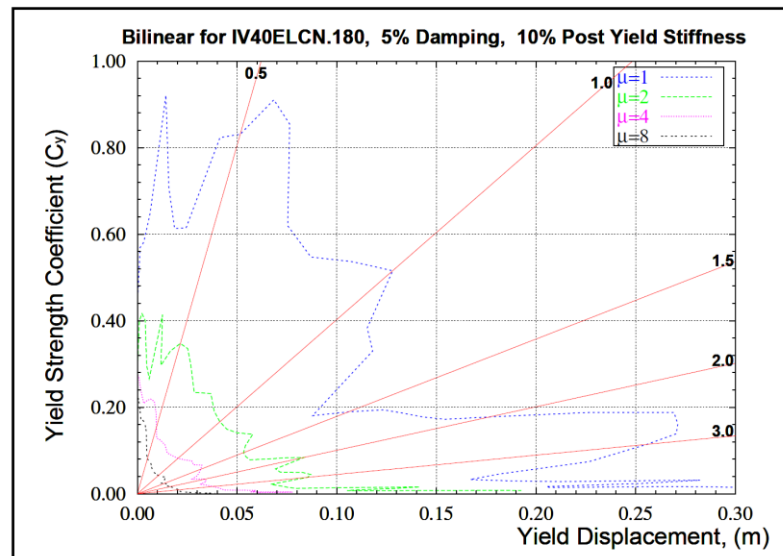


Figure **Error! No text of specified style in document.**-5 Yield Point Spectra of the 1940 El-Centro record (after Aschheim & Black, 2000)

Beside adopting the appealing graphical form of the Capacity Spectrum representation, the Yield Point Spectra method has an added advantage, where it is not just limited to estimation of structure's displacement ductility and ultimate displacement when the period and strength are known, but can also be used in the reverse process to determine the minimum strength and stiffness required to limit drift

and displacement ductility demands to prescribed values. This advantage particularly pertains to performance-based design, since target displacement values can be associated with a performance level, and accordingly displacement constraints' branches for the various performance objectives can be constructed and superimposed on the same graph to generate a permissible design region of combinations of strength and stiffness. In this manner, the yield point spectra method offers engineers a practical approach to design structures to satisfy various performance objectives simultaneously in a single design step by choosing a point within the boundaries of the permissible design region.

This graphical procedure has some disadvantage. The yield acceleration-displacement representation of seismic demand is not in common with current practice and would make inefficient use of the already established databases of response spectra. The authors recommend that the yield point spectra may be determined similar to the inelastic response spectrum method first proposed by Priestley and Calvi (1997) In that sense, Yield point spectra can be jagged if they are generated exactly from ground motion records using specialized computer programs that compute the largest strength required to limit ductility responses to specified values over a range of oscillator periods, or smooth if approximately estimated from elastic response spectra using established R- μ -T relationships to estimate strengths corresponding to various ductilities (Aschheim, 1999), including those by Newmark and Hall (1973). Another approximation is compounded in estimation of the yield displacement, where they are obtained from the elastic periods of each oscillator and the inelastic pseudo-acceleration values in accordance with initial stiffness assumptions (rather than effective stiffness), using the simple relation $\Delta_y = (T/2\pi)^2 S_a$ as suggested by Aschheim (1999). It should be also noted that after determination of the base shear coefficient, the design work continues based on conventional elastic design and capacity rules. Furthermore, similar to the equivalent static load method, this method does not account for higher mode effects, and thus is limited to design of regular low-rise structures

2.3.2.2 Performance Based Plastic Design

Performance Based Plastic Design method is a design method that directly accounts for inelastic structural behavior, by combining displacement-based and

energy-based design concepts, producing structures with targeted and predictable response. It was developed by Subhash Goel and his associates at the University of Michigan Ann Arbor, mainly for steel structures (Leelataviwat et al., 1999, 2007; Lee and Goel, 2001; Dasgupta et al., 2004; Chao and Goel, 2006a, 2006b, 2008; Chao et al., 2007; Goel and Chao, 2008; Goel et al, 2009a, 2009b,) and later modified for reinforced concrete frame structures (Liao and Goel, 2010a, 2010b, 2014). Recently, a modified version of the plastic method was proposed for self-centering buckling-restrained braced frames, whereby Liu, Shuang and Zhao (2018) studied the possibility of using the relationship between the strength reduction factor and the nonlinear displacement ratio to estimate strength demands rather than using yield displacement in order to minimize iterations.

In Performance-based Plastic design, main performance objectives are defined in terms of pre-selected target drift and desired yield mechanism that are related to the degree and distribution of accepted structural damage respectively (Liao and Goel, 2014). In order to determine the design base shear for a specified earthquake hazard level, the authors presented an approach that applies an energy balance concept similar to the basic energy approach first used by Housner (1956, 1960), whereby the amount of work needed to push the structure monotonically up to the design target drift is equated to the input energy required by an equivalent elasto-plastic single degree of freedom (EP-SDOF) system to reach the same drift state, as derived using suitable inelastic response spectra such as the idealized Newmark-Hall inelastic response spectrum (Newmark and Hall, 1982). Figure 2-6 illustrates the energy concept of the Performance-based Plastic Design together with an example selected yield mechanism of a typical moment frame.

As shown in Figure 2-6, all inelastic deformations are controlled to be formed in intended yielding points, based on the chosen yield mechanism, for example near the end of beams and at the base column for moment frames. Plastic analysis is then used for design and detailing of the yielding members with consideration of equilibrium and plastic strength conditions, while design of non-yielding members is performed applying the capacity design approach to ensure formation of the selected yield mechanism.

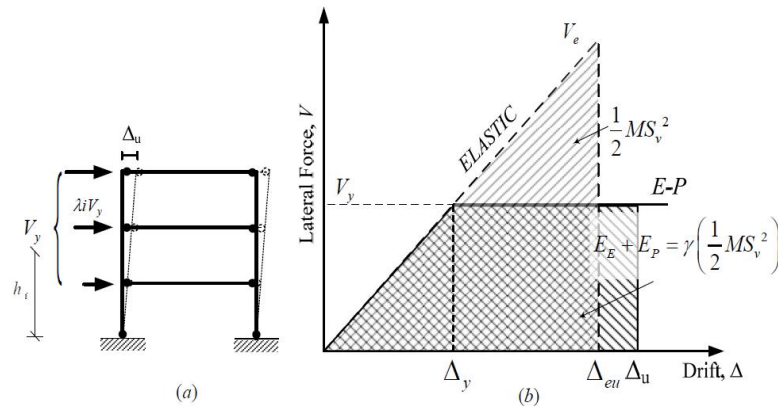


Figure Error! No text of specified style in document.-6 (a) selected yield mechanism for desirable response in a typical moment frame (b) energy equating concept for deriving design base shear of PBD method (after Liao and Goel, 2014)

The method has the advantage that drift control and definition of the desired yield mechanism is directly integrated in the start of the design process, thus minimizing the need of iterations while at the same time ensuring more enhanced structural behavior in accord with targeted performance. Another advantage is that by selection of yielding members at the appropriate locations, innovative structural schemes can be employed. However, this method still has some disadvantages and limitations. First of all, the approach requires a major shift from the norms of seismic design practice. Also, the method has some approximations, like assuming the inelastic spectra by Newmark and Hall still valid for multi-degree of freedom systems, and ignoring the effect of the structural period on energy dissipation capacity and over-strength, which can render designs not uniformly conservative for structures of variable periods. The plastic analysis approach is more suitable for highly ductile systems such as steel and its application for reinforced concrete may not be justified.

2.3.2.3 Hybrid force/displacement method

A seismic design method has been developed over the past 15 years specifically for performance-based engineering applications for steel frames, where it combines the advantages of the familiar force-based and displacement-based seismic design methods in a partial force/displacement-based design format. The method, referred to by its authors as “Hybrid force/displacement-based design”, was first proposed roughly for seismic design of framed structures by Bazeos N. and Beskos D.E. (2003), then it was further detailed as a comprehensive design method for plane steel frames based on the

EC8 (Karavasili, T.L. et al., 2006a, 2006b, 2006c, 2007a, 2007b and 2008a). It was presented as a novel performance-based design procedure in some books for example “Engineering Against Fracture” (Pantelakis, S. and Rodopoulos, C., 2009) and “Advances in Performance-Based Earthquake Engineering” (Fardis, M.N., 2010).

The main idea of this methodology is that starts by transforming target values of the inter-story drift ratio (indicator of nonstructural damage) and local ductility (indicator of structural damage) to a target roof displacement using relations that are developed as a factor of the building geometrical attributes, and then calculates the appropriate strength reduction factor required for limiting ductility demands to those of the estimated target roof displacement ductility. The design criteria are repeatedly defined as associated with three basic performance levels, i.e. immediate occupancy, life safety and collapse prevention, and in this way the design ensures control of both strength and drift performance for several seismic events (Tzimas A.S. et al, 2013). In addition to the benefit of using both drift and ductility demands as input variables for the initiation of the design process, the hybrid force/displacement approach has the major advantage of avoiding the use of a substitute single degree of freedom system as done by DDBD while retaining the use of conventional elastic response spectrum analysis and design in line with current seismic codes and common practice. Also, the proposed method considers the influence of the number of stories and the type of the lateral load resisting system.

The superiority of this proposed method over other displacement-based and force-based methods has been proven for Moment-resisting steel frames (MRF) (Bazeos, 2009; Karavasilis et al., 2009), and intricately evaluated against nonlinear time-history analysis results (Karavasilis et al., 2010b). Modifications for two types of concentrically braced frames (CBF) have been developed namely x-bracing (Karavasilis et al., 2007a) and chevron bracing (Stamatopoulos and Bazeos, 2011). Some factors were added to the method, for example, to account for setbacks (Karavasilis et al. 2008c) and for vertical mass irregularities (Karavasilis et al. 2008d). Extension of the method to the case of pulse-like earthquake ground motions has been also studied (Karavasilis et al., 2010a). The most refined form of the hybrid force/displacement methodology has been presented in the work by Tzimas, Karavasilis, Bazeos and Beskos (2013) that combines all the aforementioned factors in

one comprehensive design guide and demonstrates the validity and consistency of the method in identifying the performance level which truly controls the design. Those same researchers have extended the use of the hybrid method to space moment-resisting steel frames and proposed new empirical expressions which includes accidental eccentricity to account for torsional effects that were neglected in planar frames (Tzimas et al., 2017). Research on the hybrid force/displacement method is still ongoing for broadening its range of applicability to eccentrically-braced frames and buckling restrained frames.

While all the aforementioned studies remain on steel structures, latterly there has been an initiative on the application of the same procedure to the case of composite steel/concrete structures. Skalomenos et al. (2015) studied the extension of the hybrid methodology for composite plane moment-resisting frames (MRFs) consisting of I steel beams and concrete filled steel tube (CFT) with refined modeling than in Tzimas et al. (2013), and, by comparing realistic design examples using FBD and HFD methods on the basis of nonlinear time-history analysis of the designed structures, proved that the advantages of the hybrid method over the force-based method in terms of better rational, efficiency and accuracy in achieving intended performance remains valid for composite structures, as well.

The current study represents one of the first initiatives in applying the HFD method to reinforced concrete structures. Concurrently, a group of researchers have been working in the same line where, very recently, they proposed the hybrid force/displacement design method for reinforced concrete moment resisting frames (Piana et al., 2018). They used a frame-element software called Ruaumoko (Carr, 2006) for nonlinear analysis combined with MATLAB (2009) routines to automate the post-processing of results. All beams and columns were modeled by frame elements with concentrated hinges at their two ends, to account for inelastic behavior. The simplicity and efficiency of such nonlinear modeling technique allowed studying 38 frames with varying dynamic and mechanical characteristics. On the other side, the work presented in this thesis involves less but much more intricate number of nonlinear analysis, where fiber-element modeling is used which monitors nonlinear behavior across the cross-sections as well as along the whole length of the elements, and also accounts for geometrical nonlinearity which is quite important in large displacement analysis. This

extension is by no means trivial because due to the complex behavior of concrete compared to steel, detailed and rigorous modeling of the nonlinear material behavior along the whole member depth and length can substantially affect the displacement results.

2.4 RELATIONSHIP BETWEEN PERFORMANCE AND DISPLACEMENT DEMAND

A relationship between the displacement demand of structures and specified performance objectives would allow bringing displacement to the initial steps of design as advocated by the HFD design described in Section 2.3.2.3. Extension of the HFD method to concrete moment-resisting frames requires the use of relationships that has been specifically formulated for this lateral load resisting system and that covers various damage levels. Research efforts in this direction are limited in the literature and are discussed herein. It should be noted that all the presented equations define the damage of concrete frames (and thus performance) in terms of one response parameter which is the inter-story drift ratio, and which is also the damage metric chosen in the current study as will be discussed subsequently in Chapter 4 (Section 4.4.2).

2.4.1 Relations Valid Only in the Elastic Range of Behavior

One of the first relations are those that have been developed by Loeding et al. (1998) to define the characteristics displacement profiles of plane concrete frames at maximum response in terms of maximum inter-story drift ratio and the number of stories. Employing linear multi-modal dynamic analyses of RC frames, and relating maximum displacement at each floor with the inter-story drift at the same floor, they developed the following equation which they proposed for design purposes:

$$\begin{array}{l}
 \text{For } n \leq 4: \quad \Delta_i = \theta_d h_i \\
 4 \leq n < 20: \quad \Delta_i = \theta_d h_i \left(1 - \frac{0.5(n-4)h_i}{16h_n} \right) \\
 n \geq 20: \quad \Delta_i = \theta_d h_i (1 - 0.5 h_i/h_n)
 \end{array} \quad \left. \vphantom{\begin{array}{l} \text{For } n \leq 4: \\ 4 \leq n < 20: \\ n \geq 20: \end{array}} \right\} \dots\dots\dots (2.2)$$

where Δ_i is the design displacement at story (i), θ_d is the design drift ratio, n is the number of stories, h_i is height of story (i) from the base, h_n is the total height of the

building. The researchers proved that these approximate relations are adequate for design purposes specifically DBD. However, since they do not cover the nonlinear response of structures, these equations cannot be applied for various limit states and performance-based design. Also using such type of equations to estimate the global maximum displacement at the roof level in terms of the global maximum damage will be inaccurate because the maximum story displacements are generally asynchronous and the story of the maximum inter-story drift is not the same as that of the maximum absolute displacement.

Miranda (1999) developed another displacement predictive model with the objective of providing an approximate estimate of lateral displacement demands and maximum inter-story drifts in multistory frame buildings. The relation was developed mathematically using a fourth-order differential equation based on the continuum model of Heidebrecht and Stafford Smith (1973) It modifies the SDOF response (spectral displacement) through four parameters in order to arrive at the MDOF behavior, where it is given in the general form of:

$$IDR_{max} = \beta_1\beta_2\beta_3\beta_4 \frac{S_d}{H} \dots\dots\dots(2.3)$$

where IDR_{max} is the maximum inter-story drift ratio, S_d is the elastic spectral displacement (for a SDOF); H is the total building height; and β_s are modification factors defined as:

- β_1 : factor that represents the approximate modal participation factor
- β_2 : the ratio between elastic maximum IDR and elastic maximum roof drift ratio
- β_3 : empirical factor for modification of elastic demands to inelastic demands.
- β_4 : factor that accounts for the combined effects of inelasticity, number of stories and mechanisms in the post-elastic range.

While Miranda’s proposed equation is not aimed directly at relating maximum displacement and maximum inter-story drift of MDOF systems, one of the factors included in the predictive model (β_2) serves to amplify the roof drift ratio to reach the maximum inter-story drift, which is basically the ratio of roof drift and inter-story drift. Focus herein is on this factor, which is only provided in the model for the elastic range, while inelasticity is handled by another factor to arrive at the inelastic displacement.

The derivation of this factor is based on the continuum model that approximates the displacement profiles of buildings that deform under combined flexural and shear behavior. This factor is specific for each model building and can be calculated as the product of the derivative of the lateral deformation profile, $u(z)$ with respect to height, i.e. $(du(z)/dz)$, and the total height to top displacement ratio of the continuum model, i.e. $H/u(H)$, as given in the following equation:

$$\beta_2 = \max \left[\frac{du(z)}{dz} \frac{H}{u(H)} \right] \dots \dots \dots (2.4)$$

Thus, β_2 -factor is considered more as a representation of the distribution and concentration of inter-story drifts along the height of the building. There are several limitations for using this equation in directly relating maximum displacement to IDR. It is only applicable in the linear range; it is based on several approximations related to the continuum model like having uniform stiffness and mass distribution, and it requires an existing design to pre-develop an approximate shape function.

Adopting the forms proposed by Miranda (1999), another group of researchers (Gaetani d'Aragona et al., 2018) provided simplified formulae for the β_2 factor that can be used rapidly for relating lateral displacement and inter-story drift ratios of RC frame buildings, based on few geometrical parameters which are the number of floors and the infill opening configuration (measured by the closure percentage in each floor). By performing elastic time-history analysis, all scaled to the same intensity level, on equivalent cantilever models of the prototype buildings varying in height and infill distribution, then analyzing the response data, the following equation was developed:

$$\beta_2 = f_2(\alpha_1, \alpha_{2-n}/\alpha_1) \cdot H^{g_2(\alpha_1 \alpha_{2-n}/\alpha_1)} + h_2(\alpha_1, \alpha_{2-n}/\alpha_1) \dots \dots \dots (2.5)$$

where H is the building height (in meters); α_i is the closure percentage at floor (i), n is the number of floors and f_2 , g_2 and h_2 are functions which are linearly dependent on the closure percentage of the first floor (α_1) and on the ratio between the closure percentage of the upper floor and that of the first floor (α_{2-n}/α_1) as follows:

$$f_2 = 0.37 + 1.20\alpha_1 - 2.69 \alpha_{2-n}/\alpha_1 \dots \dots \dots (2.6)$$

$$g_2 = 1.04 - 0.49\alpha_1 - 0.76 \alpha_{2-n}/\alpha_1 \dots \dots \dots (2.7)$$

$$h_2 = 3.13 - 2.22\alpha_1 + 1.21 \alpha_{2-n}/\alpha_1 \dots \dots \dots (2.8)$$

Despite being a novel contribution in considering the effect of infill walls distribution that greatly affects the stiffness distribution and damage potential, the presented equations are only developed for the linear range of behavior, and are thus recommended by the authors for use when inter-story drift ratios do not exceed 1%, which represents only the serviceability limit state. There is also a lot of approximations involved in adopting the equivalent cantilever models that can affect the accuracy of the developed relations.

2.4.2 Relations Valid Up to the Inelastic Range of Behavior

Attempting to include the effect of nonlinear behavior on the lateral displacement profiles of RC frames, Jiang, Lu and Kubo (2009) proposed new expressions that relate the maximum displacement of regular RC frames to the inter-story drift ratio at three discrete damage levels, as a function of some structural characteristics of the frame which are the fundamental period (by varying the number of floors from 3 to 15 in three-floor increments), and the column-to-beam strength ratio. They conducted nonlinear time-history analysis on two-dimensional full frame models employing lumped plasticity for capturing the nonlinear behavior of the frames by using zero-length plastic hinge models at specified member-end locations. Separate equations are generated for each damage level, which took the form of:

$$D_j = (P_1 x_j + P_2 x_j^2 + P_3 x_j^3) H \theta_{s,max} \dots \dots \dots (2.9)$$

where D_j is the maximum floor displacement at floor (j); x_j is the relative height of floor (j) normalized by the total height, i.e. $x_j = H_j/H$, in which H_j is the height of floor (j) measured from ground level; $\theta_{s,max}$ is the maximum inter-story drift ratio along the height; and P_1 , P_2 and P_3 are parameters that depend on the damage level and include higher mode effects, and which were defined as follows:

For slight damage

$$\left. \begin{aligned} P_1 &= 0.851 - 0.175 T_1 \\ P_2 &= 0.528 + 0.077 T_1 \\ P_3 &= -0.513 \end{aligned} \right\} \dots \dots \dots (2.10)$$

For moderate damage

$$\left. \begin{aligned} P_1 &= 1.563 - 0.456\eta_c + \left(0.246 - \frac{1.155}{\eta_c + 1.162}\right)T_1 \\ P_2 &= -0.888 + 0.853\eta_c + (0.414 - 0.217\eta_c)T_1 \\ P_3 &= 0.066 - 0.322\eta_c \end{aligned} \right\} \dots\dots\dots(2.11)$$

For severe damage,

$$\left. \begin{aligned} P_1 &= 1.698 - 0.449\eta_c + \left(-0.203 - \frac{0.060}{\eta_c - 0.553}\right)T_1 \\ P_2 &= -1.678 + 1.224\eta_c + (0.493 - 0.249\eta_c)T_1 \\ P_3 &= 0.489 - 0.548\eta_c \end{aligned} \right\} \dots\dots\dots(2.12)$$

where T_1 is the elastic fundamental period of the frame in seconds, and η_c is the column-to-beam strength ratio. Using the above formulations in the context of the next-generation performance-based design is rather delimited because they are specified for discrete damage levels, while the future guidelines are directed towards the concept of continuity in performance levels. Also, using the factor of column-to-beam strength ratio requires knowledge about the reinforcement of the structural elements and thus cannot be directly used in preliminary designs without iterations and is thus more applicable for existing designs. Besides, nonlinearity can be better modeled as distributed for better capturing of the complex behavior of reinforced concrete structures.

Along with the development of a predictive model for maximum inter-story drift ratios, Azak (2013) and Azak and Akkar (2014) provided an approximate correlation between the maximum roof displacement ratio (MRDR) and maximum inter-story drift ratio (MIDR) for RC frames using just constants independent of the ground motion or structural characteristics like building height or fundamental period. The proposed relation is based on the results of hundreds nonlinear time-history analyses of two-dimensional frame models, with varying height from 3 to 9 in one-floor increment, and subjected to a range of ground motions with variable characteristics and scaled to different intensities. The nonlinear structural behaviour was modeled quite accurately using the fiber-based element approach employed in OPENSEES (2006) software. A linear fit was established on the logarithmic MRDR and MIDR values as

presented in Equation (2.13). It is evident that the provided fit is quite approximate and becomes weaker with smaller values of MIDR and MRDR, which implies the need to improve the regression by using more variables.

$$\log_{10}(MRDR) = 0.995 \log_{10}MIDR^{-0.135} \dots\dots\dots(2.13)$$

In the context of applying the HFD performance-based design method to RC frames, Pian et al. (2018) recently provided relations that associate the maximum roof displacement $u_{r,max}$ to different damage levels as represented by the inter-story-drift ratio (IDR_{max}) based on nonlinear time-history analysis of RC frames of different heights. The development of the relationship followed the same format and methodology presented by Karavasilis, Bazeos and Beskos (2008a, 2008b, 2008c) for HFD design of steel MRFs, which adopts the notation provided by Miranda (1999), given as $\beta = u_{r,max}/(H*IDR_{max})$, where H is the height of the frame from its base. The following predictive equation for the ratio β was provided:

$$\beta = 1 - 0.17 \cdot (n_s - 1)^{0.75} \cdot \rho^{0.07} \cdot \alpha^{-0.4} \dots\dots\dots(2.14)$$

where n_s is the number of floors; ρ is the column-to-beam strength ratio; and α is the beam-to-column stiffness ratio. The authors concluded that the β factor had a strong dependence on the number of floors, with less dependence on the column-to-beam strength ratio, and minor dependence on the beam-to-column stiffness ratio. This proposed relation has some limitations. Similar to the comments about the method developed by Jiang et al. (2009), there is a need for better modeling of concrete nonlinear behavior by capturing plasticity along the member cross section and length. Likewise, the use of a variable that represents column-to-beam strength ratio requires knowledge about the reinforcement of the structural elements and thus requires an existing design as a prerequisite. Additionally, in the author’s opinion, there is multicollinearity in the regression when involving both beam-to-column stiffness ratio and column-to-beam strength ratio as variables, which affect the stability of the prediction equation.

Chapter 3

PROPOSED FORCE/DISPLACEMENT-BASED DESIGN

3.1 INTRODUCTION

According to PBD philosophy, it is necessary to determine drift and displacement demands with sufficient accuracy during the seismic design process. Potential economic, social and human life losses and decisions of repair or replacement are related to the damage of buildings during earthquakes, which is in its turn directly related to displacement response. Therefore, for a truly performance-based design process to be implemented with success, displacement has to be associated to the design criteria at the input stage, in a multiple-level format, while at the same time retain the simplicity of force-based procedures which are a mainstream in seismic design. This chapter presents the proposed application of the hybrid force/displacement-based design method to RC moment-resisting frames, which modifies the force-based procedure by correlating estimates of the maximum roof displacement (based on the predefined performance objectives) to the seismic strength requirements. First, the objective of the proposed methodology is discussed with the intended advantages, then the theoretical basis of relating displacement to the strength reduction concept used in the force-based design is briefly presented, and finally, the steps of the procedure are elaborated and the research methodology for developing the required displacement estimate relationships is outlined.

3.2 MODIFICATION ENVISAGED

The outlook of the proposed modification is to shift the performance-based criteria to the beginning of the seismic design process, so that design can be based on performance, and the structures can be designed to achieve – rather than be bound by – multiple performance objectives. Figure 3-1 depicts the current method of force-based design as compared to the proposed procedure. In a sense, the prospect method can be considered a mix between the displacement-based and force-based methods described in Section 2.3.1.1, where the design starts with a displacement estimate, yet continues with calculation and distribution of forces. The scope of application is RC moment-

resisting frames (MRF's) with limited ductility and the method is in line with the hybrid force/displacement based (HFD) design developed earlier for several types of steel structures as discussed in Section 2.3.2.3. The intended properties of the envisaged design method are that

1. it can be directly used in conjunction with the conventional elastic pseudo-acceleration design spectra with 5% damping for seismic design of RC MRFs.
2. it involves only an elastic analysis scheme.
3. it can automatically account for displacement demands at several performance levels without requiring displacement checks at the end of the design process.
4. it includes simplified displacement formulas that can be used with limited knowledge of the building characteristics, and depending on few geometrical parameters, so that they can be used at the design input stage.

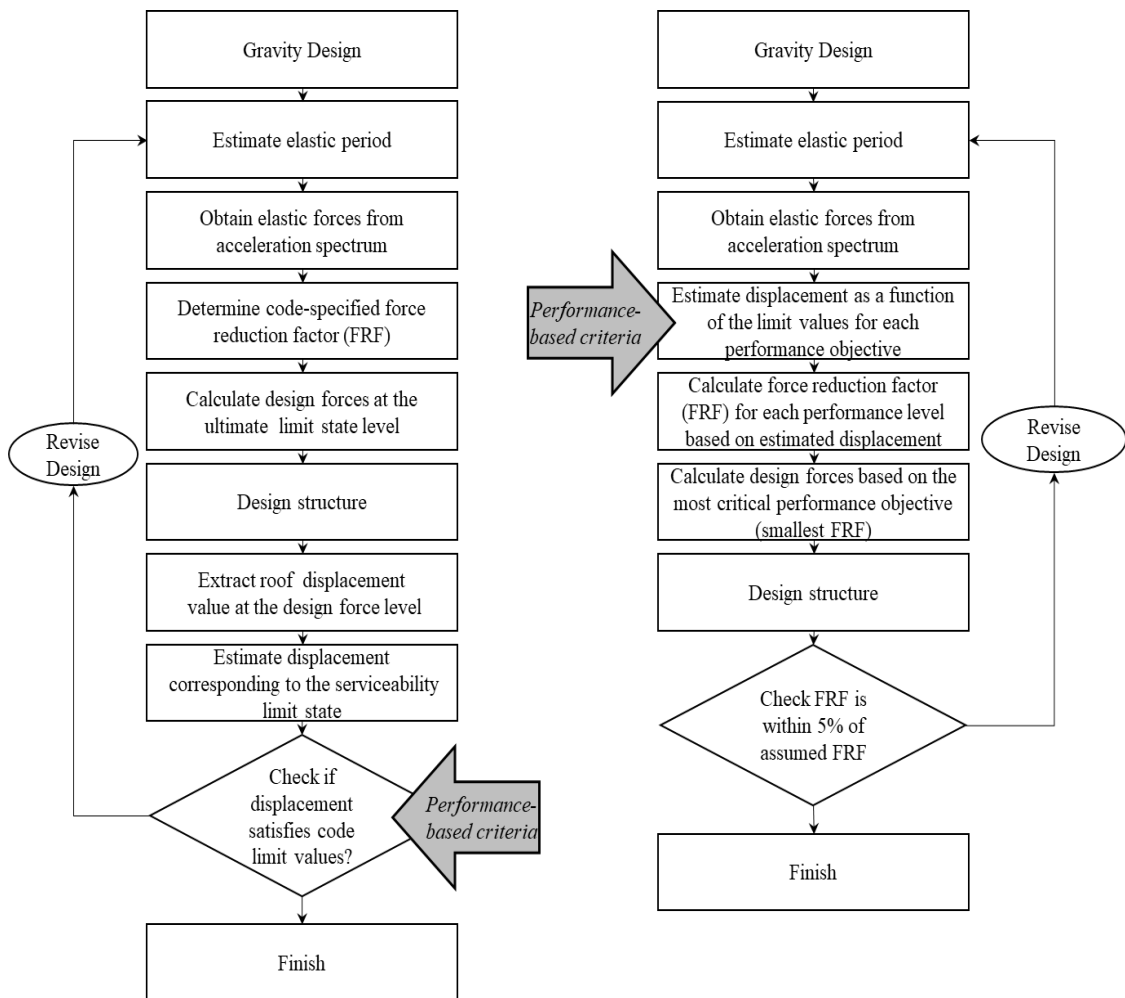


Figure 3-1 Sequence of code force-based method (left) and proposed modification (right)

Development of such modified procedure for seismic design can have the following advantages:

1. The design is more rational than the force-based procedures because displacement better represents actual earthquake physical behavior.
2. The limitation of the force-based methods in using empirically stipulated force reduction factors is avoided
3. The approximation of the displacement-based methods in using equivalent linear SDOF idealizations is also avoided, and thus the proposed method can be easily applied for the design of new buildings.
4. The design method has higher prospect of being integrated into the future performance-based design framework, where there is possibility to design for multiple performance levels, and the design has higher reliability in achieving the targeted displacement values and performance.
5. The design steps and iterations are reduced where the displacement check is already accounted for during the strength design, and therefore more efficient designs are achieved.

3.3 THEORETICAL BASIS

The theoretical basis behind the proposed design method can be explained by understanding the global load-displacement curve of a structure from the point of view of both traditional design and performance-based design. The concept of the force-based procedure is based on the reduction of the elastic demand (as obtained from the elastic design spectrum) by the force reduction factor (R) which is based on typical inelastic response of different structural systems. This reduction is conceptually based on the equal displacement rule (Newmark and Hall, 1982), as previously discussed in Section 2.3.1.1; it is justified by the expected system ductility, overstrength and redundancy. For simplification of the concept, only the ductility component is considered herein while the overstrength and redundancy are assumed to be inevitably included later in the design due to the inherent strength in the materials used, the design equations, and the specified lateral force resisting system.

Figure 3-2 illustrates the concept of typical earthquake design. Based on the equal-displacement assumption that the displacement of an elastic and an elasto-plastic

SDOF's are equal, the actual inelastic displacement of the structure is assumed approximately equal to the displacement of the structure if it is to be designed to behave completely elastic in case of the design level earthquake, i.e. inelastic displacement (Δ_u) \cong elastic displacement (Δ_e). Also understanding that earthquake-resistant structures are intentionally designed to yield under earthquake loading (damage is allowed), whereby the analysis domain is brought down to the linear stage, it can be assumed that the yield point is hypothetically the design ultimate point in the analysis domain, i.e. design displacement (Δ_d) \cong yield displacement (Δ_y) and design base shear (V_d) \cong yield base shear (V_y). Consequently, it can be concluded that the R-factor that reduces the elastic forces (V_e) (as calculated from codes of practice elastic response spectrum) to the design force level ($V_d \cong V_y$) can be calculated from the displacement coordinates as equivalent to the system ductility (μ) as follows:

$$R \cong \mu = \Delta_u / \Delta_y \dots \dots \dots (3.1)$$

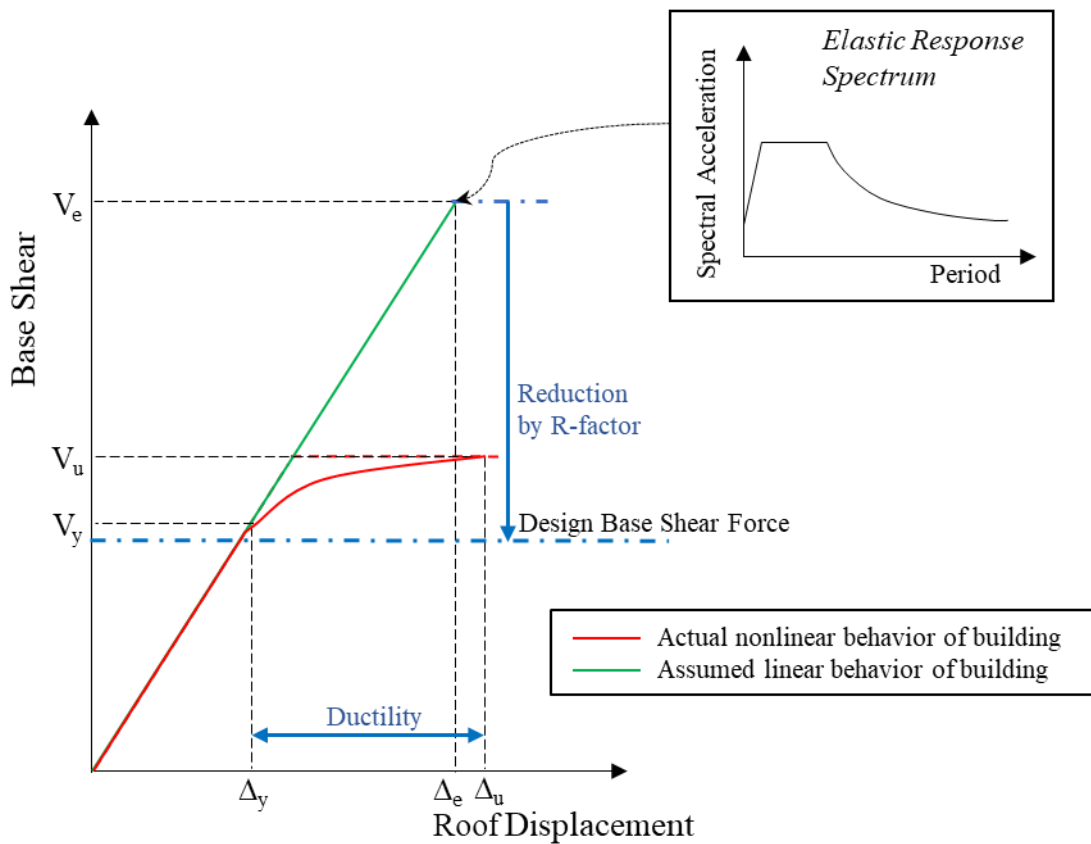


Figure 3-2 Design concept of the traditional force-based method

A similar load-displacement curve can be used to describe the various performance levels of a structure, as previously presented in Figure 2-3, in Section 2.3.3.2. However, absolute roof displacement values are not a direct and efficient measure of the global damage within a structure because structures in reality do not deform uniformly and concentrated damages may occur in certain stories depending on the structural properties and modes of vibration. Therefore, damage states are better related to the intensity of the seismic load by using other structural response quantities (engineering demand parameters) that have already established relations with damage. Inter-story Drift Ratio (IDR) is the chosen response parameter to be included in the proposed method because there is consensus in the literature that it best correlates to damage at the global level (Algan, 1982; Moehle, 1984; Gulkan and Sozen, 1999; and Aslani and Miranda 2005). IDR is defined as the relative lateral displacement between two successive floors normalized by the height between the floors. Figure 3-3 displays a typical performance curve using the inter-story drift as the response quantity that defines damage and performance levels.

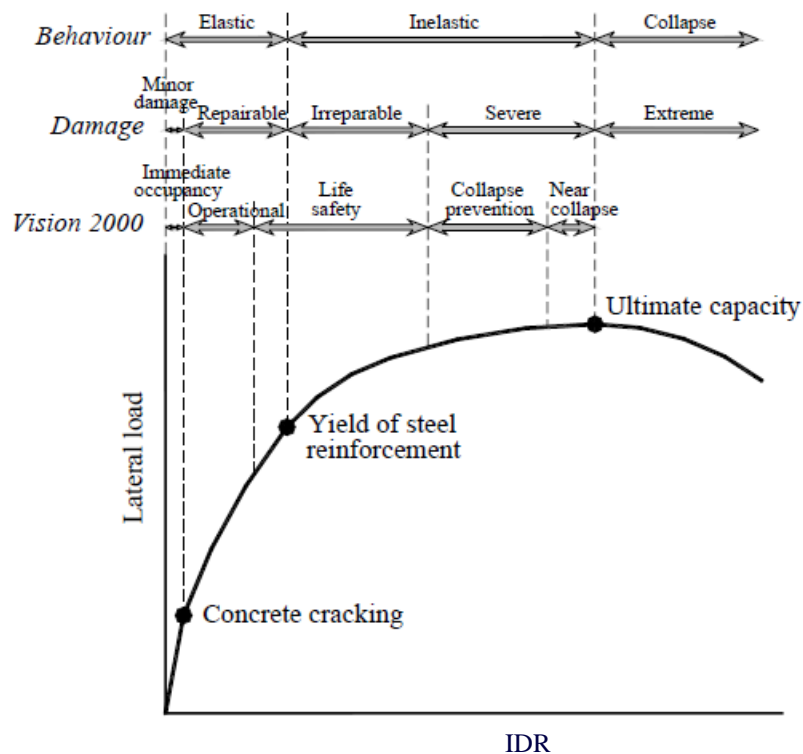


Figure 3-3 Typical performance levels of an RC structure with associated damage states (after Ghojarah, A., 2004)

The proposed design method aims to superimpose the concepts described by Figures 2-2 and 2-3, by developing a relationship between the maximum roof

displacement and the IDR at various performance levels, that can be used to calculate more rational values of the R-factor associated with different target performance levels employing Equation (3.1).

3.4 PROCEDURAL STEPS OF THE PROPOSED HFD METHOD

This section presents the steps of the proposed HFD design method. They are based on the procedure described by Tzimas et al. (2013) for steel frames after being appropriately adjusted for extension to the present case of RC MRFs, and are summarized as follows:

1. Definition of building attributes

Some building characteristics such as the number of stories, n_F , and the number of bays, n_B , are identified. Code's criteria for application of the FBD method are checked, for example, regularity in plan and elevation.

2. Selection of performance levels

Based on the stakeholders' requirements and the building functional use, the designer selects the appropriate design performance levels. According to the PBD philosophy, a performance level is defined by a pair of a post-earthquake damage and functional state objective and a level of seismic action. For example, a common multiple performance objective is Immediate Occupancy (IO) under the frequently occurring earthquake (FOE), Life Safety (LS) under the design basis earthquake (DBE) and Collapse Prevention (CP) when the building is subjected to the maximum considered earthquake (MCE). The spectral acceleration associated with the DBE (S_a)_{DBE} is the one given in seismic codes' elastic response spectrum, while those corresponding to the FOE and MCE, (S_a)_{FOE} and (S_a)_{MCE} respectively, can be estimated from (S_a)_{DBE} based on hazard studies.

3. Definition of performance criteria

Limiting values of the response parameter involved, i.e. $IDR_{\max i}$, associated with each damage level are identified (i). These limits can be based on performance-based guidelines for example FEMA-273 (1997a) or FEMA-356 (2000).

4. Estimation of the maximum roof displacement

Using the limiting values of IDR, the maximum roof displacement, $\Delta_{r,max}$, is estimated for each performance level “i”, using a relationship that will be developed in the subsequent chapters, given as:

$$(\Delta_{r,max})_i = f(\text{IDR}_{max\ i}, n_F, n_B, H) \dots \dots \dots (3.2)$$

where H is the total height of the building; IDR_{max} is the maximum inter-story drift ratio along the height of the building (for design purpose, it is set equal to the limiting values obtained in step 3); and n_F and n_B are defined in Step 1.

5. Elastic design under the FOE

Perform an elastic design of the frame with a force-reduction factor (R) = 1 only for strength requirement under the FOE, in order to obtain the resulting roof displacement as an estimate of the global yield displacement $\Delta_{r,y}$. Gravity load combination, capacity design rules, and code stipulations for stiffness reduction to account for cracking should be accounted for. Alternatively, empirical equations for estimating IDR associated with first yield of RC frames can be used, such as those developed by Priestley (2000) based on beams dimensions.

6. Calculation of the force reduction factor, R

Based on equation (3.1), the R- factor is calculated for each performance level “i”, using input from steps 4 and 5, as follows:

$$R_i = (\Delta_{r,max})_i / \Delta_{r,y} \dots \dots \dots (3.3)$$

where R_i represents the force reduction factor that will bring the elastic level spectral forces corresponding to the defined performance “i” to the design level forces. The most critical case will be the R_i resulting in the highest design level forces. In order to select the most critical (smallest) R-factor for various performance levels, one should convert the R-factor to its DBE equivalent, by multiplying it by the ratio of the spectral acceleration corresponding to the DBE, $(S_a)_{DBE}$, to the spectral acceleration corresponding to the concerned performance level. For example, in case of the 3-level performance objective stated in Step 2, the most critical R-factor (to be applied to the

code elastic response spectrum corresponding to the DBE) will be

$$R_{cr} = \text{The smallest of } (R_{LS}, R_{IO} \frac{(S_a)_{DBE}}{(S_a)_{FOE}}, R_{CP} \frac{(S_a)_{DBE}}{(S_a)_{MCE}}) \dots\dots\dots(3.4)$$

where R_{cr} is the most critical force reduction factor to be applied to the DBE; R_{IO} is the force reduction to be applied to the FOE to satisfy the IO performance level; R_{LS} is the force reduction factor to be applied to the DBE to satisfy the LS performance level; and R_{CP} is the force reduction factor to be applied to the MCE to satisfy the CP performance level.

7. Design of the structure

The chosen R_{cr} -factor is used to derive the design spectrum from the 5% damping elastic acceleration response spectrum provided in the code, then the base shear forces are calculated and distributed following the conventional force-based method and employing the same capacity and design rules.

3.5 DEVELOPMENT METHODOLOGY

The extension of the HFD design method to RC MRFS relies principally on the derivation of the relationship between maximum roof displacement and inter-story drift ratio (damage metric) in terms of some structural attributes as described by equation (3.2). This relationship should be based on appropriate modeling of the nonlinear behavior of concrete structures, in order to properly account for inelastic displacement behavior. Figure 3-4 summarizes the methodology undertaken in the subsequent chapters to develop such equations. First, prototype RC frame buildings with varying geometrical properties are selected for the study. Nonlinear time-history analysis is chosen to simulate the performance of these buildings under increasing levels of earthquakes. Based on limiting values of the damage metric chosen (IDR) which can be obtained from performance-based guidelines, the scale factor corresponding to the selected study performance levels are identified. The displacement response of the structures at the identified performance levels are post-processed and analyzed. The parameters affecting the maximum roof displacement relation to IDR are studied. Finally, nonlinear regression is performed, using the identified parameters as variables, in order to develop an estimate equation for the maximum roof displacement at various

performance levels. The estimate equation is converted to prediction charts that can be used in the context of the HFD design method, at Step 4 of the procedure described in the previous section.

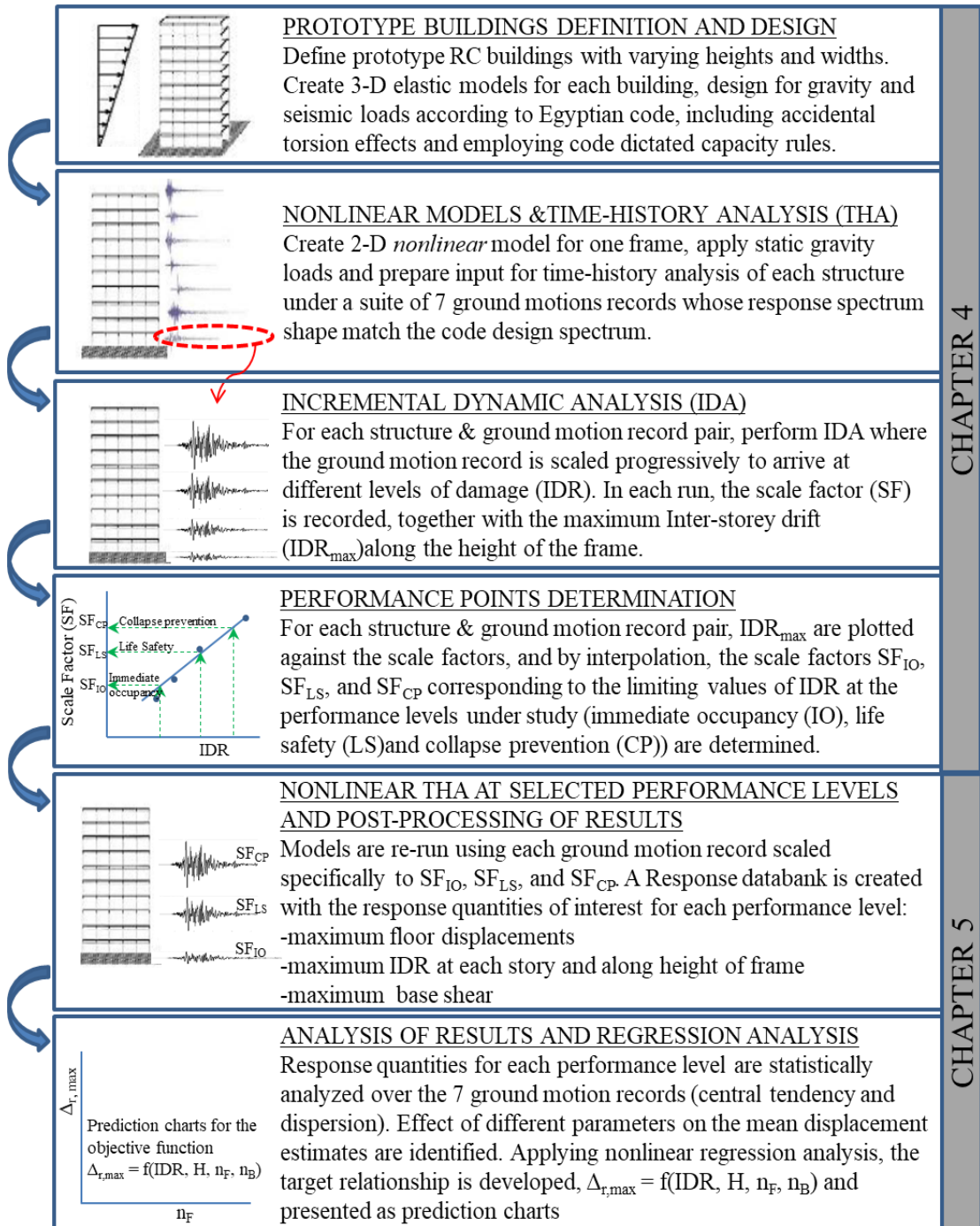


Figure 3-4 Flowchart for the methodology of development of displacement prediction equations for RC MRFs to be used in the context of the HFD design method.

Chapter 4

NONLINEAR TIME HISTORY ANALYSIS

4.1 INTRODUCTION

In order to be able to use the maximum roof displacement as a starting design variable in the context of the proposed HFD methodology, there is a need for development of relationships between roof displacement and damage potential for variable geometrical attributes and performance levels. Such relations should be independent of the frame sections to be used at the initial design stage. Analytical models are more suited for this purpose because otherwise full-scale models with varying parameters would be needed which would render experimental work prohibitively expensive. Also, simulation testing usually involves errors in estimating displacement because acceleration signals are measured and processed to arrive at displacement equivalents. Therefore, nonlinear time-history analysis remains the best approximation of reality when examining seismic displacement response. This chapter describes the methodology undertaken for numerical analysis. First, the prototype buildings chosen for study are defined with their geometry, structural system and design assumptions. Then, the analysis program used for time history analysis is presented with details of nonlinear modeling and assumptions, followed by the selection and scaling of ground motion records. Finally, the incremental dynamic analysis procedure is explained together with the output of this stage.

4.2 DESCRIPTION OF PROTOTYPE BUILDINGS

4.2.1 General Description and Geometrical Configuration

Nine prototype buildings, representative of the range of mid-rise building stock in Egypt, are selected to generate the displacement relations needed for application of the HFD method for RC structures. The buildings are assumed to have a constant floor height of 3.0 m and bay width of 6.0 m, with the number of floors and bays being varied as 4, 7 and 10 floors, and 3, 5 and 7 bays, respectively. The structural system chosen is moment-resisting frames (MRFs) since it reflects the type of concrete construction commonly used in Egypt, and as its design is generally more controlled by drift

limitations than shear wall systems or combined systems, and as discussed earlier, drift ratio is the response of interest in the proposed method. Office use and symmetrical square layouts are assumed to maintain generality in the developed findings. The prototype buildings' configurations and notations are summarized in Table 4-1, and their elevations are presented in Figure 4-1.

Table 4-1 Prototype Buildings' description and notation

Structure reference	Number of stories	Number of bays
F04B3	4	3
F04B5	4	5
F04B7	4	7
F07B3	7	3
F07B5	7	5
F07B7	7	7
F10B3	10	3
F10B5	10	5
F10B7	10	7

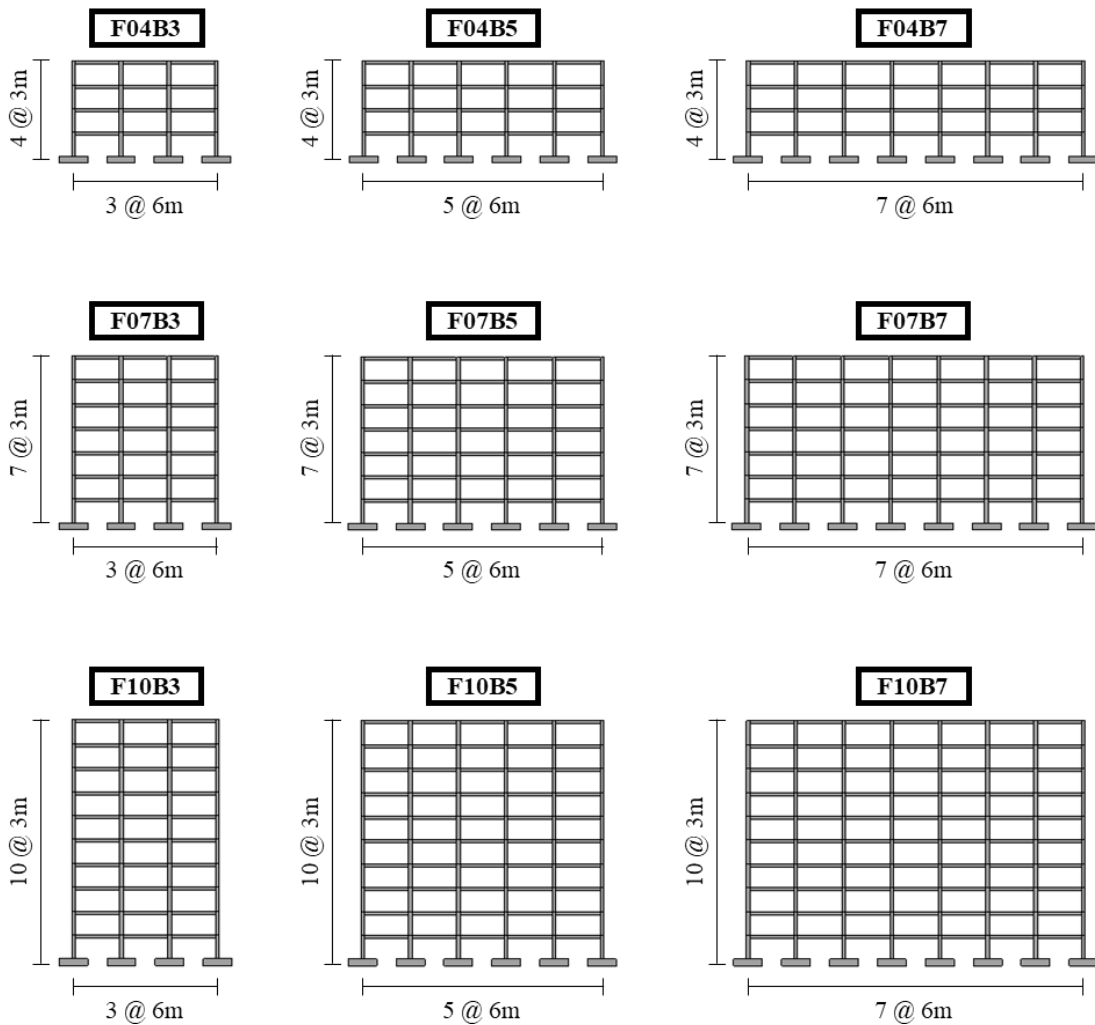


Figure 4-1 Elevations of the prototype frames

4.2.2 Design Details and Assumptions

The buildings are designed and detailed to resist combination of gravity and seismic loads, according to the Egyptian Code of Practice ECP-203 (2007), and ECP-201 (2012), which is fundamentally in line with the regulations of Eurocode 8 (EN 1998-1, 2004), a typical modern seismic code applicable to many countries with different seismicity, soil conditions, and construction practice. The buildings are assumed to reside in the highest seismic zone in Egypt (Zone 5B), with a peak ground acceleration (PGA) of 0.3g. The reason for the selection of this design peak ground acceleration, despite Zone 5B just covering secluded areas of the country, is to provide some generality in the results. This value would correspond to merely a medium seismic hazard in other highly seismic locations in the world like California in the United States. Also, choosing this high seismicity serves to magnify the seismic effects in order to attain significant difference between nonlinear and linear behavior.

For gravity loading, the considered dead load comprises the self-weight of the concrete structural elements, a typical floor finishing of 1.5 kN/m^2 , and weight of masonry infill panels of 120- and 250-mm thickness on interior and exterior beams, respectively with a density of 18 kN/m^3 . A live load of 3.0 kN/m^2 is also included. For seismic design, the lateral load resisting system is chosen as a space frame. The acceleration elastic response spectrum for shallow crustal earthquakes in non-Mediterranean areas is adopted known as Type 1 in ECP-201 (2012), and as Type 2 in EC8 (EN1998-1, 2004), for a "Soil Class C" which is soft soil, or dense or medium-dense sand, gravel or stiff clay as given in ECP-201(2012) and EC8 (EN1998-1, 2004). The design spectrum is scaled by an "Importance factor" of 1.2 to reflect the added conservatism for public office buildings. Based on the norm and know-how of reinforcement detailing in Egypt and many other countries with similar low-to-moderate seismicity, limited ductility frames are chosen and thus, a FRF with a value of 5 is used in the design. Characteristic material properties are utilized, and they are presented in Table 4-2 using units consistent with those that will be used in the program for nonlinear time-history analysis, as noted in Section 4.3.2.4.

Gravity and seismic loading are combined using the appropriate coefficients from ECP-203 (2007), so the buildings are designed to satisfy both of the following code's combinations:

$$U_1 = 1.4D + 1.6L \dots\dots\dots(4.1)$$

$$U_2 = 1.12D + \alpha L + S \dots\dots\dots(4.2)$$

Where

U : ultimate load

D: dead load

L : live load

S : Seismic load

α : live load factor representing the live load percentage existing during earthquakes and taken as 0.5 for public and office buildings.

The only capacity design rule applied is that resulting from the prescribed reduction in effective flexural stiffness of members where the stiffness reduction for beams (50%) is higher than that for columns (30%). All floors are assumed to have a solid rigid slab with a constant thickness of 150 mm, and columns are selected to have a square cross-section and to be symmetrically reinforced on the four sides, in order to have equal resistance to the changing direction of earthquake loading. The reinforcement is selected minimally according to the structural analysis and code requirements, to avoid overstrength and unnecessary margins reflecting personal designers' choices. Member cross-section sizes and reinforcements are summarized in Table 4-3,

Table 4-2 Properties of materials employed in design and time-history analysis

	Material parameter	Values used
Concrete	28d compressive cube strength, f_{cu}	25 N/mm ²
	Modulus of elasticity, E_c	22 kN/mm ²
	Poisson's ratio	0.2
Steel (36/52)	Yield strength, F_y	360 N/mm ²
	Ultimate strength, F_u	520 N/mm ²
	Modulus of elasticity, E_s	206 kN/mm ²

Table 4-3 Member dimensions and reinforcement of the prototype frames

Building	Floor #	Outer Columns		Inner Columns		Beams (width =250mm)		
		Size (mm)	Rein-forcement	Size (mm)	Rein-forcement	Depth (mm)	Top Rein-forcement	Bottom Rein-forcement
4-story	1-4	450	8 ϕ 22	600	16 ϕ 20	750	8 ϕ 18	4 ϕ 18
7-story	1-4	550	12 ϕ 20	650	16 ϕ 22	750	7 ϕ 20	3 ϕ 20
	5-7	450	8 ϕ 22	450	8 ϕ 22	650	7 ϕ 18	5 ϕ 16
10-story	1-4	650	20 ϕ 22	750	20 ϕ 22	750	7 ϕ 20	3 ϕ 20
	5-7	550	12 ϕ 22	650	16 ϕ 22	650	6 ϕ 20	3 ϕ 20
	8-10	450	8 ϕ 22	400	8 ϕ 20	600	7 ϕ 16	3 ϕ 18

The following are the assumptions considered in this design stage:

1. Floor diaphragms are sufficiently rigid relative to the lateral force resisting system, so they distribute the seismic load among the MRFs without significant deformation.
2. A change in sections of beams and columns every three stories has been adopted as a representative choice of concrete design practice.
3. Due to symmetry, only MRFs in the X-direction are studied and vertical accelerations are ignored.
4. Columns are designed for combinations of axial compression and moments due to the framing action, using the interaction diagrams.
5. Beam-column joint shear deformations are neglected.
6. Only torsion due to accidental eccentricity is considered due to symmetry.
7. Combined shear and torsion effect is neglected.
8. Lateral loads due to wind are not considered in the design.
9. Masses are distributed on structural elements following the dead load distribution.
10. Non-structural elements are fixed so as not to interfere with structural response.
11. No-second order effects (P-delta effects) are taken into consideration at the design stage (however they are considered in the nonlinear time history analysis presented in the sequel)

4.3 NONLINEAR TIME-HISTORY ANALYSIS

4.3.1 Theoretical Basis

Time history analysis (THA) is chosen for the numerical study because it uses real-representation of earthquakes in the form of ground motion time-history acceleration records as the applied loading, and therefore is considered the closest simulation of reality and actual structural loading. In THA, elements can be modelled as elastic (linear time-history analysis) or inelastic (nonlinear time-history analysis), with the latter being more rigorous, especially when employing materials of nonlinear nature like RC. Despite having the prospect of providing the most accurate results due to the realistic modeling of loading, the response (displacement or force) is typically sensitive to the choice of ground motion record applied and therefore several time-history runs are mandated for each structural analysis case, using different earthquake records. Also, because the procedure is considerably lengthy and complex, substantial effort and special precaution is required in the processing of input and output data.

Numerical-wise, THA provides the solution to the fundamental equation of motion, which defines the dynamic response of structures, at selected time steps for a defined duration, as given by

$$[M]\{a_t\} + [C]\{v_t\} + [K]\{u_t\} = -[M]\{1\}a_{gt} \dots\dots\dots(4.3)$$

where all variables containing the “t” subscript are time-dependent and are defined as:

- [M] = Mass matrix
- {a} = Acceleration vector
- [C] = Viscous damping matrix
- {v} = Velocity vector
- [K] = Structural stiffness matrix
- {u} = Displacement vector relative to the ground
- a_{gt} = Ground acceleration

The solution is incrementally repeated in an iterative process until equilibrium is achieved and then a step-wise numerical integration scheme is employed to solve the system of equations of motion at each time step (Chopra, 1995). The analysis time-step

is usually initially specified as the same time-step of the applied acceleration loading (a_g), and if convergence is not realized, the analysis time-step is repeatedly reduced. In case of nonlinear analysis, the stiffness matrix is revised at each solution time-step (so it becomes also time-dependent) to reflect any variation in stiffness at the material, section, member or structure level.

4.3.2 Analysis Program

In this study, the analysis and simulation platform of the Mid-America Earthquake Center (MAE), called “ZEUS-NL”, is selected for nonlinear THA. ZEUS-NL was developed at the Newmark Laboratories of the University of Illinois at Urbana-Champaign (Elnashai et al., 2003) specifically for earthquake engineering applications, and it was based on the analysis packages ADAPTIC (Izzuldin and Elnashai, 1989) and INDYAS (Elnashai et al., 2000) that were earlier developed at Imperial College in London. The stability and robustness of ZEUS-NL in its present or previous forms have been extensively tested by many researchers during the past 20 years, including among others the work by Izzudin (1991), Madas and Elnashai, (1992), Elnashai and Elghazouli (1993), Broderick and Elnashai (1994), Martinez-Rueda (1997) and Lee(1999) The finite element code has been further validated against full-scale test results (Jeong and Elnashai, 2005), and against SAP2000 (Elnashai et al., 2004). It has been also formerly validated by the author (Elkassas, 2010).

4.3.2.1 Pertinent features and advantages

Because the current study requires analytical models capable of capturing the nonlinearity of the structure under extreme dynamic reversed cyclic loading, the use of ZEUS-NL is deemed quite applicable since it is specially developed for large displacement analysis of complex frames considering the effects of both geometric and material nonlinearities. ZEUS-NL has the following relevant features:

1. Ability to apply constant or variable loading as forces, displacements or accelerations, at supports or at nodes, and varying proportionally or independently in the time domain.

2. Ability to represent the spread of inelasticity within the member cross-section and along the member length through utilizing the fiber approach, which is described in Section 4.3.2.2.
3. Ability to impose equilibrium in the deformed state of the structure and thus represent geometrical nonlinearity and P-delta effects.
4. Several analysis options including constant static loading, conventional pushover, adaptive pushover, eigen-value, linear and nonlinear time-history and incremental dynamic analysis, of two-dimensional and three-dimensional structures.
5. Ability to model really large structures, with thousands of nodes and elements.
6. Completely visual and efficient user-interface including model templates and views, tables, plots, animation of modes, deformed geometry display as well as cross-platform support with Microsoft Excel for database editing.
7. Expansive library of RC, steel and composite sections, and variety of well-tested material constitutive models, some of which used in the present work are discussed in Sections 4.3.4.1 and 4.3.4.2.

4.3.2.2 Nonlinear modeling approach

As mentioned earlier, ZEUS-NL uses the fiber analysis approach in modeling nonlinear behavior. This type of models, usually referred to as the *distributed plasticity* models, is considered a middle ground between the computationally efficient *lumped plasticity* models which represent inelasticity as a zero-length hinge with hysteretic properties, only at defined locations at ends of elements (for example SAP2000 and ETABS) and *continuum analysis* which monitors stress-strain behavior through every single point of the entire structure (for example ABACUS and ANSYS). The latter is unquestionably the most accurate and powerful modeling method; however, because of its excessive computational demand, and difficulty in applying time-varying loads, it is more suitable for modeling individual members or sub-assemblages or at the maximum overly simple structures (El Tawil and Deierlin, 1996). The fiber modeling approach is often the method of choice for research about large displacement analysis of frame structures in the inelastic range. Its reliability in predicting response that compares well

to experimental and full-scale tests has been reported by several researchers (e.g. Broderick, 1994; Pinho, 2000; Casarotti and Pinho, 2006).

In distributed plasticity models, cross-sections at specific integration points along the element length are divided into fibers where each fiber is associated with a uniaxial stress-strain relationship (constitutive model) for one material. The number of section fibers needs to be defined by the user and they usually range between 100 and 200. During the entire multi-step analysis, making use of the Euler-Bernoulli assumption that plane sections remain plane after bending, fiber stresses are calculated from the fiber strains considering the migration of the position of the section neutral axis during the loading history. Then, sectional stress-strain state in the form of moment-curvature relationship is obtained through the integration of the nonlinear response of the individual material fibers over the cross-sectional area, thus fully accounting for the spread of inelasticity across the whole section depth. This is followed by integrating the section's moment-curvature relationship along the length to obtain the moment-rotation response, thus simulating the distributed inelasticity along the member length. This discretization process is illustrated for an RC frame in Figure 4-2.

Some of the advantages of the fiber element method are that: it directly simulates interaction between axial force and bending moment; it does not need any prior moment-curvature analysis of members; and it automatically accounts for concrete cracking and growth in crack length, as well as gradual progression of steel yielding through the member cross sections and lengths. However, cracking is only considered to be smeared and normal to the member axis, due to the plane section assumption. Also, local buckling of steel reinforcing bars or steel webs and flanges can be reasonably modeled by using a steel constitutive model that degrades the structural properties of the steel elements when they reach a certain critical buckling stress.

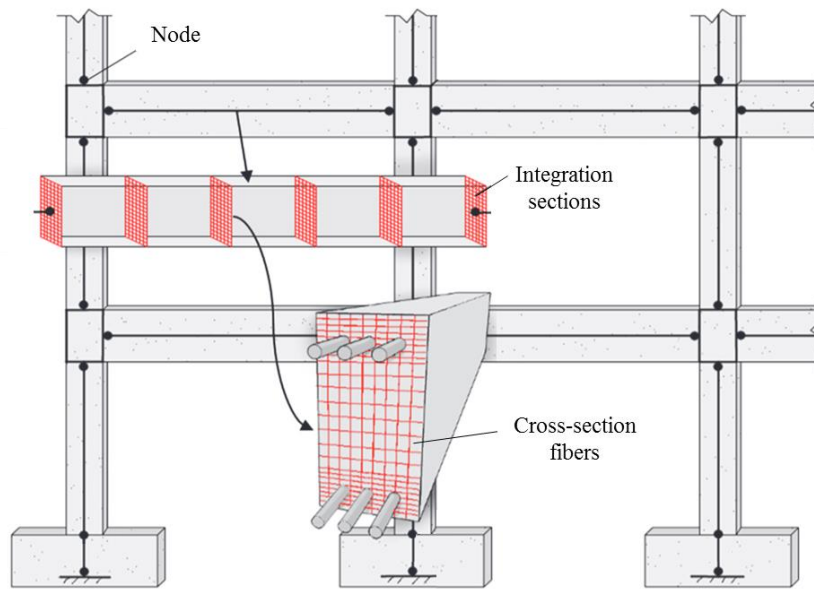


Figure 4-2 Fiber-element modeling of a reinforced concrete frame (after ATC, 2016)

4.3.2.3 The solver

This section briefly lists the algorithms used by ZEUS-NL for solution. For more information regarding the numerical details, the reader can be referred to the manual of the software (Elnashai et al., 2003).

1. Equilibrium solution iterative strategy can be full or modified Newton-Raphson iterative procedures, where convergence can be defined either based on force-moment or displacement-rotation criteria.
2. In time-history analysis, integration of the nonlinear equations of motions is performed either using the unconditionally stable Newmark time integration method or the Hilber-Hughes-Taylor algorithm (Broderick et al., 1994). The more common Newmark integration algorithm was employed in the present study.
3. Eigen-value analysis employing Lanczos algorithm for determination of natural frequencies and modes of vibration.

4.3.2.4 Limitations

The following are some limitations of ZEUS-NL, and the corresponding adjustments in modeling when applicable:

1. The program limits the user to only using the SI units of N-mm-sec.
2. Analysis may result in extremely large output files, sometimes more than 500MB, and may take up to 20 hours of runtime. Initial run time-step is usually specified the same as the ground motion record time-step, however if convergence is not achieved, the time-step must be reduced and thus results in long processing time.
3. Material constitutive models provided are based on the United States standard specimens for testing. Therefore, for example, the concrete compressive strength f_{cu} assumed in the study based on the cube tests (as of common practice in Egypt) had to be converted to its cylindrical counterpart, where the cylinder strength was considered 20% less than the cube strength following the specifications of the ECP- 203 (2007), resulting in cylindrical compressive strength (f_c) of 20 N/mm². This same value was used in the calculation of confinement factors in Table 4.5 for input to the confined concrete model.
4. The program uses only the classic displacement-based finite-element formulation (Hellesland and Scordelis, 1981; Mari and Scordelis, 1984) for fiber modeling, while it does not include the more recent force-based formulations (Spacone et al., 1996; Neuenhofer and Filippou, 1997). In a force-based frame element, beam section forces are expressed in terms of the nodal forces through force shape functions, without restraining the displacement field of the element and therefore this formulation is exact within the small-deformation Euler-Bernoulli beam theory. While in displacement-based elements, beam displacements are expressed as functions of the nodal displacements using imposed shape functions (usually cubic), which consequently means linear curvatures that is not quite accurate because in case of nonlinear materials the curvature can be highly nonlinear. This limitation is solved by using high discretization in the modeling of each structural element, thus increasing the number of global degrees of freedom, to be able to accept the assumption of linear curvature inside each sub-element.

5. The program does not have the option of applying distributed load. To overcome this, distributed gravity loads are converted to concentrated loads at several loading points on a beam. Employing the concentrated load equivalents factors presented in Table 5-16 of the LRFD of AISC (2001), three nodes are defined dividing each beam element into quarters and then equivalent point loads are calculated as shown in Figure 4-3 (Bai and Heuste, 2007). However, in case of masses definition, the number of masses is further lumped to be placed only at beam-column connections, in order to reduce the size of the mass matrix and thus save computational demand in dynamic analysis.

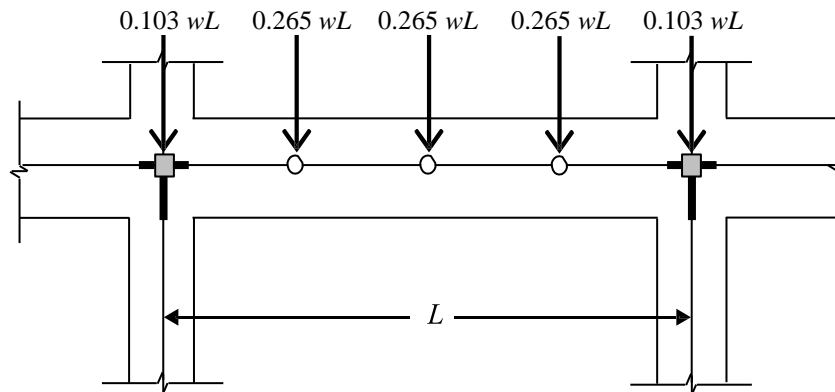


Figure 4-3 Equivalent point loads applied on beams

4.3.3 Modeling Assumptions

The following are the assumptions considered in conducting nonlinear THA:

1. Due to the symmetry of the buildings, only a two-dimensional frame for each prototype building is modelled to reduce the run time and simplify the post-processing of results.
2. The frames are assumed to be fixed at the foundation top level, therefore no soil-structure interaction is considered.
3. There is no history of nonlinear deformation where at initial conditions, displacement and velocities are zero.
4. Accidental torsional effects are ignored in THA

5. Masses are assumed to be lumped at beam-column intersections.
6. P-delta effects are included.
7. Beam-column connection is modeled without rigid links or shear joints. A study by Jeong and Elnashai (2004) validates this assumption, where they compared the results of ZEUS-NL numerical models of a moment-resisting RC frame having different combinations of rigid links and shear joints or none at all, to those from a full-scale experimental model, and proved the viability of the models with no rigid links in closely estimating actual experimental displacement results.
8. Shear deformation of members are ignored. This assumption is supported by a comparative study between experimental results and numerical models on the older form of ZEUS-NL, ADAPTIC, which proved that the effect of inclusion of shear modeling on the displacement results is quite minor for members controlled by flexure such as those employed in the present study, and therefore they can be ignored (Elnashai et al., 1999; Lee, 1999).
9. Modeling infill walls is not included in the nonlinear dynamic analysis, except for their masses considered. This decision is based on the following reasons: infill walls usually get damaged at low drift values and thus their contribution to stiffness stops at relatively low seismic action (Bertero et al., 1988); when infill walls alter the response of frames, it is usually in a quite unpredictable way that needs to be studied on a case-by-case basis based on their actual distribution; and the effect of infill walls is not as critical on the displacement behavior, which is the core of this study, as it is on the stress behavior, where they create stresses by acting as compression struts that impart loads to the frame.

4.3.4 Description of Nonlinear Model Input

The following sections describe the input data and details of creating the nonlinear model. A detailed description of available elements and material models in ZEUS-NL is beyond the scope of this study. Only the element formulations and material models pertinent to the present work are briefly presented when applicable.

4.3.4.1 Material models

i. Concrete model

In this study, it is chosen to use the uniaxial nonlinear concrete model (program reference name: con2) presented in Figure 4-4 due its balance of simplicity and accuracy. The model was implemented by Madas and Elnashai (1992) adopting the constitutive relationship formulated by Mander et al. (1988) which has been validated against experimental values and recommended by several researchers (Kappos et al., 1998); Rossetto, 2002). Additionally, it incorporates the improved cyclic rules proposed by Martinez-Rueda and Elnashai (1997) to predict the continuing cyclic degradation of strength and stiffness, and to achieve better numerical stability in case of large displacements analysis.

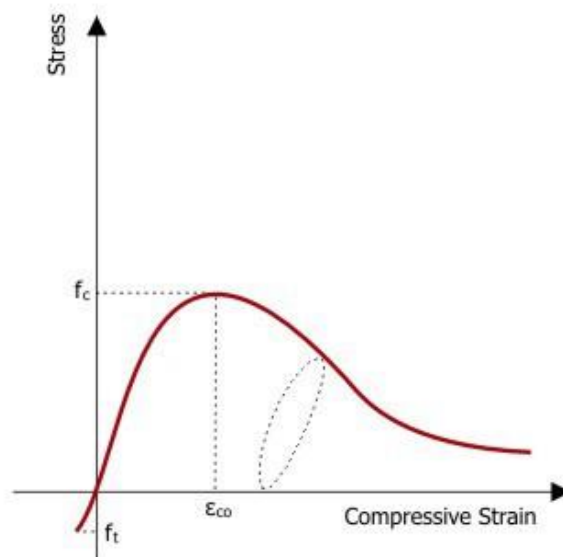


Figure 4-4 Uni-axial constant-confinement concrete material model

In the current study, each cross-section is defined by two separate concrete material models for the core concrete (confined) and cover concrete (unconfined). This model is valid for both confined and unconfined concrete, and for various cross-section shapes where it considers the increase in strength and ductility due to confinement. It assumes constant active confinement pressure throughout the entire stress-strain range, usually considered as the maximum confining pressure that occurs at yielding of transverse reinforcement. Four calibrating parameters are required: compressive

strength, tensile strength, crushing strain and a confinement factor that is introduced to scale up the whole stress-strain curve. The associated values used in this work to fully describe the concrete material model are tabulated as follows (Table 4-4).

Table 4-4 Input parameters for concrete uniaxial constant confinement model

Parameter	Description	Values used
f_c	Unconfined 28d compressive strength	20 N/mm ²
f_t	Tensile strength	2.2 N/mm ²
ϵ_{co}	Strain at peak stress	0.002 (mm/mm)
K	Confinement factor	1 (unconfined) Table 4-5 (confined)

The difference in stress-strain behavior between unconfined and confined concrete as described by Mander et al. (1989) is represented in Figure 4-5. The main effect of increasing confinement, as attained by providing closer-spaced transverse reinforcement, is increasing the strain capacity of members. This is attributed to delaying the buckling of longitudinal reinforcement and restricting the lateral expansion of concrete, which thus allow sustaining more compression stresses (Mwafy, 2001).

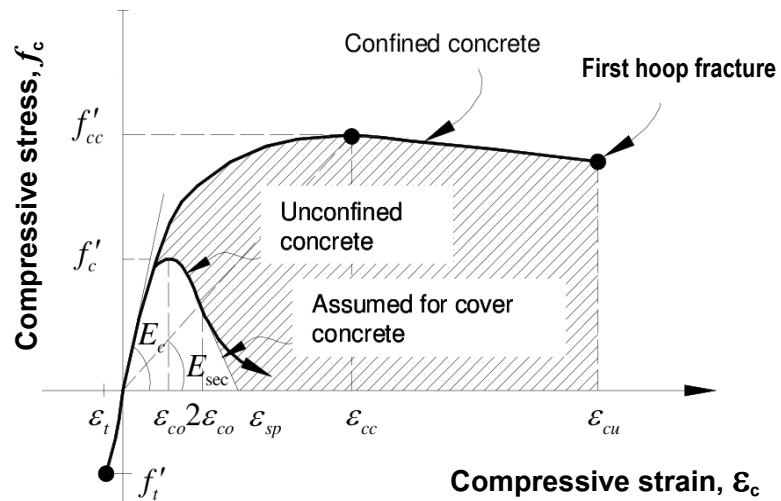


Figure 4-5 Unconfined and confined concrete monotonic stress-strain behavior (after Mander et al, 1989)

The confinement factor is defined as the ratio of confined concrete strength (f_{cc}) to unconfined concrete strength (f_c), and its calculation based on the arrangement of

lateral and longitudinal reinforcement is described hereinafter. Confinement factors are calculated for all columns according to the following steps, and the results are presented in Table 4-5 where they ranged between 1.19 and 1.44. Beams are assumed unconfined in all cases (confinement factor =1) due to the limited effect of transverse reinforcement of beams in improving flexural deformation.

STEP 1: The effective lateral confining stress (f_l) that can be developed at yield of the transverse reinforcement is calculated by:

$$f'_{lx} = k_e \cdot \rho_x \cdot f_{yh} \dots \dots \dots (4.4)$$

$$f'_{ly} = k_e \cdot \rho_y \cdot f_{yh} \dots \dots \dots (4.5)$$

in the x and y directions respectively, where:

ρ_x and ρ_y : are effective section area ratios of transverse reinforcement to core concrete cut by planes perpendicular to the x and y directions, respectively.

k_e : is a confinement effectiveness coefficient relating the minimum area of effectively confined core to the nominal core area bounded by the centerline of the peripheral hoops. This factor depends on the distribution of longitudinal steel and the resulting tie configuration and spacing. A typical value is provided by Pauley and Priestley (1992) as 0.75 for rectangular sections, which is used in this study.

f_{yh} : is yield stress of the stirrups.

STEP 2: When the concrete core is confined by equal lateral confining stresses (i.e. $f'_{lx} = f'_{ly}$) as is the case for the symmetrically reinforced square columns employed in this study, Equations (4.4) and (4.5) make one equation that defines f'_l , and the confined compressive strength of concrete is calculated as:

$$f_{cc} = f_c \left(-1.254 + 2.254 \sqrt{1 + \frac{7.94 f'_l}{f_c}} - 2 \frac{f'_l}{f_c} \right) \dots \dots \dots (4.6)$$

Therefore, the confinement factor is given by:

$$K = \left(-1.254 + 2.254 \sqrt{1 + \frac{7.94 f'_l}{f_c}} - 2 \frac{f'_l}{f_c} \right) \dots \dots \dots (4.7)$$

where:

f_{cc} : confined concrete strength

f_c : unconfined concrete strength

Table 4-5 Calculations of confinement factors of columns for model input

Building Reference	Floor	Column location	Column section	Dimension (mm)	Core Dimension (mm)	Spacing between stirrups (mm)	No. of stirrup legs	Transverse RNF area (mm ²)	ρ (10 ⁻³)	k_e	f_1	K
F04B3 F04B5 F04B7	1-4	Outer	Middle	450	392	200.0	8.00	402.1	5.1	0.75	0.92	1.29
			End	450	392	142.9	8.00	402.1	7.2	0.75	1.29	1.39
		Inner	Middle	600	542	200.0	8.00	402.1	3.7	0.75	0.67	1.21
			End	600	542	142.9	8.00	402.1	5.2	0.75	0.93	1.29
F07B3 F07B5 F07B7	1-4	Outer	Middle	550	492	200.0	9.33	469.1	4.8	0.75	0.86	1.27
			End	550	492	142.9	9.33	469.1	6.7	0.75	1.20	1.37
		Inner	Middle	650	592	200.0	8.00	402.1	3.4	0.75	0.61	1.20
			End	650	592	142.9	8.00	402.1	4.8	0.75	0.86	1.27
	5-7	Outer & Inner	Middle	450	392	200.0	8.00	402.1	5.1	0.75	0.92	1.29
			End	450	392	142.9	8.00	402.1	7.2	0.75	1.29	1.39
F10B3 F10B5 F10B7	1-4	Outer	Middle	650	592	200.0	8.80	442.3	3.7	0.75	0.67	1.22
			End	650	592	142.9	8.80	442.3	5.2	0.75	0.94	1.29
		Inner	Middle	750	692	200.0	8.80	442.3	3.2	0.75	0.58	1.19
			End	750	692	142.9	8.80	442.3	4.5	0.75	0.81	1.25
	5-7	Outer	Middle	550	492	200.0	9.33	469.1	4.8	0.75	0.86	1.27
			End	550	492	142.9	9.33	469.1	6.7	0.75	1.20	1.37
		Inner	Middle	650	592	200.0	8.00	402.1	3.4	0.75	0.61	1.20
			End	650	592	142.9	8.00	402.1	4.8	0.75	0.86	1.27
	8-10	Outer	Middle	450	392	200.0	8.00	402.1	5.1	0.75	0.92	1.29
			End	450	392	142.9	8.00	402.1	7.2	0.75	1.29	1.39
		Inner	Middle	400	342	200.0	8.00	402.1	5.9	0.75	1.06	1.33
			End	400	342	142.9	8.00	402.1	8.2	0.75	1.48	1.44

ii. Steel model

A bilinear (elasto-plastic) model with kinematic strain-hardening (program reference name: stl1) is employed in the current study to model the inelastic response of steel longitudinal bars of the RC beam-column elements. Using this simple bilinear uniaxial relationship have been demonstrated to correlate well with experimental results as verified by many researchers, for example Bursi and Ballerini (1996) and Salari et al. (1998). As depicted in the model in Figure 4-6, a linear function expresses the elastic range and unloading phase and is defined by a constant value which is the Young's modulus of steel. In the post-elastic range, a kinematic hardening rule for the yield surface is assumed and represented by a linear function of the initial stiffness (Elnashai and Elghazouli, 1993; Elnashai and Izzudin, 1993). Three input parameters are required to define this model and the associated values utilized in the present work are presented in Table 4-6.

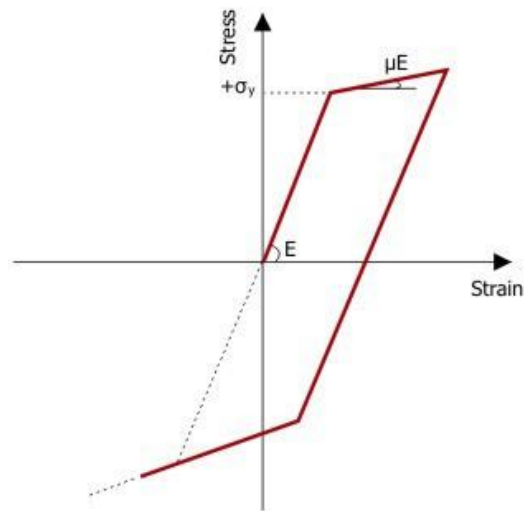


Figure 4-6 Uniaxial elasto-plastic steel model with kinematic strain-hardening

Table 4-6 Input parameters for uniaxial bilinear steel model with kinematic strain hardening

Parameter	Description	Values used
E	Young's modulus	205900 N/mm ²
σ_y	Yield strength	360 N/mm ²
μ	Strain hardening parameter	0.005

4.3.4.2 Cross-sections

The cross-sections of each element are defined based on their design details and the material models chosen, where confined concrete is used for the concrete core, unconfined concrete for the concrete cover, and steel for the reinforcing bars. In order to account for the slab contribution to beam stiffness and strength, all beam sections are modeled as T-section with effective flange width equals to threefold the slab thickness on each side, corresponding to the specifications of ECP-203 (2007) in case of seismic loading and amounting to 1.15m. Columns are modeled using square section. ZEUS-NL built-in section models rcts (RC T-section) and rrs (RC Rectangular section) are used to model beams and columns respectively as shown in Figure 4-7. Each structural member is modeled using several elements having different cross sections to reflect the change in reinforcement detailing along the member length, as previously presented in section 4.2.2. The cross-section definition covers the actual

arrangement of longitudinal reinforcement while the arrangement of transverse reinforcement is approximated through the confinement factor in the constitutive material model as discussed earlier. Figure 4-7 also illustrates the discretization of the cross-section into fibers at the material level. The accuracy of the model increases as the number of fibers discretization increases; thus, it was chosen to use 200 monitoring points per section to monitor nonlinear behavior.

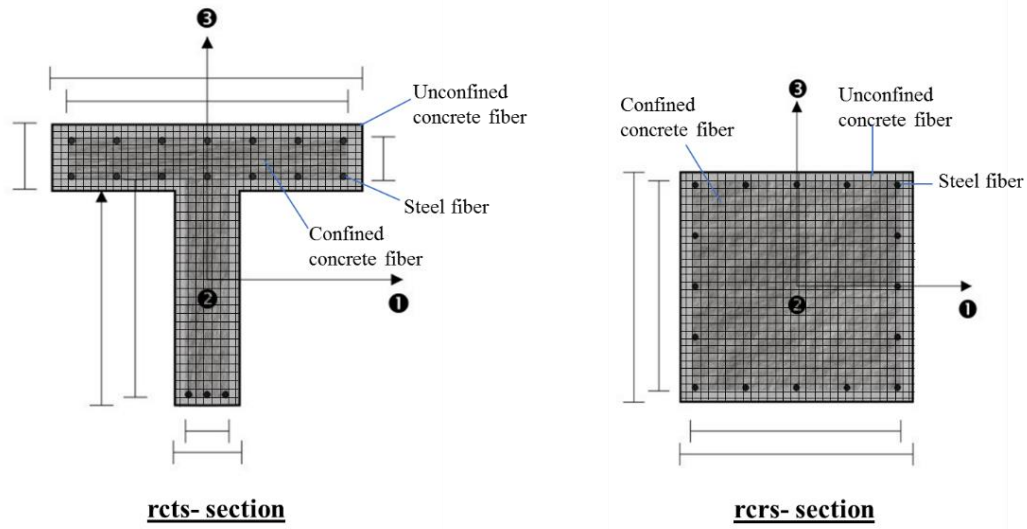


Figure 4-7 Cross sections used in modeling beams and columns

4.3.4.3 Element formulations

ZEUS-NL requires definition of three classes of elements for model building in case of THA. These are:

- Beam-column elasto-plastic element, to model frame elements
- Rayleigh damping element, to model viscous damping of the structure
- Lumped mass element, to model masses at beam-column joints

i. Beam-column elasto-plastic element

A 3-D cubic elasto-plastic element formulation is applied to model the spatial behavior of both column and beam elements accounting for inelasticity across element depth and length (Izzudin and Elnashai, 1993). As the name implies, this elasto-plastic

element utilizes a cubic shape function to provide the transverse displacement as shown in Figure 4-8, where this function is given by:

$$v(x) = \left(\frac{\theta_1 + \theta_2}{L^2}\right) x^3 - \left(\frac{2\theta_1 + \theta_2}{L}\right) x^2 + \theta_1 x \dots\dots\dots(4.8)$$

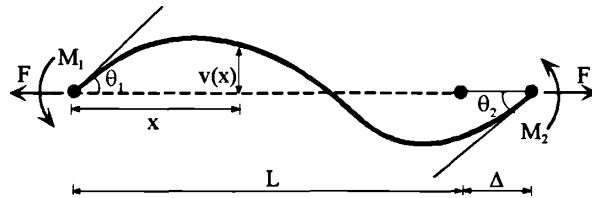


Figure 4-8 Forces and displacements of the cubic formulation for the beam-column element

For evaluation of the element forces and displacement, numerical integration of the cubic formulation equation is performed at two Gauss integration points whose location is depicted in Figure 4-9. The cross-section at each Gauss point is divided into a number of monitoring areas as discussed earlier, where the appropriate material constitutive model is applied, and strains and stresses are monitored and then integrated to model the response of the whole element cross-section and length employing the fiber approach as discussed in Section 4.3.2.2. Due to the limitation of the element having a displacement-based formulation as aforementioned in section 4.3.2.4, and also having just two integration points, short length elements are used in order to ensure reasonable accuracy in inelastic modeling.

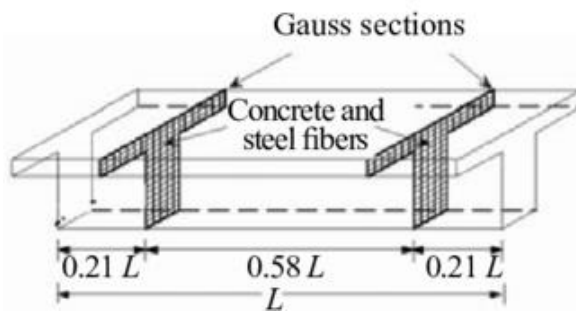


Figure 4-9 Locations of the two Gaussian sections

ii. **Rayleigh damping element**

Rayleigh damping elements are selected to model equivalent viscous damping in the structure which can result from friction in concrete opened micro-cracks and interaction of nonstructural elements. Although, this damping part is rather small

compared to the more important hysteretic damping due to inelastic behavior and yielding (which is already implicitly accounted for within the nonlinear material models which allows energy dissipation though cyclic loading), it is chosen to still employ some viscous damping in order to provide numerical stability, where the damping matrix results in stabilizing the system of equations of motion. It is chosen to model Rayleigh damping as only stiffness proportional, and without mass-proportional damping. This decision is supported by the work of Pegon (1996), Wilson (2001), Abbasi et al. (2004) and Hall (2006), which argued that mass-proportional damping generally causes excessively unrealistic energy dissipation when a structure is not sensitive to rigid body motion. Additionally, because the support of the building is not restrained in the direction of loading of earthquake, using mass proportional damping will lead to wrong results because it will be applied to the absolute velocity rather than the relative velocity.

For this end, stiffness-proportional Rayleigh damping coefficient is calculated based on the periods of the structure in the first two modes of significant mass participation (Chopra, 1995). Although the Egyptian Code of Practice ECP-201 (2012) provides the design spectrum based on 5% first mode critical damping, this percentage also indirectly comprises the effect of inelastic behavior, which is covered in the material models in nonlinear analysis. Smyro, Priestly and Carr (2012) has proposed using reduced damping ratio for the first-mode of vibration than the rest of the modes in order to avoid excessive unrealistic damping in the post-yield phase. A popular fiber-element THA program, Seismostruct (Seissoft, 2013), recommends using values of 4% and 6% in the first and second mode respectively. However, in the present study, for added conservatism, only 2% critical damping in the first mode is considered following the code provisions for wind load analysis in which structures are assumed to behave completely elastically, while 5% of critical damping is assumed in the second mode,

The Rayleigh damping element in ZEUS-NL requires input of two parameters: mass-proportional (α) and stiffness-proportional (β) damping coefficients. Since mass-proportional damping is ignored, its coefficient is input as zero, while the coefficient of stiffness-proportional damping is calculated following equation (4.9) (Clough and

Penzien,1993), and as presented in Table 4-7. It should be noted that the periods used in calculating the stiffness-proportional damping coefficient are based on un-cracked sections, because cracking and stiffness reduction is considered in the nonlinear analysis itself and thus only the initial stiffness is used in the damping parameters calculations

$$\beta = \frac{2\omega_i \xi_i - 2\omega_j \xi_j}{\omega_i^2 - \omega_j^2} \dots\dots\dots(4.9)$$

Table 4-7 Stiffness-proportional damping coefficients used in the prototype buildings

Building Reference	T ₁ (s)	T ₂ (s)	ω ₁ (rad/s)	ω ₂ (rad/s)	ξ ₁	ξ ₂	β
F04B3	0.451	0.147	13.93	42.68	0.02	0.05	0.00228
F04B5	0.442	0.143	14.22	43.86	0.02	0.05	0.00222
F04B7	0.438	0.142	14.35	44.11	0.02	0.05	0.00221
F07B3	0.749	0.292	8.39	21.49	0.02	0.05	0.00463
F07B5	0.745	0.295	8.44	21.32	0.02	0.05	0.00478
F07B7	0.744	0.295	8.45	21.26	0.02	0.05	0.0047
F10B3	1.015	0.392	6.19	16.05	0.02	0.05	0.00619
F10B5	1.005	0.396	6.25	15.86	0.02	0.05	0.00629
F10B7	1.001	0.399	6.28	15.76	0.02	0.05	0.00634

iii. Lumped mass element

Since the current work focuses on estimating structural global responses (like roof drift) rather than local stress state of members, masses are represented by lumped 2D mass elements at beam-column intersections in dynamic analysis, in order to reduce computational demand.

4.3.4.4 Nodes and mesh configuration

After defining the element classes, the mesh configuration of the model is addressed. Apart from the nodes required to define the geometry of the buildings, where each structural node is restrained out-of-plane and support nodes are fully fixed except in the direction of acceleration loading, additional nodes are required as follows:

- To allow application of equivalent gravity point loads, as discussed in Section 4.3.2.4 (point 5)
- To reflect changes in cross-section reinforcement along the member length
- To ensure proper discretization of each member into several short elements for accurate capturing of inelastic action by providing more elements near member edges where dissipative zones are expected, as explained earlier in Section 4.3.2.4 (point 4) and Section 4.3.4.3 (i).
- To define the orientation of local axis of elements, using one extra non-structural node for each element, therefore each element is designated using two structural nodes at its two ends, and one nonstructural node.

These meshing criteria resulted in modeling beams and columns employing 10 and 7 elements, respectively. Figure 4-10 presents the discretization in the F04B3 building as an example.

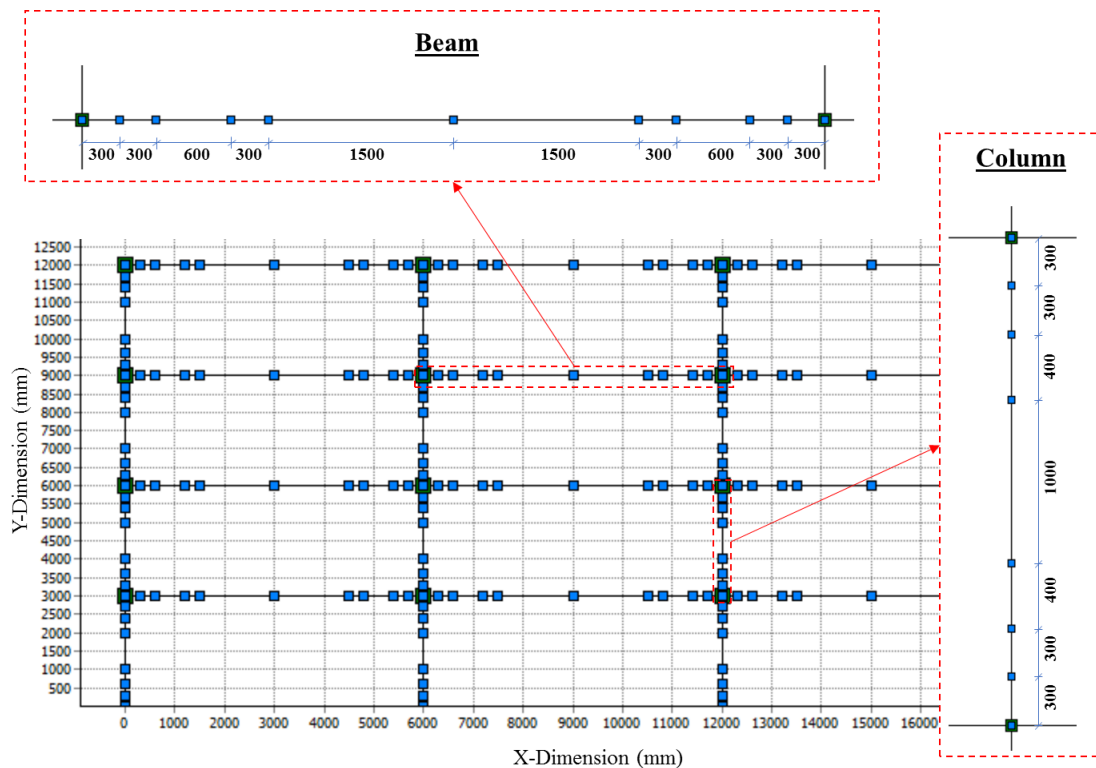


Figure 4-10 Meshing of the elements

4.3.5 Eigenvalue Analysis

Before conducting THA, eigenvalue analysis is performed to determine the periods and mode shapes of vibration of the prototype buildings. The analysis is done using the same model input files and element discretization (except for employing linear material models) so that it can additionally serve as a first insight into the validity of the analytical models before executing the rigorous nonlinear analyses, by showing their deflected shapes under free vibration. Two sets of modal analyses are performed, as follows:

1. Using cracked section properties, pursuant to the provisions of the Egyptian design code, ECP-201 (2012), where the stiffness of beams and columns is reduced by 50% and 30% respectively. The results are used for validation purposes and for comparing to the fundamental period values using the empirical formulae provided in the code.
2. Using uncracked section properties. The results are used for calculation of the parameters of the Rayleigh damping element as formerly explained in section 4.3.4.3 and presented in Table 4-7.

Cubic elastic elements (program reference name: stl0) with a cubic shape function for estimating transverse displacement is used which requires a single parameter input, the modulus of elasticity. This formulation accounts for geometric nonlinearities but doesn't account for material inelasticity. Code stipulated member stiffness reduction to account for cracking is accomplished by reducing the moduli of elasticity for each member with their respective factor, using the base concrete modulus of elasticity " E_c " predefined in Table 4-2. T-sections (symmetrical I or T section: sits) are used to model beams and square section "Rectangular solid sections: rss) to model columns, where the slabs contribution to beam stiffness and strength is reflected by the T-section effective flange width. The cross-sections and material properties employed are shown in Figure 4-11.

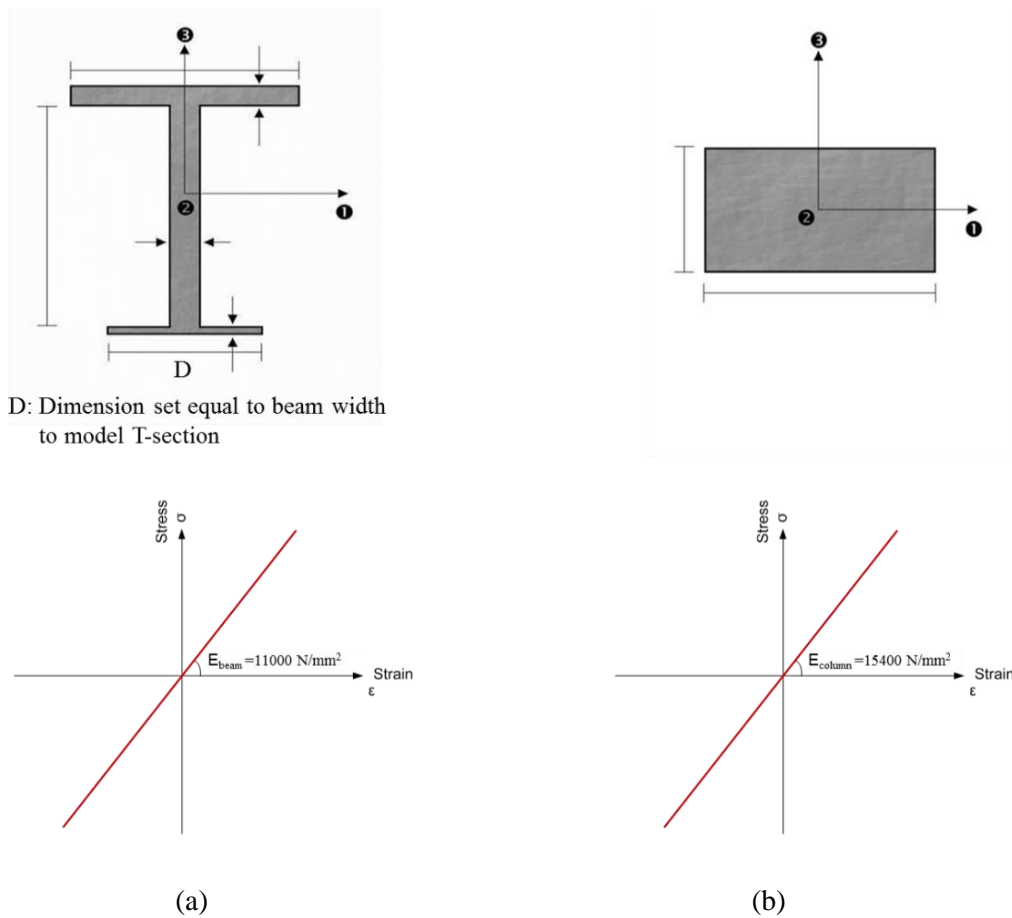


Figure 4-11 Elastic model cross sections and materials for (a) beams ;(b) columns

From the modal analysis, it is verified that all prototype buildings satisfy the regularity criteria provided by ECP-201 (2012) for application of the equivalent static load method for analysis, where they are regular in plan and elevation, and vibrate predominantly in the first mode with a period of less than any of $4.0 T_c$ (where $T_c = 0.25$ for soil Type C) and 2.0 seconds. A summary of the outcome of this modal analysis is shown in Table 4-8. Although the behavior of the frames is dominated by the first translational mode, there is some contribution of higher modes that increases with increasing height as indicated by the modal mass participation factor. It is clear that the periods are directly related to the height of the structure, where the longest period is for the tallest 10-story buildings while the shortest period is for the stiffest and shortest 4-story 7-bays building. The effect of the number of bays is quite insignificant. The periods resulting from the modal analysis are in general longer than that calculated using the code empirical equation (ECP-201, 2012) because cracked sections are used, and the effect of infill walls are ignored which results in overestimated periods.

Table 4-8 Modal Analysis Results

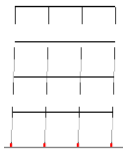
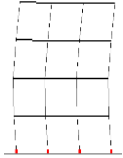
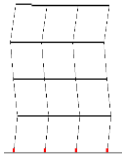
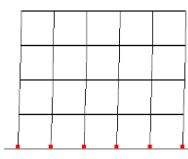
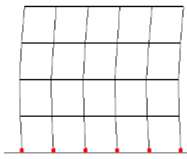
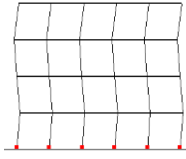
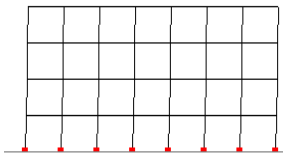
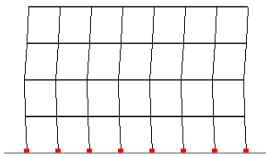
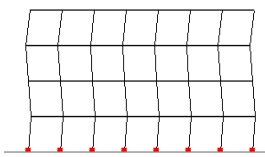
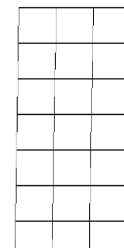
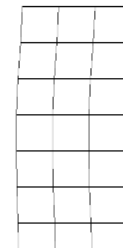
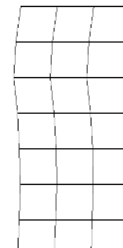
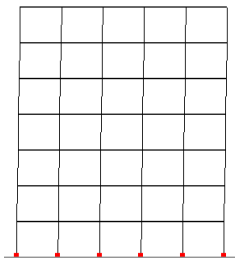
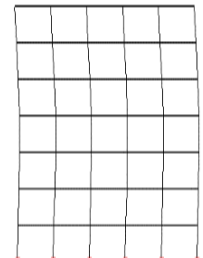
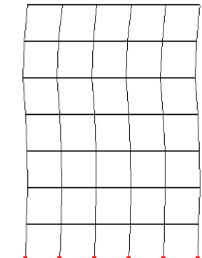
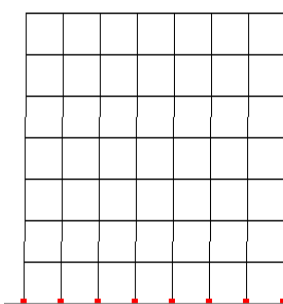
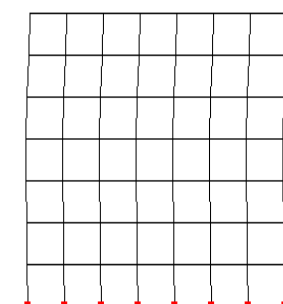
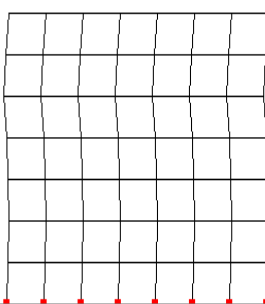
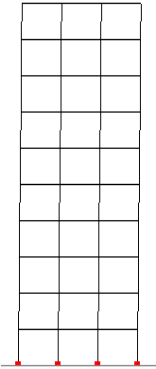
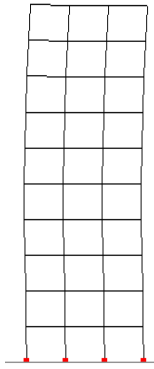
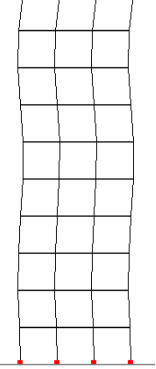
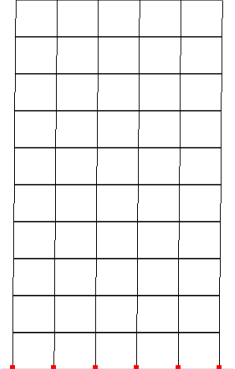
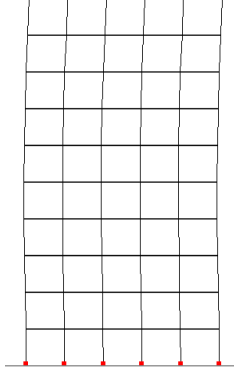
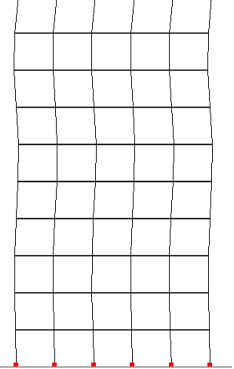
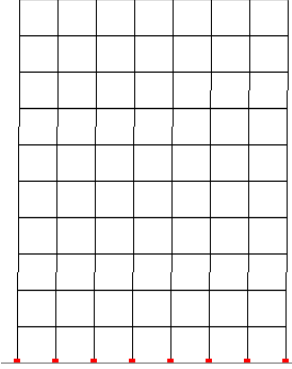
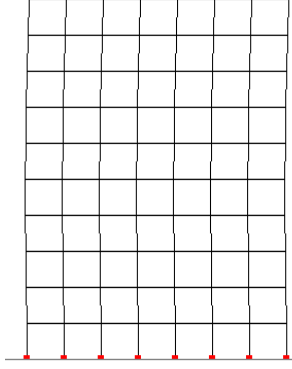
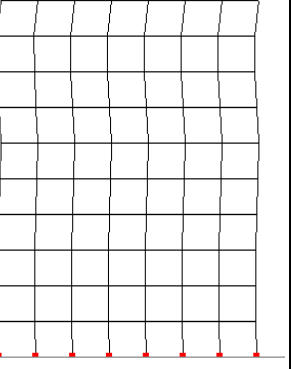
Building ($T=0.075H^{0.75}$)	Modal Period (sec) / Mass Participation Factor(%) Mode Shape		
	1 st mode	2 nd mode	3 rd mode
F04B3	0.582/ 95 	0.186/ 4.25 	0.106/ 0.79 
F04B5	0.57/ 95 	0.182/ 4.08 	0.103/ 0.74 
F04B7	0.565/ 95 	0.18/ 3.99 	0.102/ 0.71 
F07B3	0.969/ 92 	0.374/ 5.99 	0.204/ 1.29 
F07B5	0.965/ 92 	0.377/ 5.83 	0.207/ 1.23 
F07B7	0.964/ 92 	0.378/ 5.76 	0.209/ 1.2 

Table 4-8 Modal Analysis Results (continued)

Building ($T=0.075H^{0.75}$)	Modal Period (sec) / Mass Participation Factor(%) Mode Shape		
	1 st mode	2 nd mode	3 rd mode
F10B3	1.325/ 90 	0.503/ 7.25 	0.3/ 1.67 
F10B5	1.311/ 90 	0.509/ 7.06 	0.305/ 1.62 
F10B7	1.306/ 90 	0.512/ 6.97 	0.307/ 1.59 

4.3.6 Seismic Input and Selection of Ground Motion Records

The accuracy of the results of inelastic THA relies mostly on the competence of the employed earthquake representation. In order to properly benefit from the rigorous refined modelling approach endorsed in the present study, the seismic input must be

carefully selected. It is well established that structural response is highly sensitive to individual earthquake characteristics, therefore several ground motion records must be used for each prototype building model for effective assessment of seismic response. With interest in response induced from general earthquake loading for future code applications, the adopted approach for specifying seismic input for THA does not need to be strictly site-specific, and thus it is selected to use an ensemble of artificial accelerograms (acceleration time history ground motion records), with a single criterion which is compatibility of their 5% damped elastic spectra with the code spectrum used in the seismic design of the buildings over the period range of significance. Using artificial records provide the advantage of best fit to target spectrum as well as limiting the variability in results. In this study, it is opted to use a suite of seven ground motion records, and then to average the results pertinent to the provisions of ECP-201 (2012) for THA. The code also permits using only three ground motion records while considering the maximum of their results, nevertheless many researchers have pointed to the bias created when relying on the maximum response because it still reflects a single earthquake action.

Seven 20-seconds artificial accelerograms are generated using the program SIMQKE (Gasparini and Vanmarcke, 1976) such that their average matches the ECP-201 (2012) “Type 1” elastic response spectrum for soft soil class “Type C”. This software code constructs a time history record from a given spectrum by smoothing the spectrum and building a power spectral density function for it and then creating sinusoidal signals of random amplitudes and phase angles. The records are selected to have reasonable variability of frequency and energy content to reduce the bias in response. The software SEISMOSIGNAL (Seismosoft, 2008) is used to evaluate some of the characteristics of the generated records, where maximum acceleration to maximum velocity (A/V) ratio serves as an energy content indicator, and the earthquake predominant period, T_p , as a frequency content indicator. Characteristics of the records that have been used with their reference notation are given in Table 4-9, while their acceleration response spectra for 5% damping as matched to the code spectrum (Type (1) for zone 5B and soil type C) are shown in Figure 4-12. Figure A.1 in Appendix A depicts each separate unscaled artificial ground motion time-history record, with its corresponding 5% damped elastic spectrum as compared to the code spectrum.

Table 4-9 Characteristics of selected artificial ground motion records

Earthquake reference	Predominant period (T_p)	A_{max}/V_{max}
EQ1	0.26	11.2
EQ2	0.12	8.6
EQ3	0.2	13.9
EQ4	0.28	9.4
EQ5	0.18	11.8
EQ6	0.16	14.1
EQ7	0.22	10.5

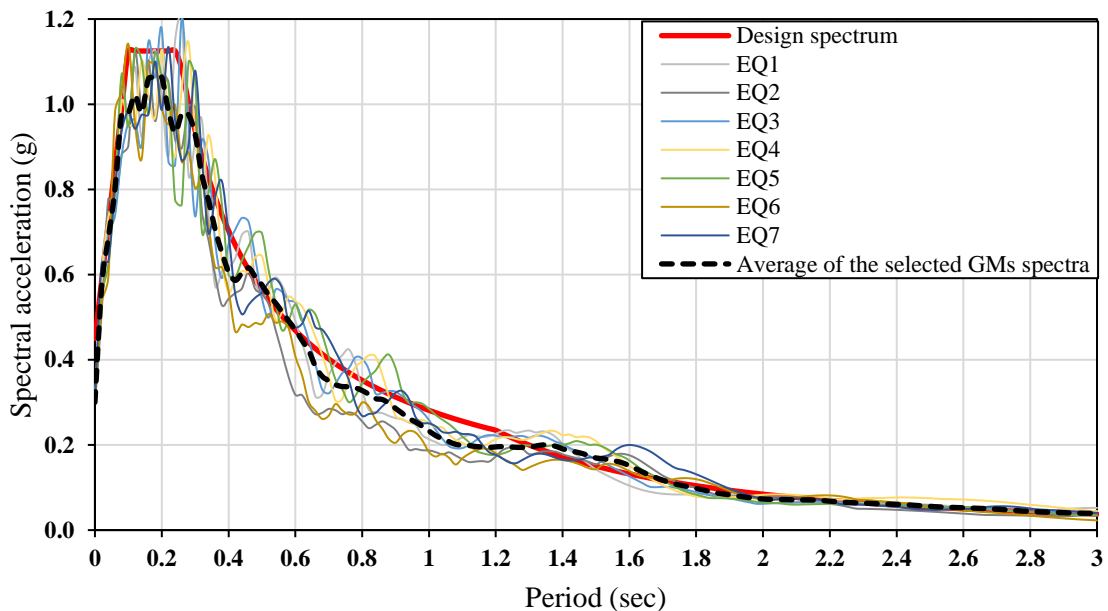


Figure 4-12 5% damped spectra of the selected artificial ground motion (GM) records compared with the target spectrum

For input in ZEUS-NL, the records are scaled by 9810 ($g \times 1000$) to be consistent with the program system of units and by 1.2 reflecting the importance factor ($\gamma_1=1.2$) used in design of buildings category III of public use. This approach follows the recommendations of ECP-201 (2012) and EC8 (EN1998-1, 2004) in including the importance factor in scaling the records themselves rather than the elastic response spectrum used in generating the records. It should be noted that the records scaled by the importance factor are considered the base case i.e. Scale factor=1, when performing incremental dynamic analysis described hereinafter.

4.4 INCREMENTAL DYNAMIC ANALYSIS

In order to derive maximum displacement expressions for RC frames corresponding to different levels of performance, it is required to study each prototype structure under various levels of seismic actions to investigate the factors that influence its maximum displacement pattern. This type of parametric analysis involving the extension of a single nonlinear THA into an incremental one by progressively scaling the seismic load is generally referred to as “Incremental Dynamic Analysis” (IDA). The scaling interval and limit is selected to adequately push the structure through the entire range of behavior under study, from elastic to inelastic and finally to collapse (or close to collapse). IDA concept has been first mentioned by Bertero (1977), and then has been developed in different ways by many researchers including among others, the work of Bazurro and Cornell (1994), Mehanny and Deierlein (2000), Nassar and Krawinkler (1991), and Psycharis et al. (2000). Lately, it has been established by the U.S. FEMA guidelines as the state-of-the-art method to determine global collapse capacity and nowadays for studying the change in nature of structural response as the intensity of ground motion increases. Appropriate postprocessing can present the structural response results as IDA curves, for each ground motion record, of the structural response parametrized by a seismic intensity level. According to the terminology used in next-generation Performance-based Earthquake Engineering guidelines, as depicted in the PEER framework in Figure 2-5 in Section 2.2.32. of Chapter 2, the structural response is measured by an engineering demand parameter (EDP), while the seismic intensity level is represented by an Intensity Measure (IM). Therefore, the resulting IDA curves are representation of IM versus EDP. The selected IM and EDP are discussed in the following sections.

4.4.1 Intensity Measure and Scaling

In Incremental dynamic analysis, possible choices for the Intensity Measure are the peak ground acceleration (PGA), peak ground velocity (PGV) and the 5%-damped spectral acceleration at the first-mode period of the structure ($S_a(T_1)$). The latter is the most widely used IM measure used to scale the ground motion by multiplying its amplitude by a constant scalar factor necessary to reach a target spectral acceleration

level at the fundamental natural period of the structure (Shome et al., 1998; Bradley et al., 2008). However, $S_a(T_1)$ has a major deficiency when used in analysis involving high excursion into the inelastic response range, where it does not consider the elongation of the first modal period of vibration as a result of nonlinear behavior. Also, it has been proved by Shome et al. (1998) that the use of $S_a(T_1; 5\%)$ as IM is only more consistent than other IMs when used in analysis of simple structures represented by a single-degree-of-freedom system.

Due to the aforementioned reasons and additionally because relative spectral matching at all periods is closely achieved during the generation of the spectrum-compatible records which eliminates the needs to provide separate scaling factors for each different height building depending on its fundamental period, it is chosen to use the peak ground acceleration (PGA) as the IM in the present study in order to scale the accelerograms for IDA. Peak ground acceleration (PGA) is considered the most important IM from a structural point of view because the resulting inertia forces in a structure are directly proportional to the acceleration, according to Newton's Second Law. And till present PGA is the key aspect of definition of seismic hazard in most seismic design standards including the ECP-201 (2012), where it represents the first point on the elastic design response spectrum.

PGA is measured as the maximum absolute amplitude on a recorded or synthetic accelerogram. In order to be used for scaling, at each incremental step i of analysis, each record is simply multiplied by a scale factor $SF_i = a_i / a_1$, where a_i is the PGA of ground motion record used in the analysis, and a_1 is the PGA of the original unscaled earthquake record. Therefore, a $SF = 1$ means the analysis is using the unscaled accelerogram, $0 < SF < 1$ a scaled-down accelerogram, and $SF > 1$ a scaled up accelerogram.

4.4.2 Engineering Demand Parameter

An Engineering Demand Parameter (EDP) can be either “direct” responses, that are extracted straight from analysis such as the maximum inter-story drift, peak story displacement, and peak floor accelerations, or “processed” using several response values from analysis like many damage indices available in the literature as reviewed

by Whittaker et al. (2004). EDP can also be categorized into local parameters, for example, strain, moment, curvature, and global parameters, again like maximum inter-story drift and base shear. Global damage criteria and EDP are considered in the current work because the force reduction concept used in design is based on response at the structural level. The Inter-story Drift Ratio (IDR) is the damage metric that is chosen to be included in the proposed design method and thus is the response parameter used in IDA. The computed maximum IDR at each IM scale factor can be plotted together with the associated IM in order to develop IDA curves. This EDP can also be checked against established acceptance criteria related to performance as explained in the next section.

4.4.3 Definition of Seismic Performance Levels

In order to identify the factors that affect the maximum displacement at various levels of seismic action, certain levels of performance must be preselected and defined for studying their associated response. Three discrete structural performance levels corresponding to three major damage and functional states are investigated in the present work, following the definition of the guidelines of FEMA-356 (2000) previously discussed in Section 2.2.3.2 under the second-generation procedures, and reiterated herein:

1. Immediate Occupancy (IO) level, at which the structure is safe to be occupied immediately after the associated seismic event and repairs are minor, i.e. negligible damage.
2. Life Safety (LS) level, at which the structure remains stable and has significant reserve capacity at the associated seismic event, and hazardous nonstructural damage is also controlled to ensure life safety.
3. Collapse-Prevention (CP) level, at which the structure is barely standing after the associated seismic event, i.e. most severe damage before collapse.

Although this categorization of performance levels is based on the currently prevailing procedures of PBSD procedures (second-generation), it can be easily extrapolated for application in the next-generation procedures, where the performance measures advocated such as casualties, repair and replacement costs can be quantified

based on damage using loss models (FEMA, 2006). Limiting values for the chosen EDP, which is IDR, can be assumed, following the acceptance criteria specified in the FEMA-356 document (2000), and presented in Table 2-2. Therefore, the upper limits of IDR used for definition of the IO and LS performance levels are selected as 1% and 2%, respectively. The IDR for the CP level is chosen as 3% (less than the 4% stipulated by FEMA 356) for added conservatism in the global failure criteria as proved by several previous studies (Broderick and Elnashai, 1995; Kappos, 1997).

4.4.4 IDA Analysis Procedure and Results

For the purpose of IDAs performed herein, the following procedure is repeated for each pair of one structure and one accelerogram, in order to develop IDA curves and create a response databank with the post-processed results at the study performance levels.

1. Multiply the accelerogram with the initial SF_1 , which is taken as the reciprocal of the FRF used in design ($FRF = 5$); therefore $SF_1 = 0.2$.
2. Run nonlinear dynamic analysis with the ground motion record acceleration set as $a_i = SF_1 \times PGA_{design} (0.3g)$, where i represents the run number.
3. Extract nodal displacements and calculate at each time increment of the accelerogram:
 - The instantaneous story drift ratio $(SDR_{in})_j$ calculated as the maximum absolute difference between the lateral displacements of the two column ends, divided by the story height, for each story level (j).
 - The instantaneous roof displacement $(\Delta_{r,in})$ calculated as the maximum absolute difference between the lateral displacement of the roof and the base.
4. Over the entire length of the ground motion record, calculate:
 - The maximum story drift ratio $(SDR_{max})_j$ for each story (j) at any instance of all $(SDR_{in})_j$.
 - The maximum inter-story drift ratio (IDR_{max}) as the maximum of all $(SDR_{max})_j$ for $j=1$ till n_F , where n_F is the number of stories.
 - The maximum roof displacement $(\Delta_{r,max})$ at any instance of all $(\Delta_{r,in})$

5. A reasonably small increment of 0.2 is chosen for progressively increasing the scale factors. Therefore, the new scale factor is computed as: $SF_{i+1} = SF_i + 0.2$. This is equivalent to having a PGA increment of 0.06g (0.2x 0.3g).¹
6. Repeat steps 2 to 4 until the $(IDR_{max})_i$ is greater than or equal 3%.
7. Plot the SF_i versus $(IDR_{max})_i$ and by linear interpolation, determine the scale factors SF_{IO} , SF_{LS} , SF_{CP} corresponding to the three following predefined performance levels (respectively):
 - IO when IDR_{max} equals to 1%
 - LS when IDR_{max} equals to 2%
 - CP when IDR_{max} equals to 3%
8. Re-run the model using SF_{IO} , SF_{LS} and SF_{CP} and check that the IDR_{max} properly corresponds to the selected performance levels. If the target IDR_{max} is not achieved, interpolation is repeated, and scale factors are corrected until reaching the specified limits of IDR_{max} for the three study performance levels. In other words, for each pair of structure and accelerogram, three scale factors are identified for running the models.

The resulting IDA curves for all prototype frames are presented in Figures 4-13 to 4-15². It should be noted that the number of dynamic analyses for each frame (as depicted on each graph bordered title) differs based on the number of runs required in the interpolation for reaching the exact IDR limiting values associated with the objective performance levels. The whole computational volume is in the order of 1750 nonlinear THA runs. The resulting scale factors serve only to provide separate values of the earthquake intensity associated with the study performance level for each structure-accelerogram pair. The subsequent chapter will make use of statistical analysis of the THA results at those specific performance levels, in order to develop the relationship between displacement and the target performance.

¹ In some cases, for added efficiency, a smaller or larger increment than 0.2g is used when it can be predicted that it will be closer to reaching the IDR associated with the defined performance level.

² IDA curves are presented in terms of the SF rather than the intensity measure (PGA) for simplicity and because the only objective is determining the scale factors corresponding to the study performance levels, and no hazard matching is performed.

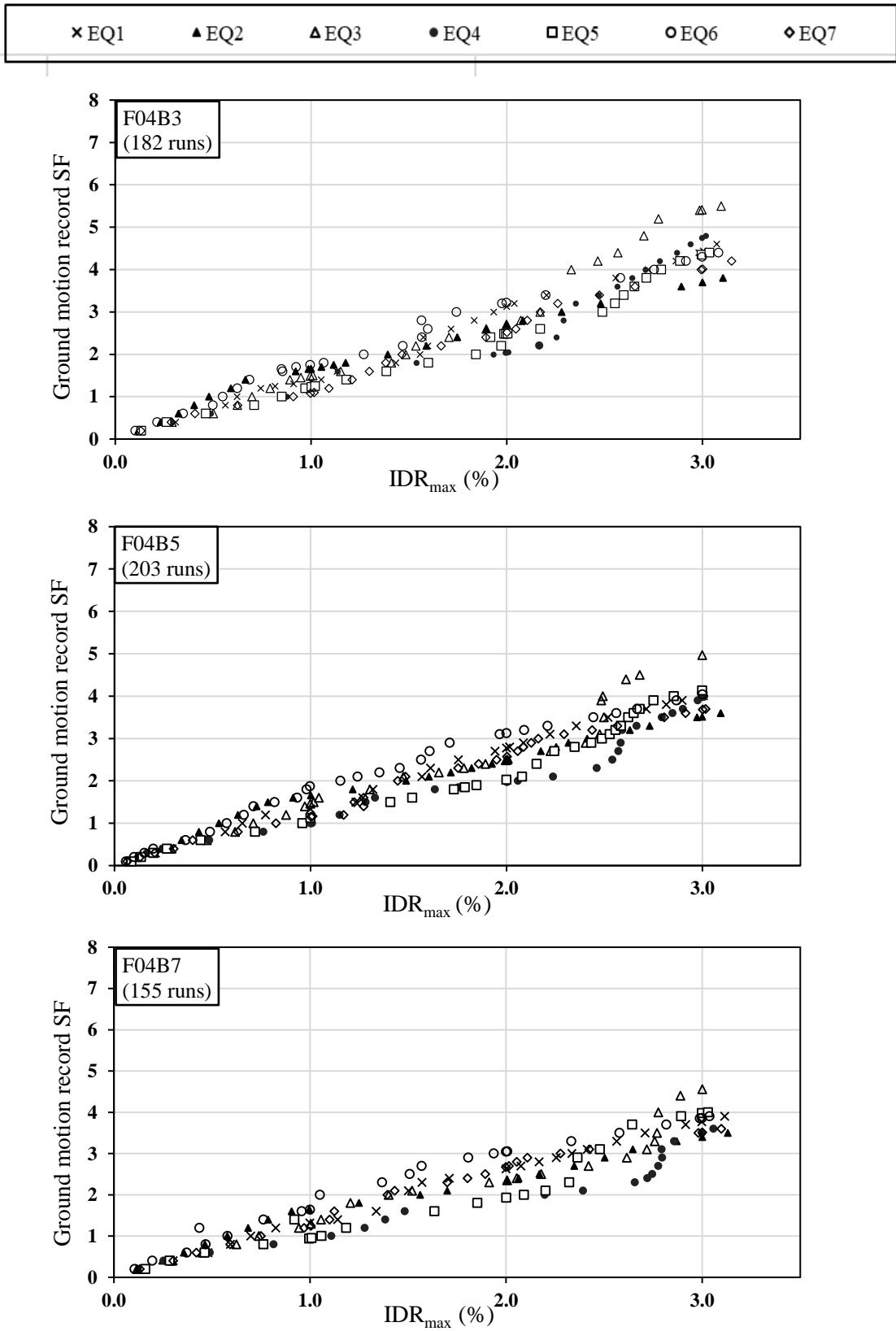


Figure 4-13 Incremental dynamic analysis results for the 4-story frames relating the maximum IDR (damage level) with the scale factor (SF) of each earthquake record

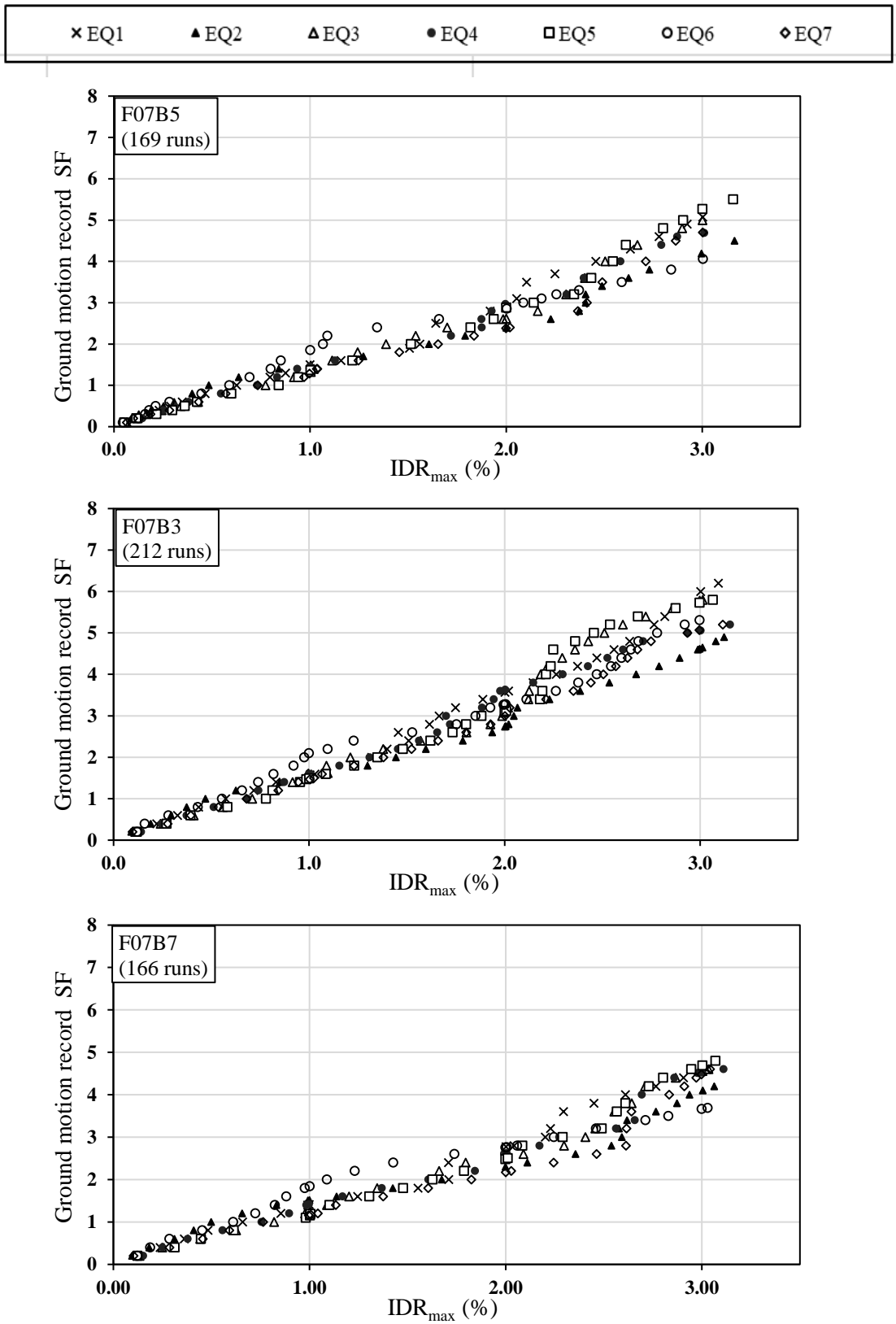


Figure 4-14 Incremental dynamic analysis results for the 7-story frames relating the maximum IDR (damage level) with the scale factor (SF) of each earthquake record

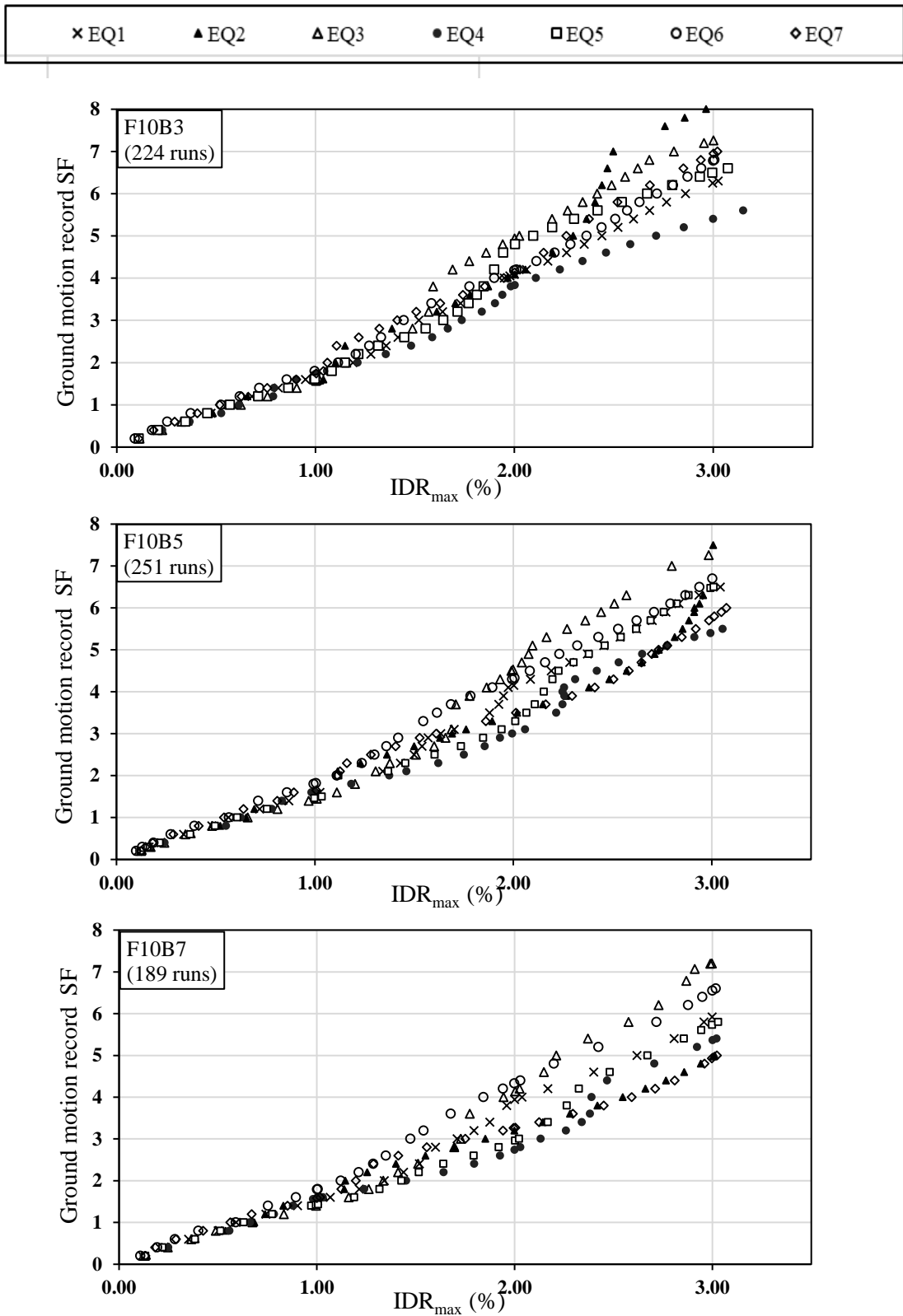


Figure 4-15 Incremental dynamic analysis results for the 10-story frames relating the maximum IDR (damage level) with the scale factor (SF) of each earthquake record

Chapter 5

PERFORMANCE-BASED DISPLACEMENT ESTIMATE

5.1 INTRODUCTION

Based on the methodology of numerical analysis previously discussed and the determined ground motion intensity corresponding to the limits of the predefined study performance objectives, this chapter serves to present and analyze the displacement results specifically at these performance levels. The height-wise distribution and amplitude of deformation demands at the various damage levels of the frames are studied. Then, the factors that most affect the roof displacement values are determined. Using nonlinear multiple regression analysis, prediction equations are developed for the maximum roof displacement in terms of the determined governing factors and its incorporation into the HFD design method is briefly discussed.

5.2 DISPLACEMENT PROFILES AT THE STUDIED PERFORMANCE LEVELS

In addition to the post-processed results from Section 4.4.4, all story absolute displacements are monitored at the occurrence of each damage limiting value, in order to study the frames' displacement patterns. The story drift profiles and deformed shapes of each prototype frame are shown in Figures 5-1 to 5-3, where the individual records responses are presented as markers, and the mean value (averaged over the 7 ground motion record cases) are indicated only as lines for clarity. For the 4-story frames in Figure 5-1, a pure shear-type deformation behavior can be clearly observed. Because the design of those shorter buildings is controlled by gravity rather than seismic loading, the flexural stiffness of the beams compared to that of columns are large enough to result in pure shear-deformation, in which columns' deformation in each floor is mainly in double curvature bending and the lower floors' deformation contributes highly to the overall top displacement. However, as the building height increases for the 7-story and 10-story frames in Figures 5-2 and 5-3, flexural-type behavior (like a cantilever's deformation) can be depicted near the lower stories due to the significant axial deformation of the columns carrying the whole building, then the lateral deformation changes back to overall shear-type behavior at higher floor levels, when the axial load

levels out. These observations are typical of well-designed low- to medium- height moment frame buildings. The number of bays does not have any effect on the displacement shape, while only slightly diminishing the amplitude of displacement demand with increasing number of bays. The contribution of higher modes of vibration is particularly evident in the displacement shapes of higher buildings, due to the larger mass vibrating in these modes as evidenced by the participation ratios formerly presented in Table 4-8.

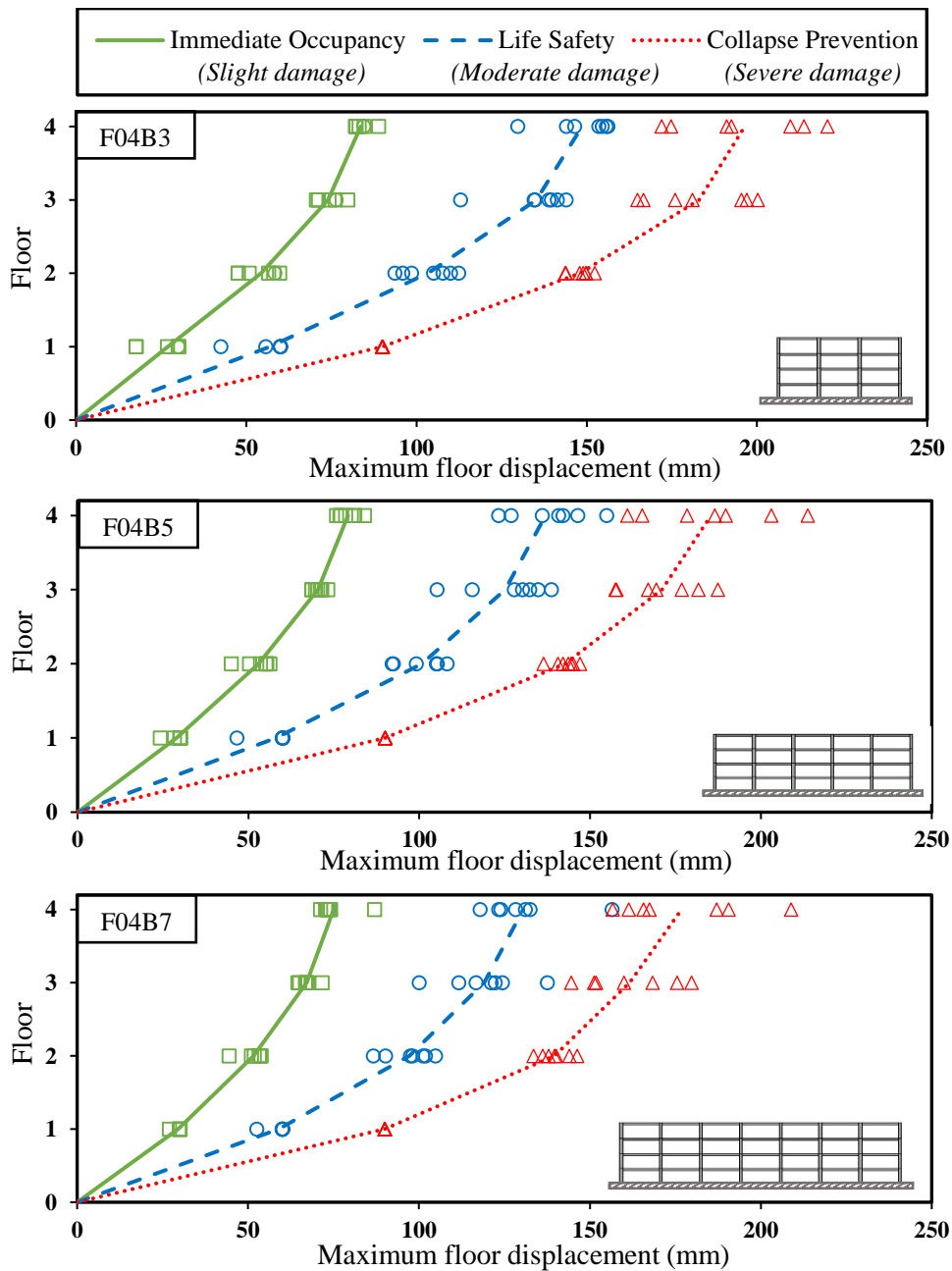


Figure 5-1 Displacement profiles of the 4-story prototype frames

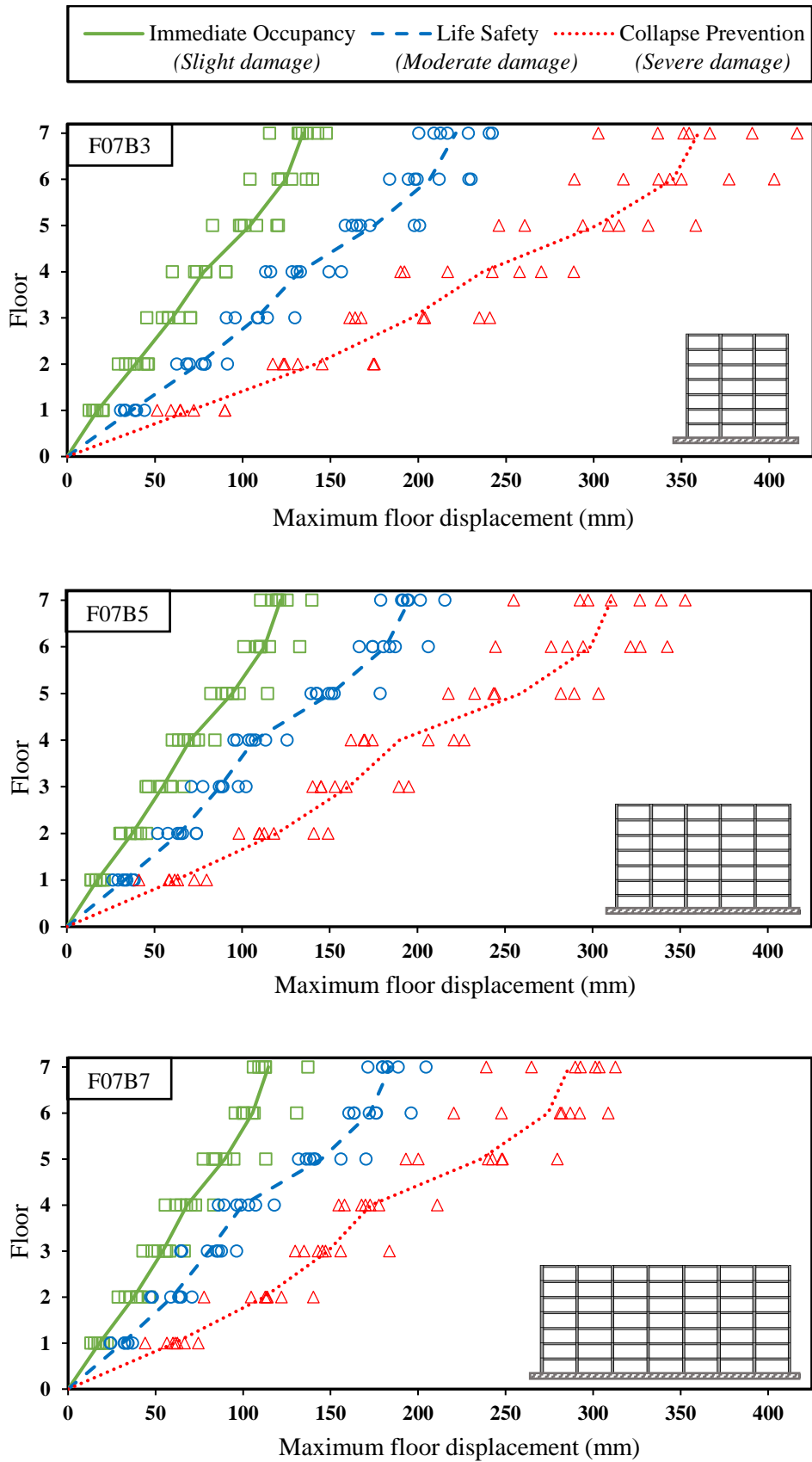


Figure 5-2 Displacement profiles of the 7-story prototype frames

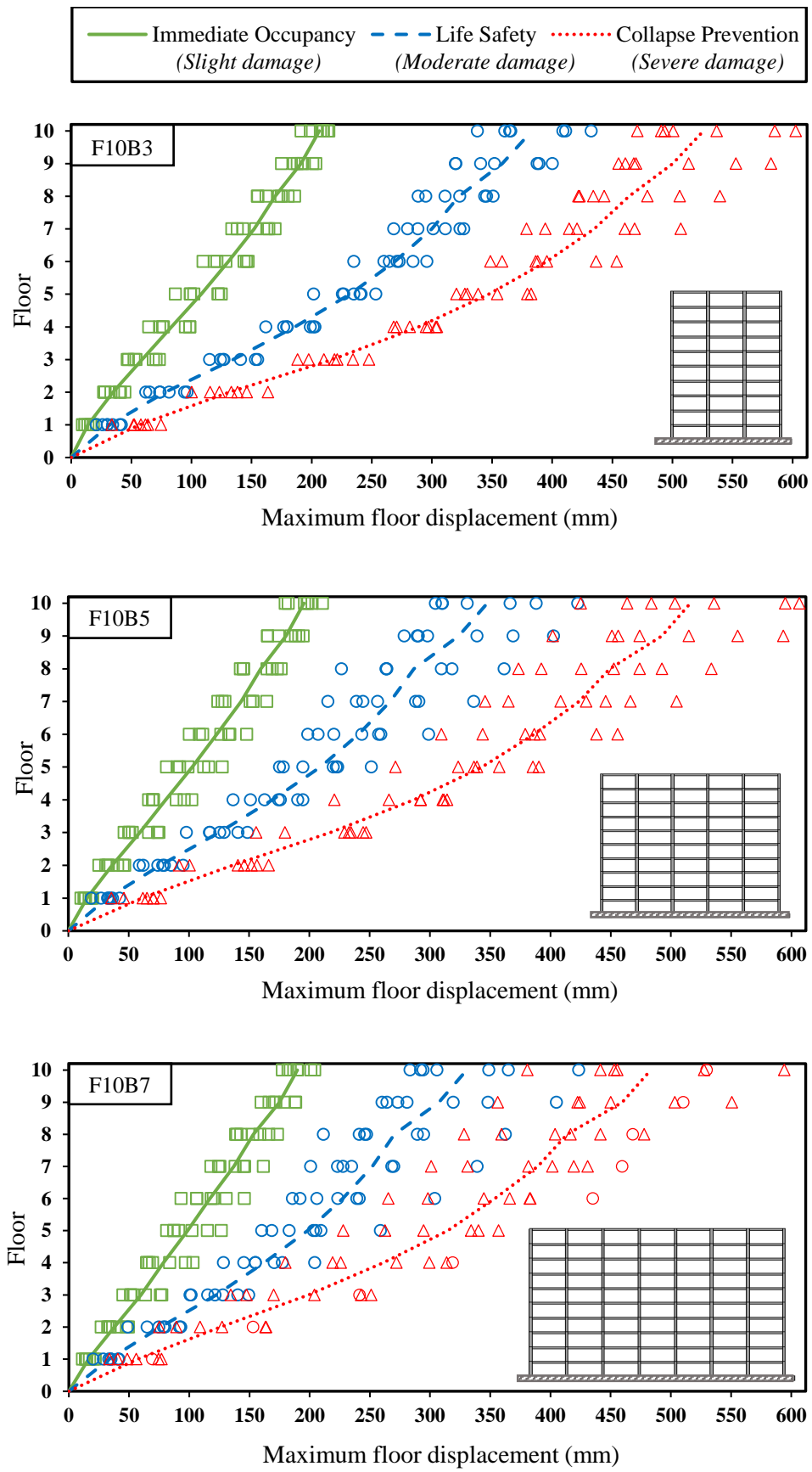


Figure 5-3 Displacement profiles of the 10-story prototype frames

5.3 ROOF DISPLACEMENT RESULTS

Seismic codes, including ECP-201 (2012) and EC8 (EN1998-1, 2004) allow considering the expected response values from THA as the average of responses from 7 ground motion accelerations; accordingly, the expected values of the maximum roof displacement given a certain IDR, ($E[\Delta_{r,max}|IDR]$), are calculated as the mean for the 7 records. Similarly the associated conditional dispersion values, ($[\sigma_{\Delta_{r,max}}|IDR]$), are computed as the standard deviation from the mean. Table 5-1 summarizes the expected maximum displacement results at the roof level of all structures at the identified study performance levels (IO: Immediate Occupancy; LS: Life-safety and CP: Collapse Prevention), while details of the maximum roof displacement for every subjected ground motion are given in Table 5-2, together with the floor at which the associated damage level (as measured by IDR) was first achieved.

Table 5-1 Summary of conditional mean $E[\Delta_{r,max}|IDR]$ and conditional dispersion $[\sigma_{\Delta_{r,max}}|IDR]$ of displacement results for all frames

Structure Reference	IDR = 1%		IDR = 2%		IDR = 3%	
	$E[\Delta_{r,max} IDR]$	$[\sigma_{\Delta_{r,max}} IDR]$	$E[\Delta_{r,max} IDR]$	$[\sigma_{\Delta_{r,max}} IDR]$	$E[\Delta_{r,max} IDR]$	$[\sigma_{\Delta_{r,max}} IDR]$
F04B3	83.6	2.8	148.6	9.6	196.4	19.0
F04B5	79.1	2.9	137.0	10.5	185.4	19.1
F04B7	74.1	6.1	130.5	12.5	176.8	19.0
F07B3	134.4	10.2	221.4	16.1	359.6	36.6
F07B5	122.0	9.1	195.5	11.2	311.0	32.9
F07B7	114.4	10.3	184.1	10.4	286.3	25.8
F10B3	206.3	8.3	383.1	34.4	525.8	50.7
F10B5	195.4	10.9	347.6	45.8	516.1	67.1
F10B7	189.8	9.9	330.4	51.3	483.3	71.1

It is evident from the tabulated results that average values of the roof displacements are correlated positively to the number of floors and negatively to the number of bays for all investigated IDR levels. This is intuitively expected due to the increase in stiffness for shorter and wider structures, respectively. Moreover, conditional dispersion for all cases increases with the increase of IDR and with the increase in height. A similar dispersion pattern can be visualized in the displacement

profiles formerly depicted in Figures 5-1 to 5-3, for the response of the individual records, which fortifies these statistical results. The variation in displacement response with each ground motion record can be explained by the sensitivity to the characteristics of ground motions, some of which are given in Table 4-9. The A/V ratio is well correlated to the magnitude-epicentral-distance relationship and is an indication of the relative frequency content (Garg et al., 2019), therefore, accelerograms with high A/V ratio (for example EQ3 and EQ6) impose greater demand on stiffer structures while those possessing low A/V ratio (for example EQ2 and EQ4) result in higher response for more flexible structures. It is not within the scope of this research to study the exact effect of ground motion characteristics on the displacement response but this remark is rather included for explanation of the variability of the results. It follows that the dispersion becomes more prominent for higher structures due to the higher domination of seismic loads (which are sensitive to the ground motions) over the gravitational loads, and also the variation increases with increase in damage level due to the associated higher earthquake amplitudes. It may, however, generally be observed that there is no specific trend for the conditional dispersion with the change in number of bays, due to the insignificance of the number of bays on the fundamental period (as previously discussed in Section 4.3.5 and tabulated in Table 4-8) and accordingly on the sensitivity to the ground motion dynamic properties. Lastly, it should be noted that having this range of response variance and then averaging over seven records has been proven to be quite satisfactory for providing unbiased expected results (Iervolino et al., 2008), which is essential for the purpose of the current study.

Another observation from Table 5-2 concerns the location of the limiting values of the maximum IDR along the height of each buildings, where it is achieved at different floor levels for each input ground motion. It is clear that, there is no possibility to take averages of the inter-story drift distribution for the set of records and accordingly only the top displacement profiles are determined for each record separately and then averaged as shown in Figures 5-1 to 5-3. Limiting values of the IDR generally occur at the lower floors for the 4-story buildings, then they shift to stories near the mid-height of the frame for the 7-story buildings, and further to the upper stories for the 10-story buildings. This behavior is consistent with the finding of other researchers, for example Azak (2013). The shifting of damage to mid-floor levels with increasing height is

expected due to the contribution of higher mode effects, and then the further shift towards the top floors can be attributed to the dominance of the second-order P- effects.

Table 5-2 Maximum roof displacement values ($\Delta_{r,max}$) for all structure-accelerogram pairs at the three study performance levels, and the floor at which the associated limiting value of Inter-story drift ratio (IDR) first occurred

Structure Reference	EQ1		EQ2		EQ3		EQ4		EQ5		EQ6		EQ7		
	$\Delta_{r,max}$ (mm)	Floor	$\Delta_{r,max}$ (mm)	Floor	$\Delta_{r,max}$ (mm)	Floor	$\Delta_{r,max}$ (mm)	Floor	$\Delta_{r,max}$ (mm)	Floor	$\Delta_{r,max}$ (mm)	Floor	$\Delta_{r,max}$ (mm)	Floor	
Results at IO level (IDR =1%)	F04B3	84.5	1	83.1	1	82.2	2	88.8	1	84.6	1	79.9	2	82.1	2
	F04B5	77.1	1	75.8	1	76.8	1	78.5	1	81.1	1	80.8	2	84.0	2
	F04B7	73.0	1	71.2	1	74.1	1	67.2	1	73.8	1	72.7	1	87.0	1
	F07B3	131.6	5	115.4	5	134.0	5	147.6	5	132.5	5	142.8	5	136.9	5
	F07B5	121.4	5	110.5	5	120.3	5	139.7	5	125.6	5	116.7	5	119.4	5
	F07B7	110.9	5	109.1	5	112.8	5	137.1	5	112.7	5	112.6	5	105.9	5
	F10B3	191.4	9	207.3	5	209.4	9	213.2	9	209.8	9	199.0	3	214.2	5
	F10B5	182.4	9	210.7	5	198.2	9	195.9	9	179.9	9	202.1	3	198.8	9
	F10B7	177.4	9	204.3	5	190.0	9	189.6	9	184.0	9	201.0	9	182.2	9
Results at LS level (IDR =2%)	F04B3	146.4	1	154.6	1	156.2	1	144.0	1	155.8	2	129.7	1	153.5	2
	F04B5	134.8	1	140.8	1	142.0	1	136.0	1	123.2	1	126.9	1	154.9	2
	F04B7	124.0	1	131.1	1	132.5	1	128.3	1	117.9	1	123.3	1	156.5	2
	F07B3	240.6	5	228.5	5	200.3	5	242.2	5	212.7	5	216.7	5	209.0	5
	F07B5	215.6	5	201.7	5	179.1	5	194.2	5	191.8	5	191.0	5	194.9	5
	F07B7	204.6	5	188.7	5	171.2	5	182.6	5	179.6	5	179.7	5	182.3	5
	F10B3	365.7	3	411.3	9	360.7	3	364.8	3	432.5	9	409.0	5	337.9	9
	F10B5	366.5	4	388.2	9	331.0	9	310.3	9	304.6	9	422.6	4	309.9	9
	F10B7	348.7	9	365.0	9	305.8	9	292.2	9	283.3	9	423.5	3	294.2	9
Results at CP level (IDR =3%)	F04B3	172.0	1	191.1	1	213.8	1	209.8	1	220.7	1	174.8	1	192.5	1
	F04B5	161.0	1	189.7	1	203.0	1	186.5	1	213.7	1	165.3	1	178.4	1
	F04B7	161.3	1	187.1	1	190.5	1	165.7	1	208.8	1	156.7	1	167.4	1
	F07B3	390.4	5	336.5	5	354.4	5	351.3	5	416.0	1	366.1	1	302.7	5
	F07B5	339.1	5	311.5	5	292.8	5	328.1	5	352.9	5	254.8	5	297.4	5
	F07B7	303.5	5	301.3	5	264.8	5	312.8	5	289.8	5	238.9	5	292.8	5
	F10B3	493.6	3	500.7	2	585.1	4	470.8	3	602.5	4	536.9	3	490.9	3
	F10B5	503.2	4	483.7	2	594.7	5	463.7	3	606.5	3	535.8	3	425.1	9
	F10B7	453.1	9	441.6	9	594.4	5	455.6	9	527.8	9	529.7	3	381.0	9

5.4 FACTORS AFFECTING ROOF DISPLACEMENT

Using the expected displacement results presented in the previous section, parametric study is performed to evaluate the contribution of the different variables to the roof displacement. Simplified bar charts are used in Figure 5-4 to graphically present the general trend of roof displacement in relation to the three factors considered for this study, namely the number of floors, the number of bays and the damage level in terms of the IDR.

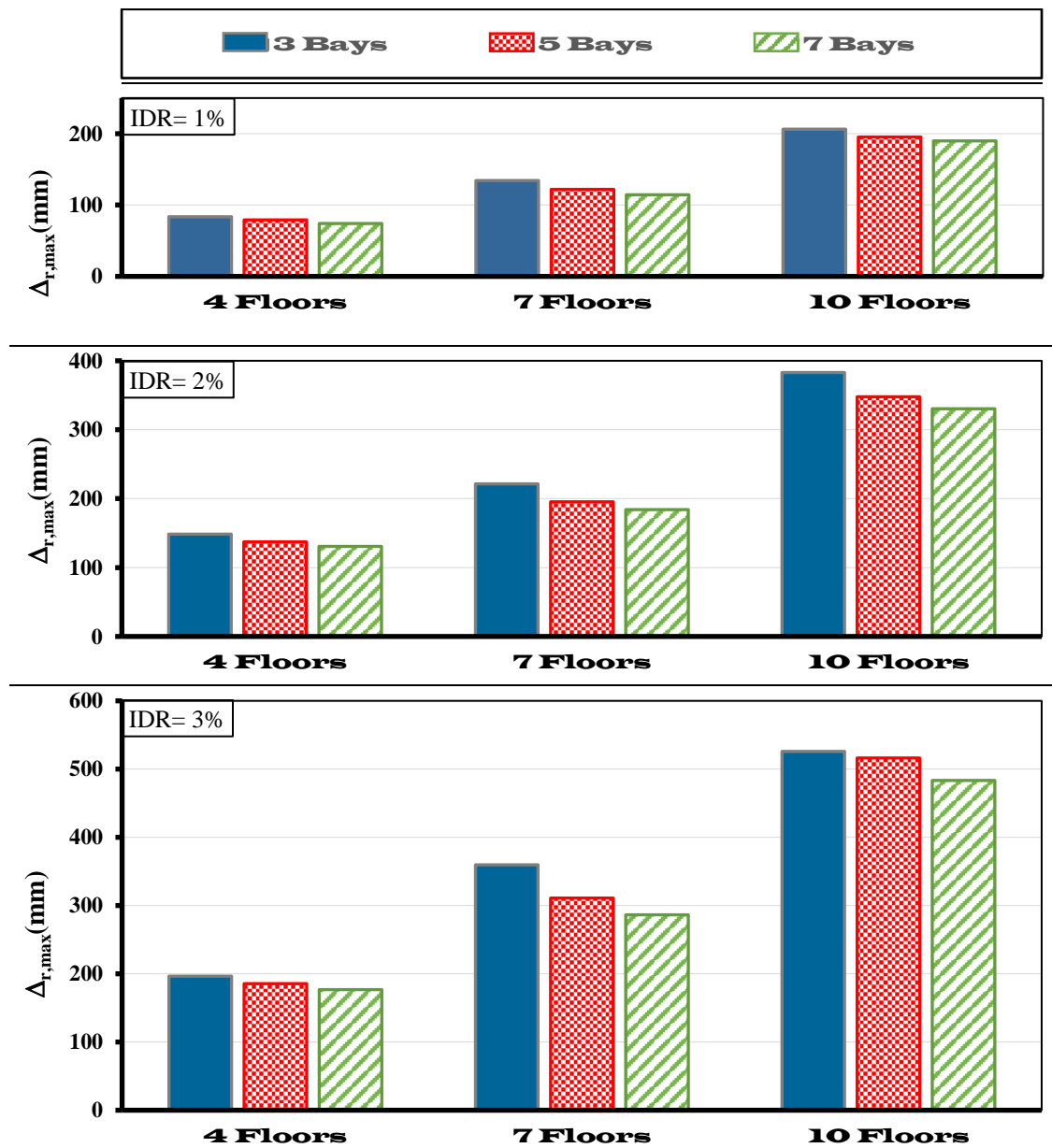


Figure 5-4 Relationship between maximum roof displacement ($\Delta_{r,max}$) and number of floors for different number of bays at fixed values of IDR (based on the average of the results given the acceptance criteria of the three studied performance levels).

5.4.1 Effect of the Number of Floors on Roof Displacement Response

First the effect of the number of floors is analyzed, by calculating the average percentage change in displacement per one-floor increase, for fixed values of the other two variables. The following is observed and is tabulated in Table 5-3 and graphically represented in Figure 5-5:

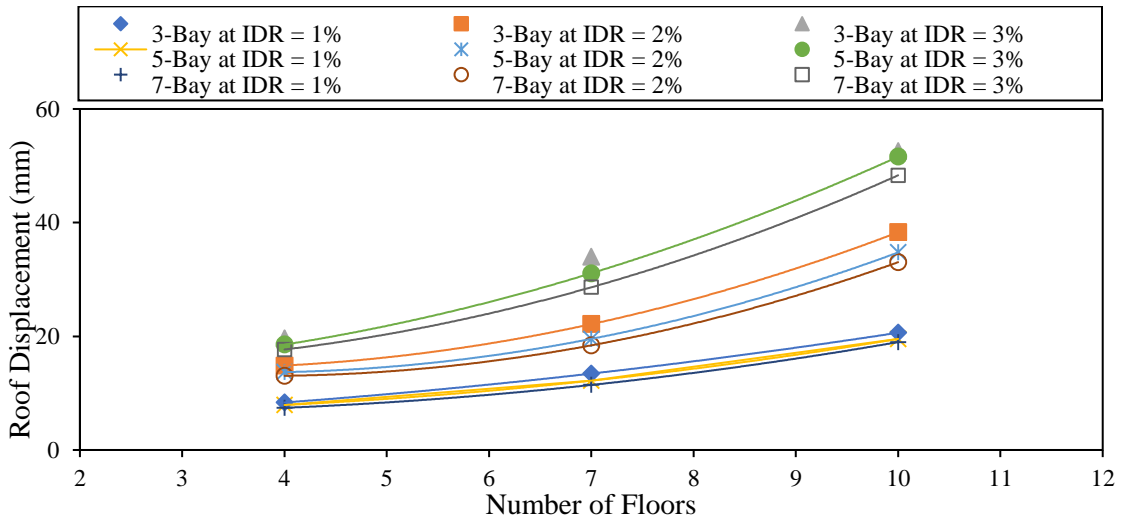


Figure 5-5 Change of the roof displacement with the number of floors

Table 5-3 Percentage change in displacement per one-floor increase for the different combinations of number of bays and inter-story drift ratio

Number of Bays	Inter-story-drift Ratio		
	1%	2%	3%
3	19	20.3	21.3
5	19	20.1	22.3
7	20	20.1	21.8

- For the 3-Bays structures, at the IO level, change in the number of floors from 4 to 7 results in 60.7% increase in the maximum displacement response, while that from 7 floors to 10 floors results in an increase of 53.5 %, therefore on average a one-floor increase results in 19% increase in displacement.
- For the 3-Bays structures, at the LS level, change in the number of floors from 4 to 7 results in 49% increase in the maximum displacement response, while that from 7 floors to 10 floors results in an increase of 73 %, therefore on average a one-floor increase results in 20.3 % increase in displacement.

- For the 3-Bays structures, at the CP level, change in the number of floors from 4 to 7 results in 74% increase in the maximum displacement response, while that from 7 floors to 10 floors results in an increase of 54 %, therefore on average a one-floor increase results in 21.3% increase in displacement.
- For the 5-Bays structures, at the IO level, change in the number of floors from 4 to 7 results in 54.1 % increase in the maximum displacement response, while that from 7 floors to 10 floors results in an increase of 60.3 %, therefore on average a one-floor increase results in 19% increase in displacement.
- For the 5-Bays structures, at the LS level, change in the number of floors from 4 to 7 results in 42.7 % increase in the maximum displacement response, while that from 7 floors to 10 floors results in an increase of 77.8 %, therefore on average a one-floor increase results in 20.1 % increase in displacement.
- For the 5-Bays structures, at the CP level, change in the number of floors from 4 to 7 results in 67.8 % increase in the maximum displacement response, while that from 7 floors to 10 floors results in an increase of 66 %, therefore on average a one-floor increase results in 20.1 % increase in displacement.
- For the 7-Bays structures, at the IO level, change in the number of floors from 4 to 7 results in 54.4 % increase in the maximum displacement response, while that from 7 floors to 10 floors results in an increase of 65.8 %, therefore on average a one-floor increase results in 20 % increase in displacement.
- For the 7-Bays structures, at the LS level, change in the number of floors from 4 to 7 results in 41.1 % increase in the maximum displacement response, while that from 7 floors to 10 floors results in an increase of 79.5 %, therefore on average a one-floor increase results in 20.1 % increase in displacement.
- For the 7-Bays structures, at the CP level, change in the number of floors from 4 to 7 results in 61.9 % increase in the maximum displacement response, while that from 7 floors to 10 floors results in an increase of 68.8 %, therefore on average a one-floor increase results in 20.1 % increase in displacement.

From the summary of results in Table 5-3, it can be concluded that the number of floors is a significant factor in estimating the displacement response, where a one-floor increase on average results in 20 percent increase in displacement. One could observe that the percentage increases are higher when the inter-story drift increases,

which proves the interaction of these two variables in their influence on displacement response. This can be explained by the second-order effects which better manifest with a combination of increasing structure's heights and large displacement into the inelastic range.

5.4.2 Effect of the Number of Bays on Roof Displacement Response

The effect of the number of bays is analyzed for fixed values of the other two variables. The top story displacement decreases with the increase of number of bays. Figure 5-6 shows that the decrease in the top story displacement is almost linear for all damage levels. The calculated average percentage change in displacement per one-bay increase is tabulated in Table 5-4.

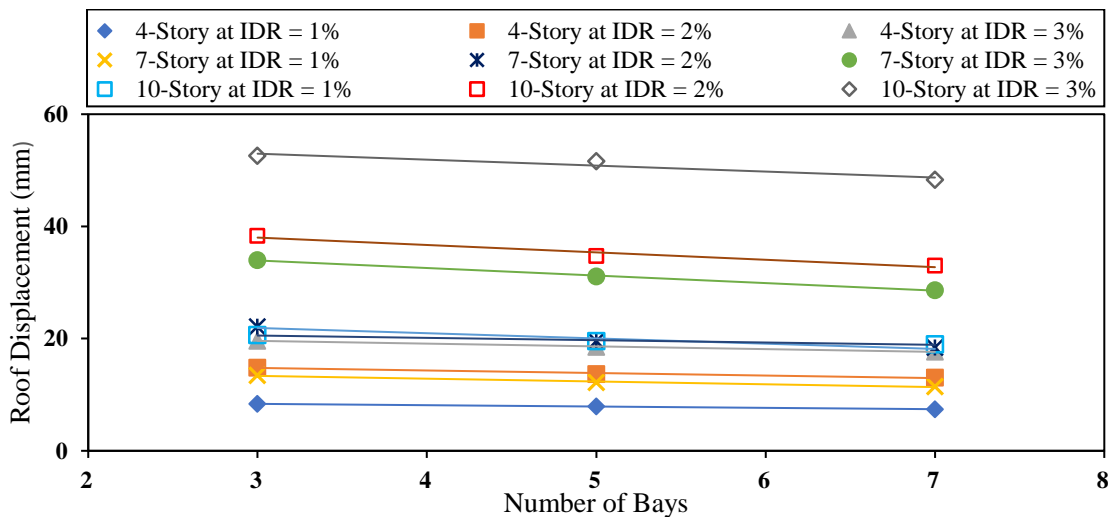


Figure 5-6 Change of the roof displacement with the number of bays

Table 5-4 Percentage change in displacement per one-bay increase for the different combinations of number of floors and inter-story drift ratio

Number of Floors	Inter-story-drift Ratio		
	1%	2%	3%
4	-2.9	-3.1	-2.6
7	-3.9	-4.4	-5.4
10	-2.1	-3.6	-2.1

The following is observed::

- For the 4-stories structures, at the IO level, change in the number of bays from 3 to 5 results in 5.3 % decrease in the maximum displacement response, while that from

5 bays to 7 bays results in a decrease of 6.3 %, therefore on average a one-bay increase results in 2.9 % decrease in displacement.

- For the 4-stories structures, at the LS level, change in the number of bays from 3 to 5 results in 7.8 % decrease in the maximum displacement response, while that from 5 bays to 7 bays results in a decrease of 4.7 %, therefore on average a one-bay increase results in 3.1 % decrease in displacement.
- For the 4-stories structures, at the CP level, change in the number of bays from 3 to 5 results in 5.6 % decrease in the maximum displacement response, while that from 5 bays to 7 bays results in a decrease of 4.6 %, therefore on average a one-bay increase results in 2.6 % decrease in displacement.
- For the 7-stories structures, at the IO level, change in the number of bays from 3 to 5 results in 9.2 % decrease in the maximum displacement response, while that from 5 bays to 7 bays results in a decrease of 6.2 %, therefore on average a one-bay increase results in ~~2.1~~ 3.9 % decrease in displacement.
- For the 7-stories structures, at the LS level, change in the number of bays from 3 to 5 results in 11.7 % decrease in the maximum displacement response, while that from 5 bays to 7 bays results in a decrease of 5.8 %, therefore on average a one-bay increase results in 4.4 % decrease in displacement.
- For the 7-stories structures, at the CP level, change in the number of bays from 3 to 5 results in 13.5 % decrease in the maximum displacement response, while that from 5 bays to 7 bays results in a decrease of 7.9 %, therefore on average a one-bay increase results in 5.4 % decrease in displacement.
- For the 10-stories structures, at the IO level, change in the number of bays from 3 to 5 results in 5.3 % decrease in the maximum displacement response, while that from 5 bays to 7 bays results in a decrease of 2.9 %, therefore on average a one-bay increase results in 2.1 % decrease in displacement.
- For the 10-stories structures, at the LS level, change in the number of bays from 3 to 5 results in 9.3 % decrease in the maximum displacement response, while that from 5 bays to 7 bays results in a decrease of 4.9 %, therefore on average a one-bay increase results in 3.6 % decrease in displacement.
- For the 10-stories structures, at the CP level, change in the number of bays from 3 to 5 results in 1.8 % decrease in the maximum displacement response, while that

from 5 bays to 7 bays results in a decrease of 6.4 %, therefore on average a one-bay increase results in 2.1 % decrease in displacement.

From the summary of results in Table 5-4, it can be concluded that the number of bays is much less significant than the number of stories in estimating the displacement response, where a one-bay increase on average results in 3.4 percent decrease in displacement. However, it is elected to still include this factor as a variable for estimating roof displacement because of the negative correlation. The displacement estimate will be used for calculation of the force-reduction factor (R), so a higher than actual displacement will result in higher reduction of forces and less conservative results. The percentage decrease does not seem to have any coherent pattern associated with the other two factors, and thus is assumed a completely independent variable in the development of the estimate equation later in this Chapter.

5.4.3 Effect of Damage Level on Roof Displacement Response

The effect of the damage level is analyzed, by calculating the average percentage change in displacement per unit increase in IDR ratio (as a measure of damage) for fixed values of the other two variables. Figure 5-7 shows the variation of displacement with change in IDR for all studied structures. The following is observed and tabulated in Table 5-5:

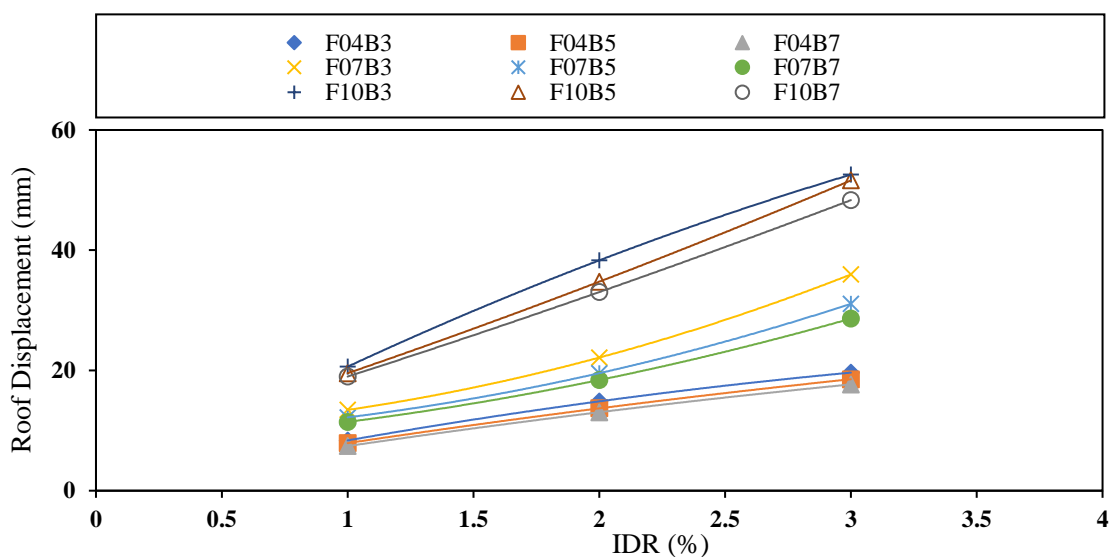


Figure 5-7 Change in the roof displacement with damage level (in terms of IDR)

Table 5-5 Percentage change in displacement per unit increase of IDR for the different combinations of number of floors and bays

Number of Floors	Number of Bays		
	3	5	7
4	54.9	54.2	55.7
7	60.6	59.7	58.2
10	61.5	63.2	60.2

- For the 4-Floor 3-Bay structure, change in performance level and IDR percentage from 1 to 2 results in 77.7 % increase in the maximum displacement response, while the change of IDR from 2 to 3 percent results in an increase of 32.2 %, therefore on average a unit increase in IDR results in 54.9 % increase in displacement.
- For the 4-Floor 5-Bay structure, change in performance level and IDR percentage from 1 to 2 results in 73 % increase in the maximum displacement response, while the change of IDR from 2 to 3 percent results in an increase of 35.3 %, therefore on average a unit increase in IDR results in 54.2 % increase in displacement.
- For the 4-Floor 7-Bay structure, change in performance level and IDR percentage from 1 to 2 results in 76 % increase in the maximum displacement response, while the change of IDR from 2 to 3 percent results in an increase of 35.5 %, therefore on average a unit increase in IDR results in 55.7 % increase in displacement.
- For the 7-Floor 3-Bay structure, change in performance level and IDR percentage from 1 to 2 results in 64.8 % increase in the maximum displacement response, while the change of IDR from 2 to 3 percent results in an increase of 56.4 %, therefore on average a unit increase in IDR results in 60.6 % increase in displacement.
- For the 7-Floor 5-Bay structure, change in performance level and IDR percentage from 1 to 2 results in 60.3 % increase in the maximum displacement response, while the change of IDR from 2 to 3 percent results in an increase of 59.1 %, therefore on average a unit increase in IDR results in 59.7 % increase in displacement.
- For the 7-Floor 7-Bay structure, change in performance level and IDR percentage from 1 to 2 results in 60.9 % increase in the maximum displacement response, while the change of IDR from 2 to 3 percent results in an increase of 55.5 %, therefore on average a unit increase in IDR results in 58.2 % increase in displacement.
- For the 10-Floor 3-Bay structure, change in performance level and IDR percentage from 1 to 2 results in 85.7 % increase in the maximum displacement response, while

the change of IDR from 2 to 3 percent results in an increase of 37.2 %, therefore on average a unit increase in IDR results in 61.5 % increase in displacement.

- For the 10-Floor 5-Bay structure, change in performance level and IDR percentage from 1 to 2 results in 77.8 % increase in the maximum displacement response, while the change of IDR from 2 to 3 percent results in an increase of 48.5 %, therefore on average a unit increase in IDR results in 63.2 % increase in displacement.
- For the 10-Floor 7-Bay structure, change in performance level and IDR percentage from 1 to 2 results in 74.1 % increase in the maximum displacement response, while the change of IDR from 2 to 3 percent results in an increase of 46.3 %, therefore on average a unit increase in IDR results in 60.2 % increase in displacement.

From the summary of results in Table 5-5, it can be concluded that the inter-story drift ratio as an indication of the damage level has the highest weight in influencing the maximum roof displacement response, where a unit increase in the IDR percentage results approximately in 59.5 percent increase in displacement. A similar observation regarding the interrelation between the inter-story drift ratio and the number of floors can be drawn, where the percentage increases due to increase in IDR are higher when the number of floors increases, which proves the interaction of these two factors. There is no consistent relation between the number of bays factor and the effect of the IDR, confirming its independence assumption. The significance of IDR in estimating the roof displacement can be intuitively explained, because more damage of a building is associated with higher amplitudes of earthquake loading and consequently larger displacements.

It is worth noting that this parametric analysis is highly simplified for the purpose of studying the general influence of the various factors on the displacement response only. The values used in expression of the percentage change in displacement with change in the different parameters are computed after several averaging steps. Thus, the results cannot be stated as absolute nor be used directly for development of a prediction model. It is essential to develop relations for estimating displacement that are based on realistic data, and that would embed the interaction of several factors like the second order P-delta effects, the contribution of higher modes of vibration, the relative dominance of the seismic loading compared to gravitational loads and inelastic effects.

5.5 PREDICTION OF DISPLACEMENT DEMAND

After analysis of the displacement response database and identifying the structural features that influence the lateral drift, it is required to develop a formula for estimating the roof displacement to be used for HFD design of RC frame structures (as previously discussed in Chapter 3). For that purpose, regression analysis is adopted to find the most suitable fit for the displacement results that can serve as a prediction model. The displacement is considered to be the dependent variable, while IDR, number of floors (n_F) and number of bays (n_B) are the three predictors.

5.5.1 Definition of the Expected Relation

In order to visualize the expected trend for the relationship between the displacement and the three predictors, it is elected to observe the results on a continuous scale for the IDR, in order to have a more accurate model that can be applicable to various performance levels, not just the ones under study. Thus, the results of the IDA presented in Chapter 4 are used to plot the roof displacement versus IDR for all the study frames together as shown in Figure 5-8. It can be inferred from the scatter plots for the 4-story buildings that a power rule with an exponent inferior to unity explains the relationship between roof displacement and IDR, while this exponent clearly increases with the increase of building height to reach almost unity and a linear relationship for the 10-story building. The number of bays does not seem to have any effect on the slope of the scatter and likewise the exponent. Therefore, it is concluded that a power rule with an exponent that is a function of the number of floors will best explain the relationship. This trend of increasing slope for higher buildings can be attributed to the redistribution of forces and deformations in a structural system, which becomes more effective as the number of structural members increase as is the case for taller buildings. In other words, shorter buildings reach damage (a specific IDR) faster (with a flatter slope) due to having less redundancy that can redistribute the responses with excursion into the inelastic behavior.

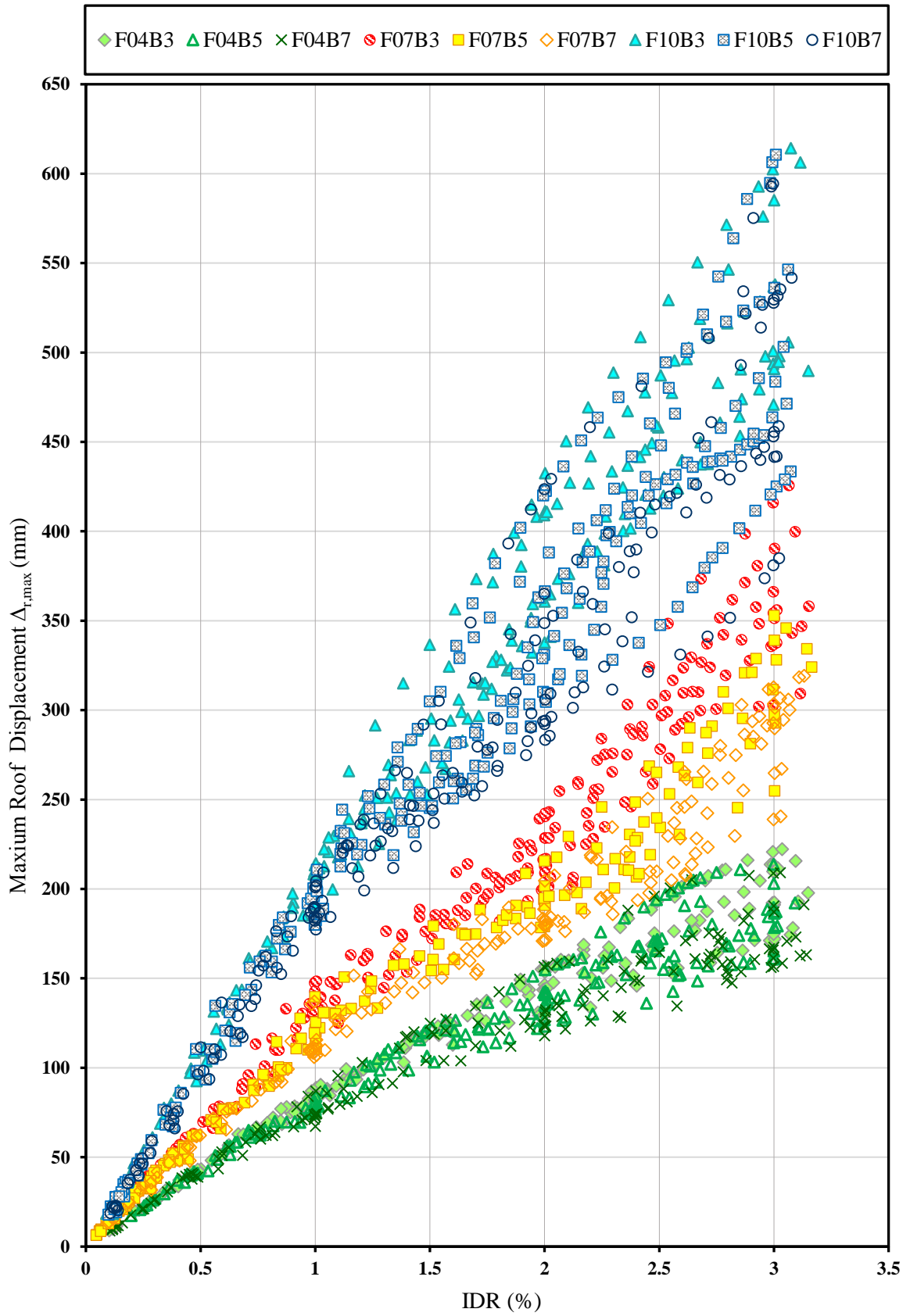


Figure 5-8 Relationship between maximum roof displacement ($\Delta_{r,max}$) and IDR for all frames based on all results of the seven ground motion records

5.5.2 Regression Analysis

The expected power-rule function cannot be expressed by linear regression, and also more than one explanatory variable is involved, therefore multi-variable nonlinear regression is employed in the present study. The analyses are performed using “LAB Fit” curve fitting software (Silva and Silva, 2011), which is a tool for treatment and analysis of data. LAB Fit performance has been validated using the Statistical Reference Datasets Project (SRD) of the National Institute of Standards and Technology (NIST). It uses the Levenberg-Marquardt algorithm to solve nonlinear regression of up to 6 independent variables with a library of almost 500 functions, in addition to the option of providing user-defined functions. In order to improve the ability of the model to realistically reflect the physical behavior, it is chosen to postulate own fitting function based on the expected relation discussed in Section 5.5.1. In order to draw reliable limits for the developed function, a physical constraint is taken into consideration, which is that the roof displacement should be equal to the IDR multiplied by the floor height, for the case of one-story buildings; in other words, when $n_F=1$, top drift and story drift are the same.

5.5.3 Proposed Prediction Equation

The proposed equation for estimating the maximum roof displacement demand (Δ_r) at the various performance levels is selected to have the following functional form:

$$\Delta_r = (P_1 H + P_2 IDR^{P_3}) IDR \dots \dots \dots (5.1)$$

where, Δ_r is the roof displacement in m, H is the building height in m, IDR is the target story drift ratio associated with the objective performance levels; and P_1 and P_2 are empirical parameters that depends on the geometry of the buildings, which are found based on the regression analysis of the response data of the study cases to be as follows:

$$\left. \begin{aligned} P_1 &= 1/n_F \\ P_2 &= 0.17 (n_F - 1)^2 n_B^{-0.3} \\ P_3 &= -1.3/n_F \end{aligned} \right\} \dots \dots \dots (5.2)$$

where n_F and n_B are the number of floors and bays of the buildings respectively.

The goodness of fit of the developed equation is expressed through the correlation coefficient (R) between the training data set used for regression analysis (the displacement values obtained by THA for all the earthquake records) and the corresponding fitted values calculated from the formulation. As illustrated graphically in Figure 5-9, the correlation coefficient is calculated to be 0.98 which indicates that the actual data are well replicated by the model. To avoid the overfitting errors introduced by having a large number of data points and variables, the adjusted correlation coefficient is also computed as 0.97 which confirms the goodness of fit. On another note, it can be recognized that the resulting equation satisfies the boundary constraint where $\Delta_r = H \cdot IDR$ for $n_F = 1$, and the signs of the coefficients agree with the theoretical observations where the number of floors are positively correlated and the number of bays are negatively correlated to the maximum roof displacement, respectively.

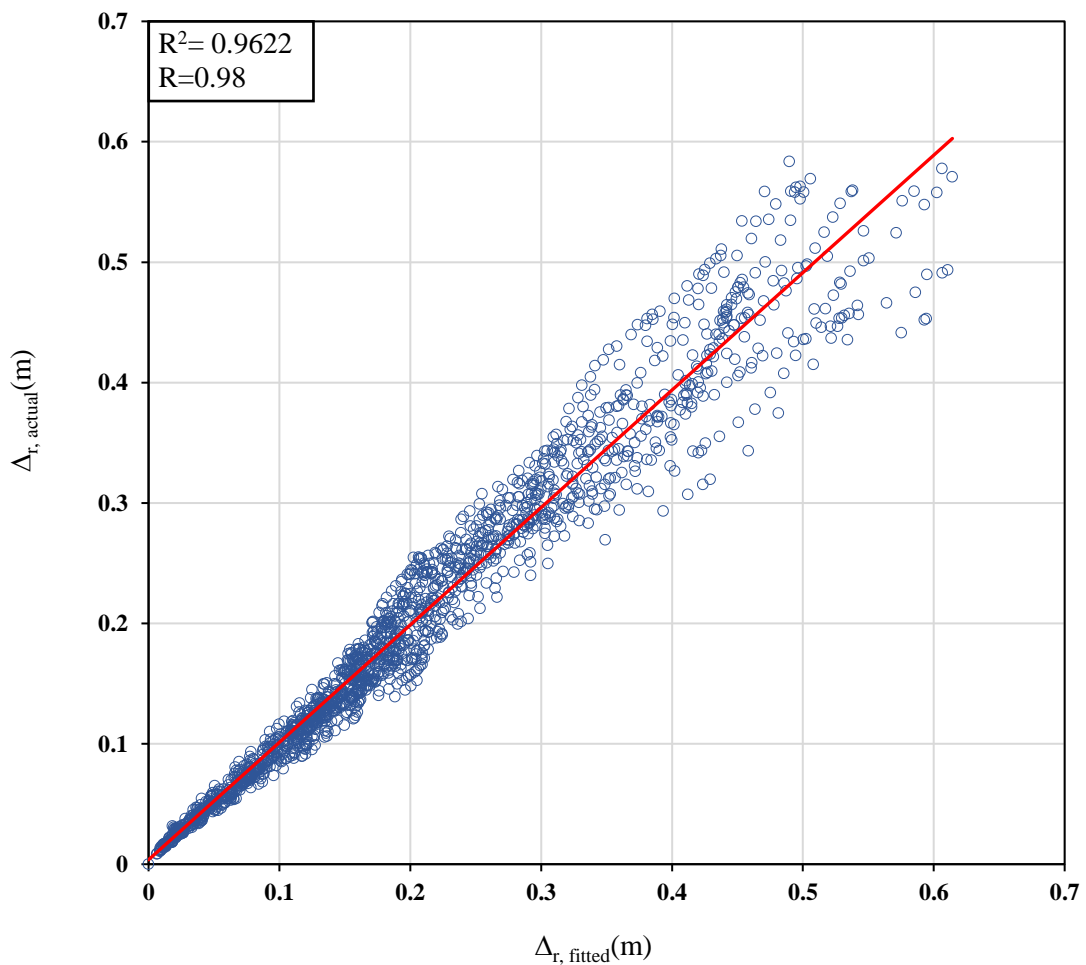


Figure 5-9 Goodness-of-fit of the regression line for estimating maximum roof displacement (Δ_r)

The quality of prediction is additionally measured by assuming the expected average values of the displacement demand shown in Table 5-1 (which can be considered as the closest approximation of real response) as a test data set, and computing the corresponding correlation coefficient, which is found to be 0.99 meaning that 99% of the observed variance is accounted for by the prediction model. Figure 5-10 shows how closely the expected values fall in with respect to the fitted regression line. The mean absolute percentage error (MAPE) is also checked to be just 5.1% which proves the accuracy of the predictive model. It should be noted that only one value of correlation coefficient and MAPE is presented for all the curves because they are based on one set of model equations (5.1) and (5.2). The relatively high correlation coefficient can be attributed to the collinearity between the predictor variables, especially the number of floors and the inter-story drift ratio, which can be expected by intuition. Nevertheless, multicollinearity is statistically accepted when the purpose of data fitting is merely providing a prediction model with reasonable accuracy, which is already proved by the goodness-of-fit tests (Kutner et al., 2005).

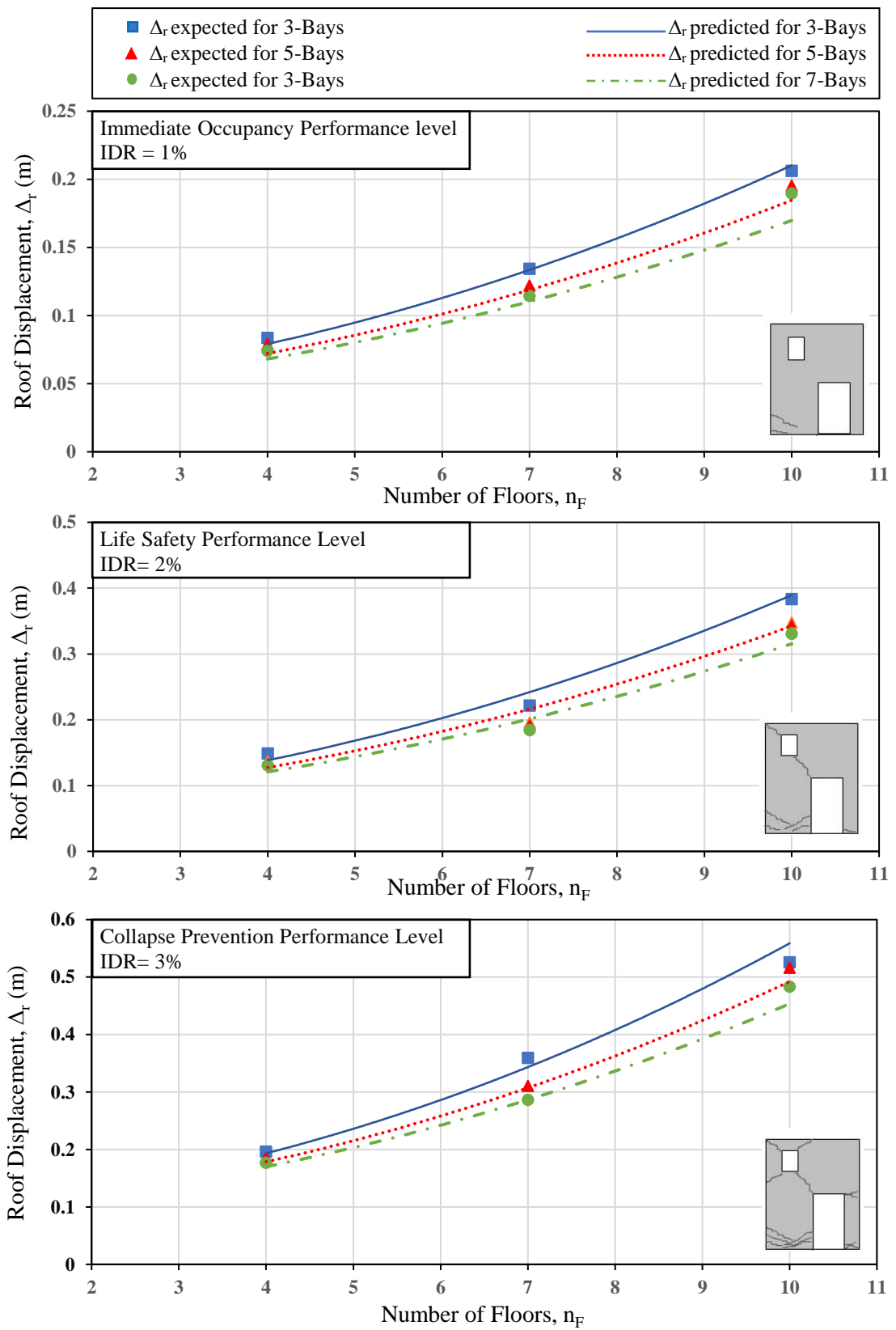


Figure 5-10 Comparison of the expected roof displacement response from THA with those resulting from the proposed relation for the three study performance levels.

5.5.4 Incorporation of Displacement Prediction into the HFD Design

The developed global roof displacement prediction equation can serve as a benchmark for creation of graphical charts for prediction of displacement, that can be incorporated in the HFD performance-based seismic design method. Subject to further modification using more structural models, types of ground motion records, types of soil, and damage limiting criteria, these prediction charts can obtain more degree of generality. Figure 5-11 represents a sample vision for such charts that is created from the displacement formula proposed by this study, with interpolation to cover more cases than the prototype ones used for development of the equation. This chart can be directly and simply used by the designer, at the start of the preliminary design stage, to predict a structure's maximum displacement at a predefined performance level, using only its geometric properties, and represents a valid contribution to the procedural step 4 of the HFD design method as described in Section 3.4. Then, by estimating the yield displacement using the design elastic model, a more rational value of force-reduction factor (R) can be calculated and design can proceed in the conventional way. The advantages of the proposed equation and prediction charts is that they incorporate IDR values rather than levels as a variable, therefore they can be still utilized with any improvement in the limiting values for performance levels and also with the future possibility of continuum between the discrete performance levels as advocated by the P-58 report.

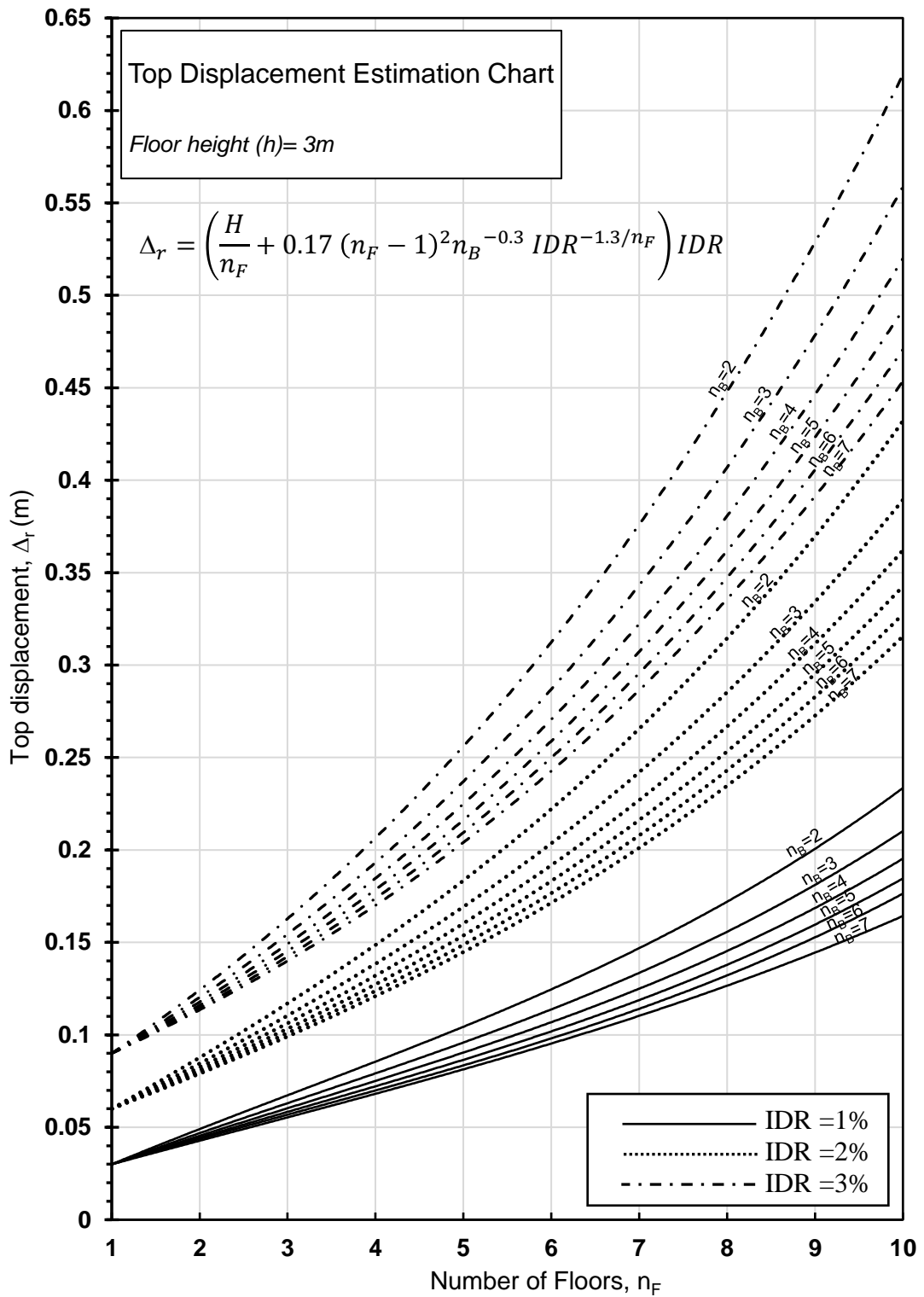


Figure 5-11 Top displacement estimation chart for incorporation in the HFD design method

CHAPTER 6

DESIGN CASE STUDY

6.1 INTRODUCTION

The use of the developed displacement prediction equation is tested in the context of the envisaged modified design, in line with the hybrid force displacement method. A prototype RC frame is chosen as a design case study and is designed using the traditional force-based code method and using the modified design procedure. The two designs are compared based on the number of iterations required, and the expected performance as compared to the results of nonlinear time-history analysis.

6.2 DESCRIPTION OF BUILDING AND DESIGN ASSUMPTIONS

The building shown in Figure 6-1 is selected for testing the modified design method. It has 8 floors and 3 bays and therefore lies in the range of applicability of the developed equations. Assuming a symmetrical layout, one internal lateral load resisting frame is designed employing two-dimensional analysis. The floor heights and the bay widths are equal to 3 m and 6 m. Assumptions, materials, load combinations, and loading are the same as those described in Section 4.2.2, except for assuming a live load of 2.0 kN/m^2 and adopting an earthquake loading with a peak ground acceleration (PGA) of $0.35g$. The design procedure is accomplished with the aid of ETABS v.17 (CSI, 2013), following the guidelines of the Egyptian Codes, ECP-201 (2012) and ECP-203(2007). For simplicity and due to the symmetry of the example building, the equivalent static load method is used. The building's members are proportioned according to the straining actions from the gravity load combinations (Appendix B), then the two seismic design models are developed. The frame designed using the code-stipulated R factors is referred to as the "Baseline frame (BL-frame)." While the frame designed using the proposed hybrid force/displacement method (employing the developed displacement relations for estimating a performance-related R factor) is given the name "Modified-design frame (MD-frame)."

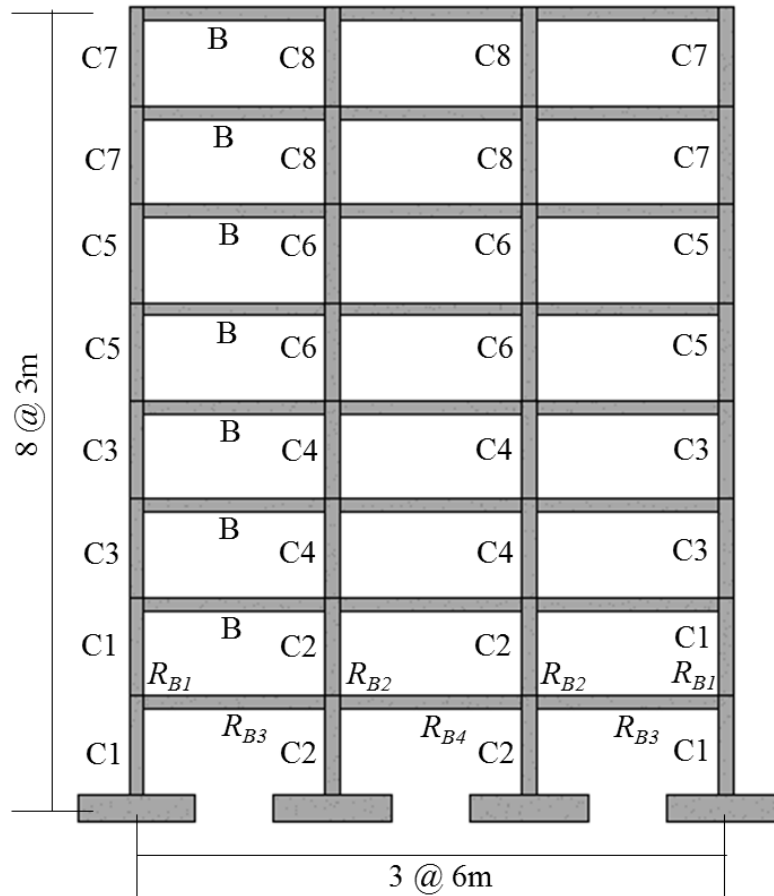


Figure 6-1 A representative layout of the design example frame, together with the notation used for numbering the columns and beam reinforcement

6.3 PERFORMANCE LEVELS CONSIDERED

The BL-frame is designed for the ultimate limit state for which the code of practice provides the elastic design response spectrum, and which corresponds to an earthquake with probability of exceedance of 10% in 50 years (475 years return period), referred to as the design-basis earthquake (DBE) as discussed in Chapter 3. The damage limitation state is checked as a post-design step, by conversion of the response values to correspond to the more frequent earthquake (FOE) with probability of exceedance of 50% in 50 years (72 years return period).

For the case of the MD-frame, the same performance levels are used in order to have a common basis of comparison, which are the Life-safety (LS) performance level and the Immediate Occupancy (IO) performance level, equivalent to the ultimate limit state and the damage state, respectively. Furthermore, one more performance level is

specified to be able to evaluate the ability of the proposed modification in mapping the traditional design procedure to the multi-performance-based design framework, which is the Collapse Prevention (CP) performance level. Design performance objectives are developed by linking each performance level to a specified earthquake level and a limiting value of IDR, as summarized in Table 6-1. The performance limiting criteria chosen are based on the guidelines of FEMA-356 (2000). The same spectral shape is assumed for all the seismic action levels, adopting a single multiplicative factor which reflect regional seismotectonic environment, as shown in Figure 6-2. Based on a hazard study of Egypt (Dorra, 2011), it is assumed that the peak ground acceleration corresponding to the FOE equals one third of that of the DBE, i.e. $PGA_{FOE} = 0.3 \times PGA_{DBE}$, while the peak ground acceleration for the maximum considered earthquake (MCE) equals one-and-a-half that of the DBE i.e. $PGA_{MCE} = 1.5 \times PGA_{DBE}$.

Table 6-1 Definition of the performance levels used in the design case study

Performance Level	Earthquake Intensity	Limiting value of IDR
Immediate Occupancy (IO)	FOE with 50% probability of occurrence in 50 years (72 years return period)	0.1
Life Safety (LS)	DBE with 10% probability of occurrence in 50 years (475 years return period)	0.2
Collapse Prevention (CP)	MCE with 2% probability of occurrence in 50 years (2475 years return period)	0.3

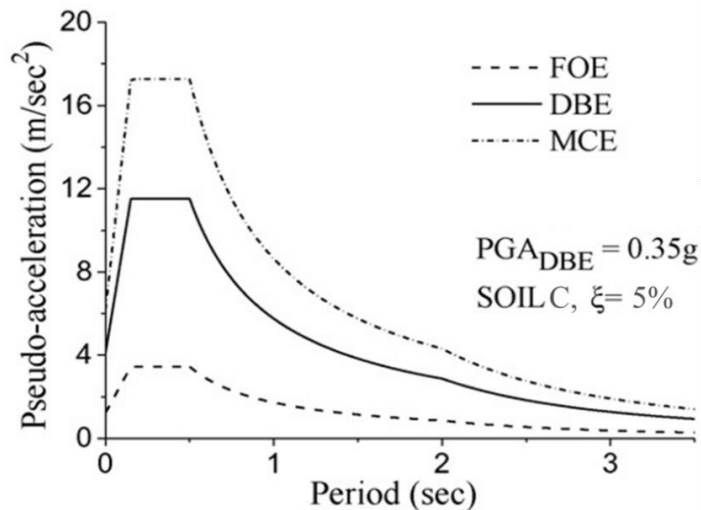


Figure 6-2 Elastic Pseudo-acceleration design spectrum associated with the three study performance levels

6.4 COMPARISON BETWEEN CODE DESIGN AND MODIFIED DESIGN

6.4.1 Efficiency and Iterations

In order to compare the efficiency of the proposed modified design method to normal design, the steps and results of the design of the BL-frame and MD-frame are presented. In both designs, all columns have square dimensions and the same beam is used in all floors for simplification. The columns' and beams' stiffness are reduced by 30% and 50%, respectively, in order to account for cracking. And the mass source includes the gravity loads with 50% of the live load.

6.4.1.1 Baseline (BL) frame

1. According to the requirements of the ECP-201 code (2012), the design seismic action for the ultimate limit state at the DBE are determined and applied to the BL-frame model. It is calculated using the elastic response spectrum for $a_g=0.35g$ reduced by a force-reduction factor (R) of 5 as prescribed for moment-resisting frames of limited ductility.
2. The resulting straining actions (presented in Figure B-1 in Appendix B) are used to determine the minimum required cross-sections and reinforcement ratios based on the strength and capacity design rules. The results are summarized in Table 6-2, based on the notation illustrated in Figure 6-1.

Table 6-2 Baseline-frame's member dimensions and reinforcement for the strength design step

Member	Dimension (mm)	Reinforcement ratio (%)
C1	400 x 400	1.90
C2	450 x 450	1.94
C3	400 x 400	0.85
C4	400 x 400	1.90
C5	400 x 400	1.90
C6	400 x 400	0.85
C7	300 x 300	2.18
C8	300 x 300	2.18
B-R _{B1}	200 x 450	1.05
B-R _{B2}	200 x 450	1.27
B-R _{B3}	200 x 450	2.1
B-R _{B4}	200 x 450	0.85

3. The designed frame is checked for deformation (second design step) for the damage limitation state at the FOE. The code uses a factor, υ , to convert the displacement response resulting from design at the DBE to its corresponding value at the FOE. This factor is specified as 0.4 for ordinary buildings. In order to convert the displacement values from the elastic design to its inelastic counterpart, the code uses a displacement amplification factor equals to $0.7R$. Therefore, the maximum interstorey drift at the DBE, IDR_{DBE} , is calculated, using the IDR output from analysis as shown in Figure C-2 in Appendix C, as follows: $IDR_{DBE} = 0.7 R IDR_{analysis} = 0.7 \times 5 \times 0.0074 = 0.026$. The corresponding IDR at the FOE, $IDR_{FOE} = \upsilon \times IDR_{DBE} = 0.4 \times 0.026 = 0.011$, which is greater than the code-specified limit of 1% for damage limitation in the case of no interaction of non-structural elements, therefore, design iteration is required.
4. Several iterations of changing member dimensions are performed, based on trial and error, until the IDR_{FOE} satisfies the limit of 1% for the damage limitation state. The final straining actions, story shear and displacement output results are presented in Appendix D, and the designed BL-frame member dimensions and reinforcement are given in Table 6-3.

Table 6-3 Baseline-frame's member dimensions and reinforcement, final after all iterations

Member	Dimension (mm)	Reinforcement ratio (%)
C1	450 x 450	1.01
C2	450 x 450	1.01
C3	450 x 450	0.85
C4	400 x 400	1.90
C5	400 x 400	0.85
C6	400 x 400	0.85
C7	300 x 300	1.4
C8	300 x 300	1.01
B-R _{B1}	200 x 450	1.05
B-R _{B2}	200 x 450	1.27
B-R _{B3}	200 x 450	2.1
B-R _{B4}	200 x 450	0.85

5. The designed BL-frame maximum values of IDR (at the FOE) is calculated to be 0.98% which satisfies the above limit values of IDR for the damage limitation state. The expected maximum roof displacement is also found to be 0.45m (0.7R x 0.1287m from Figure D-4 in Appendix D).

6.4.1.2 Modified-design (MD) frame

1. For the modified hybrid force/displacement procedure, the design seismic action is also obtained from the elastic response spectrum described in ECP-201code (2012) but using a force-reduction factor (R) that is calculated based on the most critical performance level that governs the design as previously described in Chapter 3. The first step involves estimating the maximum target roof displacement associated with each performance objective using Equations (5.1) and (5.2) or the prediction chart provided in Figure 5.11. For the number of floors (n_F) equals 8, and the number of bays (n_B) equals 3, the resulting roof displacement is:
 - For the IO performance level, $IDR_{max}=0.01$, therefore $\Delta_{r,IO}= 0.108$ m
 - For the LS performance level, $IDR_{max}=0.02$, therefore $\Delta_{r,LS}= 0.286$ m
 - For the CP performance level, $IDR_{max}=0.03$, therefore $\Delta_{r,CP}= 0.408$ m
2. The global yield displacement is estimated either using the empirical equation provided by Priestley (2000) for the yield drift (θ_y), which is $\theta_y=0.0004l_b/h_b$, where l_b and h_b are the bay length and beam height respectively, or alternatively by applying the seismic load corresponding to the FOE with $R=1$. It is selected to use the latter method because it accounts for the overall stiffness properties of the chosen frame, therefore the elastic response spectrum with $a_g=0.105g$, is applied corresponding to the PGA_{FOE} . The resulting roof displacement ($\Delta_{r,y}$) is found to be 0.075m, as shown in Figure E-3. It is also verified from the drift plot in Figure E-2 that the maximum IDR is 0.004084, which is less than the limiting value for the IO performance level (0.01) associated with the FOE seismic action applied on the model.
3. Based on the results of Step 1 and Step 2, the force-reduction factors (R_i) associated with each performance level (i) are calculated using Equation (3.3) in Chapter 3, and their equivalent at the DBE are also computed as tabulated in the Table 6.4.

Table 6-4 Calculation of performance level-dependent force reduction factors(R)

Performance level (i)	PGA_i	$\Delta_{r,i}$ (m)	$R_i = \frac{\Delta_{r,i}}{\Delta_{r,y}}$	$R_{DBE} = R_i \times \frac{PGA_{DBE}}{PGA_i}$
IO	$PGA_{FOE}=0.3 \times PGA_{DBE}= 0.105 \text{ g}$	0.156	2.1	6.9
LS	$PGA_{DBE}=0.35\text{g}$	0.286	3.8	3.8
CP	$PGA_{FOE}=1.5 \times PGA_{DBE}= 0.525\text{g}$	0.408	5.4	3.6

- The most critical force reduction factor R_{cr} is the smallest one, which corresponds to the CP performance level, and is equal to 3.6. This shows that the collapse prevention performance level governs the design.
- The seismic loads are applied based on the elastic response spectrum with $a_g=0.35\text{g}$ reduced with $R=3.6$, and the building is designed accordingly. The straining actions and drift results are given in Appendix F. The resulting member dimensions and reinforcing ratios are presented in Table 6-5.

Table 6-5 Modified design-frame's member dimensions and reinforcement

Member	Dimension (mm)	Reinforcement ratio (%)
C1	450 x 450	0.8
C2	450 x 450	0.8
C3	400 x 400	0.85
C4	450 x 450	0.8
C5	400 x 400	0.85
C6	400 x 400	0.85
C7	300 x 300	1.6
C8	300 x 300	1.8
B-R _{B1}	200 x 500	0.94
B-R _{B2}	200 x 500	1.85
B-R _{B3}	200 x 500	2.7
B-R _{B4}	200 x 500	0.85

6.4.1.3 Commentary

It should be noted that for the modified design, there is no need to check the drift requirements because they are embedded in the design process from the beginning. However, for the sake of testing, the code of practice method of checking drift is used. The collapse prevention force reduction factor is excluded (because it is not covered by the code of practice), and the smallest R factor is taken as 3.8, as given in Table 6-4.

The elastic response spectrum reduced by $R=3.8$ is applied to the designed structure and the resulting displacement results are monitored, as shown in Figure F-3 in Appendix F. The drift resulting from analysis is 0.0064, which is then multiplied by the displacement modification factor of $0.7R$, to get at its inelastic counterpart, and then by the ν factor (0.4) to arrive at the IDR corresponding to the serviceability earthquake. The resulting maximum IDR at the FOE is then equals to $0.0064 \times 0.7 \times 3.8 \times 0.4 = 0.0068$ (0.68%), which satisfies the code of practice limiting value of 1%. Therefore, the modified design is proved to be more efficient since it is performed in one step taking into account the strength and displacement demands simultaneously, unlike the code of practice method in which the second deformation check step may turn out highly iterative. Moreover, the proposed modification allows considering multiple performance levels, while identifying the performance objective that governs the design.

Regarding the value of R-factors achieved using the proposed design method, it is interesting to note that the Eurocode 8 (EN1998-1, 2004) provides a close value of 3.9 for designing MRF's with limited ductility for the ultimate and serviceability limit states, as compared to the value of 3.8 calculated in the modified design method for the life-safety performance objective. A study on the Egyptian seismic code (ECP-201, 2012) has also proposed changing the R-value specified as 5 for framed structures with low ductility to 60% of this value, which is almost 3 (Abd El Basset, Y., 2017). By performing nonlinear static analysis using the commercial software ETABS (CSI, 2013), the study proved that the proposed value of 3 is more conservative for a range of regular RC frames with different heights and located in different seismic zones (Abd El Basset, Y., 2017). This value is quite comparable to the critical R-factor of 3.6 found in this case study. Other research on the Egyptian seismic code has also advocated using a reduced value than 5 for the R-factor of framed structures (Mansour, A., 2015; and Ramadan, M., 2016). All these studies demonstrate the potential of the proposed modified method in achieving more accurate and reliable designs, in addition to the added advantage of efficiency.

6.4.2 Performance of the Designed Frames

In order to evaluate the reliability of the MD-frame design as compared to BL-frame design in achieving the intended performance objectives, nonlinear time history analysis (THA) is employed to provide a benchmark solution that reflects the closest approximation of actual behavior. ZEUS-NL is used for performing THA, using the same methodology, assumptions, material models, ground motion records and post-processing procedure described in Chapter 4.

6.4.2.1 Drift at the hazard levels associated with the performance levels

The final design MD-frame and BL-frame are modelled on ZEUS-NL, and are subjected to the seven ground motion records, described in Section 4.3.6. Three different scales, 0.3, 1 and 1.5 are applied on the PGA to match the elastic response spectrum for the FOE, DBE and MCE respectively, as illustrated in Figure 6-2. The resulting IDR values are calculated based on average and standard deviation. The average IDR values are compared to the limiting values associated with the corresponding performance levels, i.e. IO, LS and CP. Margins against reaching different performance levels are calculated by dividing the IDR limit specified for each performance level by the IDR_{max} reached at the associated hazard level, for example the margin against the IO level is calculated as 0.01 divided by the IDR_{max} achieved under the 50% in 50 years hazard level, which corresponds to PGA scale factor of 0.3. These results are summarized in Table 6-6. It is observed that the results of the BL-frame and the MD-frame are quite comparable at all hazard levels, with minimal reduced values for the MD-frame indicating more economical designs. Both designs satisfy the target drift values of the three performance levels with a considerable margin. This can be attributed to the overstrength resulting from the factors of safety employed in design, and also from the use of the equivalent static load method which results in relatively large base shear values, and accordingly overestimated displacement results.

Table 6-6 IDR response at the different hazards corresponding to the performance levels

Frame/design procedure	IDR _{average}		σ_{IDR} (dispersion due to record to record variability)		Margin $= \frac{IDR_{limit-hazard\ level}}{IDR_{average}}$	
	BL-frame	MD-frame	BL-frame	MD-frame	BL-frame	MD-frame
50% in 50 years hazard, i.e. FOE (PGA _{FOE} =0.3 PGA _{DBE})	0.27	0.30	0.03	0.04	3.67	3.39
10% in 50 years hazard, i.e. DBE	1.01	1.03	0.18	0.11	1.98	1.95
2% in 50 years hazard, i.e. MCE (PGA _{MCE} =1.5 PGA _{DBE})	1.46	1.59	0.26	0.29	2.06	1.89

6.4.2.2 Accuracy in estimating roof displacement

The roof displacement results from the THA at the limit of the LS performance level are post-processed for the BL-frame and the MD-frame, and their average compared to those estimated by the respective design method. Table 6-7 presents the THA results. The average roof displacement for the MD-frame when the IDR reaches 0.02 is 0.255m, which is quite close to the value estimated by the proposed design method which is 0.286m, as shown in Table 6-4. The modified design overestimates the roof displacement by only 12%. While the roof displacement of the BL-frame can be calculated by multiplying the displacement analysis results in Figure D-4 in Appendix D by the displacement amplification factor of 0.7R, thus amounting to $0.7 \times 5 \times 0.1287 = 0.45\text{m}$, which is 71% higher than the THA result of 0.264m. Thus, the code of practice method highly overestimates displacement response which should be accurately appraised to account for pounding and separation distances. This conclusion about the exaggeration of the code displacement estimate is consistent with the findings of many other researchers, for example El Howary, H. (2009) among others.

Table 6-7 THA results for the roof displacement at IDR=2%

	EQ1	EQ2	EQ3	EQ4	EQ5	EQ6	EQ7	Average
BL-frame	0.277	0.267	0.255	0.295	0.220	0.285	0.246	0.264
MD-frame	0.248	0.228	0.241	0.301	0.270	0.287	0.212	0.255

6.4.2.3 Fragility analysis

In order to understand the performance and damage potential of the two designed frames in a probabilistic manner, fragility curves are developed for both the BL-frame and the MD-frame, by employing Incremental Dynamic Analysis as described in Chapter 4. The fragility curves provide the probability of exceeding a certain damage state versus the different intensities of earthquake. Because only 7 ground motion records are used in the fragility analysis, the results are considered quite approximate, yet appropriate for the purpose of the comparative study between the two-design method. The damage state is expressed as the limiting value of the IDR, and the earthquake intensity used is simply the PGA. The probability values are calculated by dividing the number of records whose responses reached the limiting state by the total number of records, as presented in Table 6-8 and Table 6-9 for the BL-frame and the MD-frame respectively. It can be observed from Figures 6-3 to 6-5 that the fragility curves for both frames are approximately the same, except for the collapse prevention level, where the consideration of this performance level in the design of the MD-frame results in it having a lower probability of exceedance given a certain seismic intensity, compared to the BL-frame. Nevertheless, such observation needs to be substantiated with more comprehensive fragility analysis employing a higher number of ground motion records. It should be noted that the IDR at the hazard (FOE, DBE and MCE) associated with each performance level (IO, LS and CP) is still way less than the target IDR limiting values, due to the inherent overstrength. From the results, it can be concluded that the use of the modified hybrid force/displacement method can result in structures that have higher reliability of achieving the targeted performance objectives, which, in addition to the advantage of considering multiple performance targets in a less iterative process, proves its suitability for performance-based design applications.

Table 6-8 Probability of exceedance of the three performance levels given an earthquake intensity, for the BL-frame

PGA/g	IDR for the seven ground motion records (%) given an earthquake intensity PGA/g							Probability of IDR greater than IDR _{Performance-Level}		
	EQ1	EQ2	EQ3	EQ4	EQ5	EQ6	EQ7	P(IDR _≥ IDR=1%)	P(IDR _≥ IDR=2%)	P(IDR _≥ IDR=3%)
0.28	0.72	0.69	0.89	0.91	0.90	0.73	0.74	0.00	0.00	0.00
0.35	0.88	0.84	0.99	1.08	1.38	0.93	0.97	0.29	0.00	0.00
0.39	0.95	0.94	1.01	1.00	1.00	1.04	1.10	0.71	0.00	0.00
0.42	1.04	1.03	1.01	1.41	1.85	1.13	1.22	1.00	0.00	0.00
0.49	1.26	1.19	1.17	1.76	1.81	1.30	1.23	1.00	0.00	0.00
0.56	1.46	1.27	1.46	2.04	1.64	1.40	1.46	1.00	0.14	0.00
0.63	1.54	1.32	1.91	2.02	1.73	1.47	1.74	1.00	0.14	0.00
0.70	1.59	1.48	2.37	1.92	2.03	1.59	1.99	1.00	0.29	0.00
0.77	1.70	2.20	2.32	2.59	2.24	1.85	2.16	1.00	0.71	0.00
0.84	1.80	2.95	2.22	4.30	2.31	2.05	3.19	1.00	0.86	0.29
0.91	1.88	3.63	3.27	6.53	2.28	2.17	4.86	1.00	0.86	0.57
0.98	2.01	4.39	5.19	-	2.45	2.29	7.12	1.00	1.00	0.57
1.02	2.00	4.70	8.46	-	3.18	2.34	8.37	1.00	1.00	0.71
1.05	2.29	4.98	-	-	4.40	2.40	9.12	1.00	1.00	0.71
1.09	2.50	5.16	-	-	5.63	2.46	-	1.00	1.00	0.71
1.19	3.40	5.51	-	-	-	2.86	-	1.00	1.00	0.86
1.26	-	-	-	-	-	3.34	-	1.00	1.00	1.00

Table 6-9 Probability of exceedance of the three performance levels given an earthquake intensity, for the MD-frame

PGA/g	IDR for the seven ground motion records (%) given an earthquake intensity PGA/g							Probability of IDR greater than IDR _{Performance-Level}		
	EQ1	EQ2	EQ3	EQ4	EQ5	EQ6	EQ7	P(IDR _≥ IDR=1%)	P(IDR _≥ IDR=2%)	P(IDR _≥ IDR=3%)
0.28	0.79	0.72	0.83	0.86	0.83	0.68	0.76	0.00	0.00	0.00
0.32	0.00	0.00	0.99	1.00	0.91	0.00	0.86	0.14	0.00	0.00
0.35	0.95	0.94	1.15	1.18	1.04	0.90	1.03	0.57	0.00	0.00
0.42	0.96	1.19	1.37	1.49	1.45	1.11	1.42	0.86	0.00	0.00
0.49	1.13	1.45	1.36	1.51	1.90	1.36	1.68	1.00	0.00	0.00
0.56	1.29	1.68	1.30	1.76	2.24	1.55	1.76	1.00	0.14	0.00
0.63	1.47	1.84	1.48	1.95	2.21	1.65	1.73	1.00	0.14	0.00
0.70	1.78	1.94	1.73	2.12	2.02	1.70	1.82	1.00	0.29	0.00
0.77	2.10	1.98	1.96	2.30	2.23	1.74	2.12	1.00	0.57	0.00
0.84	2.32	2.00	2.28	2.52	2.50	1.79	2.40	1.00	0.71	0.00
0.91	2.44	2.08	2.54	2.70	2.67	1.86	2.66	1.00	0.86	0.00
0.98	2.66	2.63	2.81	2.82	2.88	1.97	2.85	1.00	0.86	0.00
1.02	2.76	2.86	2.90	3.47	3.03	2.03	2.93	1.00	1.00	0.29
1.05	2.84	3.15	2.96	4.13	3.15	2.11	2.99	1.00	1.00	0.43
1.09	2.90	3.53	3.55	4.90	3.22	2.19	3.05	1.00	1.00	0.71
1.19	3.00	4.89	-	-	3.31	2.45	4.15	1.00	1.00	0.86
1.26	-	-	-	-	-	2.63	-	1.00	1.00	0.86
1.33	-	-	-	-	-	2.83	-	1.00	1.00	0.86

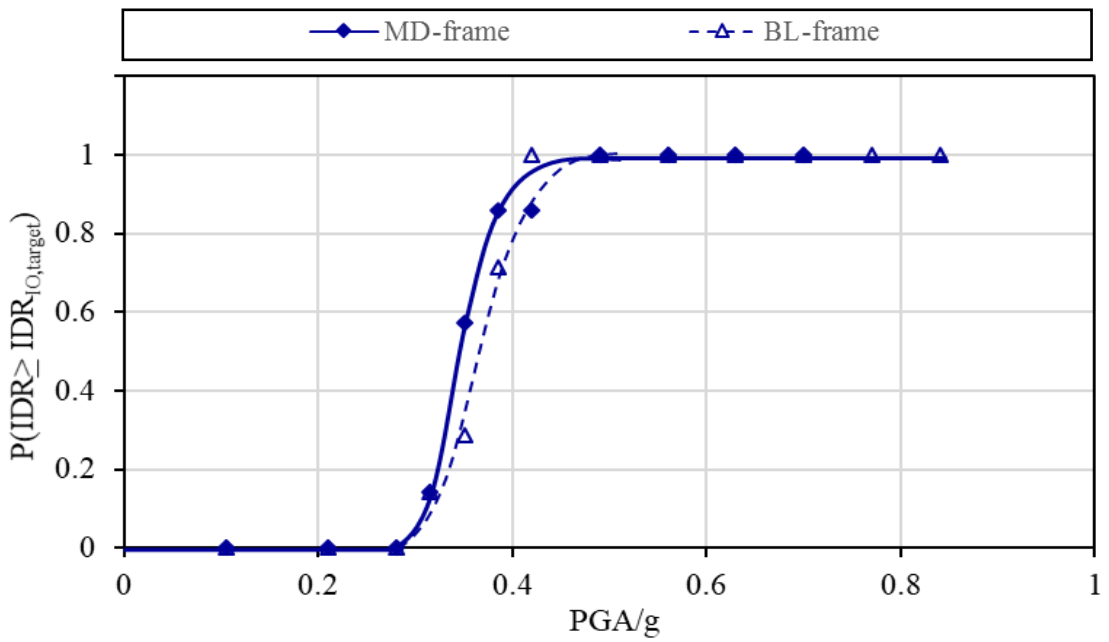


Figure 6-3 Fragility curves for the BL-frame and the MD-frame showing conditional probability of exceeding the IO performance level target IDR of 1%

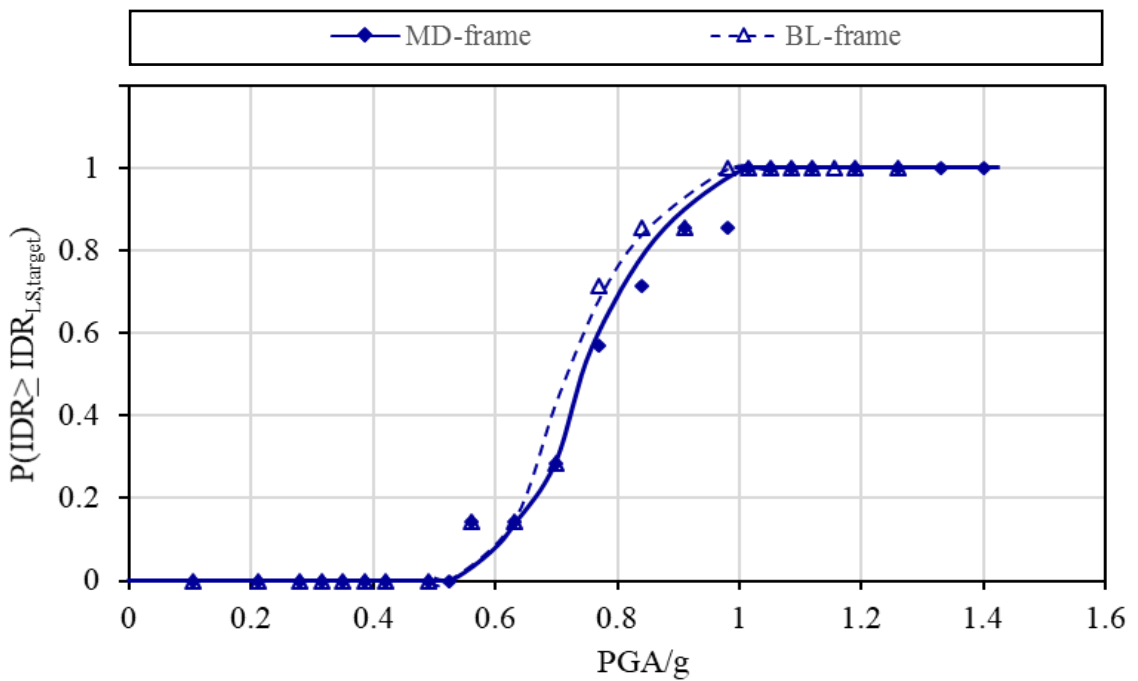


Figure 6-4 Fragility curves for the BL-frame and the MD-frame showing conditional probability of exceeding the LS performance level target IDR of 2%

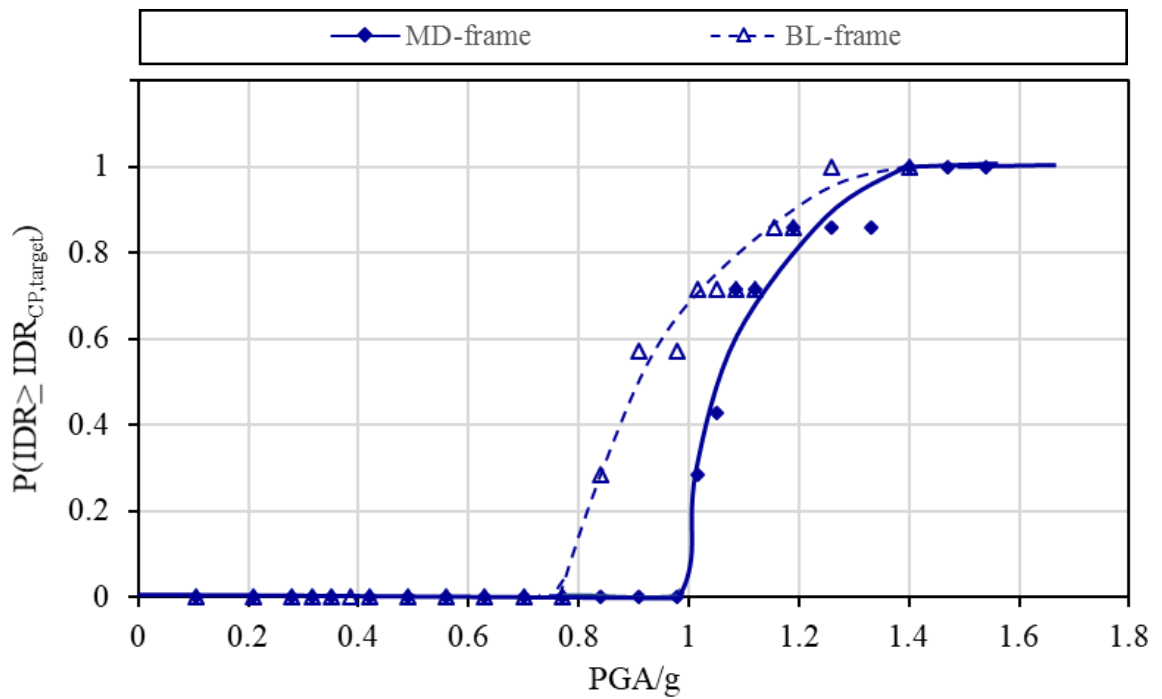


Figure 6-5 Fragility curves for the BL-frame and the MD-frame showing conditional probability of exceeding the CP performance level target IDR of 3%

CHAPTER 7

CONCLUSIONS AND RECOMMENDATIONS

7.1 INTRODUCTION

The present study is analytical/numerical in nature aiming to develop relations for estimating lateral displacement demand of low-to-medium RC moment-resisting frames that can be used for extension of a refined hybrid force-displacement (HFD) design methodology to RC structures. This chapter presents a summary of the research with the main conclusions and contribution. The limitations and the recommendations for future study are also discussed.

7.2 SUMMARY

The HFD method is a simple and direct seismic design procedure developed specifically for the purpose of performance-based design. The methodology uses preselected target inter-story drift values as key performance objectives to estimate the displacement demand which is then used as a design input parameter to determine a more realistic and performance-dependent reduction of elastic forces. This method eliminates the iterative steps required to satisfy the drift limiting criteria in traditional code design procedure. It additionally serves as a promising preliminary design method in the framework of the next-generation performance-based design, since it can design structures for various limit states associated with different levels of seismic input, and thus has better reliability of success in the subsequent performance assessment stage. The design parameters used for estimation of the displacement demand are simply the structural geometrical attributes; for example, the number of stories, the number of bays and the building height as well as the performance target objectives. The procedure involves formats common to design practitioners like the elastic pseudo-acceleration response spectrum and the force reduction factor. The HFD method has been well established and validated during the past 12 years for a variety of steel structures (Karavasilis et al., 2006-2008; Tzimas et al., 2013, 2017; Skalomenos et al., 2015; among others). This research serves as an initiative for extension of the HFD to concrete structures by proposing displacement estimating relations that can be used in the early

stage of design. Employing rigorous nonlinear modelling of RC moment-resisting frames, incremental dynamic analysis is performed to determine the earthquake intensity at which certain predefined damage levels are reached. Then, damage-window time-history analysis is conducted to monitor the displacement response at the determined loading levels associated with the pre-selected performance targets. The displacement response values are post-processed and analyzed. By utilizing nonlinear regression, equations are developed for estimation of the maximum roof displacement, and presented as displacement prediction charts. A design example (a case study) helps to prove the efficiency and higher reliability of the proposed HFD in achieving targeted performance of RC frames.

7.3 CONCLUSIONS AND CONTRIBUTIONS

The main conclusions drawn from this research are given below.

1. The HFD design method has been extended from steel structures to RC plane MRF's by developing a practical formula for estimating global displacement demand in terms of a performance measure which is the Inter-story drift ratio (IDR). The IDR is a major Engineering Demand Parameter (EDP) and a damage metric.
2. The proposed prediction equation has the following advantages:
 - It directly estimates displacement from the structure's geometrical properties (number of floors and number of bays) independent of any section dimensions so that it can be used at the beginning of design.
 - Performance is directly implemented into the predictive model, through the selected EDP, the IDR.
 - The equation is developed using a continuous scale of IDR's, and provides the IDR variable as values rather than levels. Therefore, it can be utilized with any improvement in the limiting values for performance levels and also with the future possibility of continuum between the discrete performance levels as advocated by the next-generation performance-based design guidelines.
 - The interaction of the different factors used in the equation and their relative contribution is well studied and captured by the prediction model. From the time-history analysis (THA) results, and the corresponding coefficients of the

regression equation, it is concluded that the IDR, followed by the number of floors, has the most significant effect on the displacement estimate (positively correlated factors, with interaction between them). The number of bays has a less significant, but negative correlation,

- The response data used for developing the formula are based on rigorous nonlinear time-history analysis that addresses material and geometrical nonlinearity (effect of P-delta), as well as stiffness degradation and strength deterioration which are typical characteristics of actual RC hysteretic behavior
- The displacement estimate inherently includes the inelastic displacement effects as well as the response of the multi-degree-of freedom structure.
- To an extent, the proposed predictive model can be considered as producing unbiased results with respect to the uncertainty associated with the earthquake loading, since it is based on averaging response to several ground motion records that have reasonable variability in their frequency and energy content. Still, interaction between the earthquake and structure characteristics affect the dispersion of the results.
- The calculated correlation coefficient of 0.98 and maximum absolute percentage error of 5.1% proves the accuracy of the proposed equation in estimating displacement demand.
- The developed displacement prediction equation, based on the parameters selected for study, fills a gap in the literature and can be readily used for performance-based seismic design combined with any other design method.

3. From the results of the case study design example, it is proved that

- THA results showed that the maximum roof drift (at the LS performance level) of the Modified-design (MD) structure, which is designed following the HFD method, is quite close to the values calculated by the proposed equation and assumed in the design. It also showed that the resulting inter-storey drift values fall below the target limiting values associated with each performance level. Therefore, the use of the proposed equation in combination with the HFD design method, can lead to structures that meet predefined performance objectives in terms of target inter-story drift, without the need for iteration or explicit drift check.

- The baseline (BL) frame designed in accordance with the ECP-201 (2007) excessively overestimated the maximum displacement, which can lead to cumbersome and unnecessary iterations, with no uniform indication of the real performance.
 - The MD-frame, designed according the HFD method, responded as intended in design with much improved performance over those of the corresponding BL-frame, for the added CP performance level, as indicated by the comparison of the fragility curves of the MD-frame and the BL-frame.
 - From the procedural viewpoint, the case study proves that the HFD method can complete the design directly in one step by considering the strength and deformation demands at the same time, while the code of practice method required many iterations after the deformation check step to reach the final design.
 - It is concluded that the HFD method can be successfully used for design of RC MRF's.
4. The HFD design method is a direct method, which requires no performance evaluation after the strength design step because the nonlinear behavior and performance criteria are built into the design process from the start i.e. the drift check is automatically accounted for. Compared to force-based methods, it minimizes the design iterations and avoids the oversimplified constant values of the force reduction factor. While compared to displacement-based procedures, it eliminates the errors introduced by the substitute SDOF approximation, and maintains the elastic domain of analysis with the conventional representation of earthquake action in terms of the pseudo-acceleration spectrum. Therefore, the HFD combines the advantages of both the force-based and displacement-based procedures.
5. The HFD design procedure is easy to follow and can identify the performance level which truly controls the design, and accordingly results in a structure with higher reliability in meeting the predefined performance levels. Therefore, the proposed method can be readily incorporated as a preliminary design method in the context of the broader next-generation performance-based design framework given in FEMA-445. This is especially advantageous for zones of low-to-medium seismicity where the added complexity of more complicated design methods cannot be justified.

7.4 LIMITATIONS AND RECOMMENDATIONS FOR FUTURE STUDY

1. The conclusions of the current research are confined to the assumptions and properties of the frame models utilized in development of the displacement prediction equation, which are
 - a. Code-compliant RC buildings with number of stories 4 to 10, number of bays 3 to 7, and fundamental period range of $0.5s < T_1 < 1.3s$
 - b. Moment-resisting frames with limited ductility as the main lateral load-resisting system.
 - c. Symmetrical geometries, where eccentricities and the associated torsional effects are neglected.
 - d. Equal floor heights along the building amounting to 3m.
 - e. Concrete has 28 days compressive cube strength of 25 MPa and steel of the reinforcing bars has 360 MPa yield strength.
 - f. Ground motions limited to normal far-source earthquakes with A/V ratio between 8 and 14 s^{-1} . Near-source earthquakes have rather distinctive characteristic which are not covered by this study.
 - g. Site conditions restricted to soils with deep deposits of dense or medium-dense sand, gravel or stiff clay, having an average shear wave velocity of the top 30m of the soil profile between 180 and 360 m/s and plasticity index between 70 and 250 kPa, which are the properties of soil class C, as described in the code.

Application of the proposed methodology to other structural systems, higher heights, and different site conditions needs further verification employing similar studies.
2. The numerical accuracy of the nonlinear model used in THA can be improved by
 - a. Using a greater number of ground motions with different characteristics.
 - b. Modeling soil-foundation-structure interaction.
 - c. Using more precise hysteretic characteristics, and modeling variations of confinement effect through the history of loading.
 - d. Including panel zone and bond slip effects.
 - e. Conducting correlation studies to calibrate the properties of the modelled structure against field results.
 - f. Including a parameter that reflect the initial stiffness assumed in the design.

3. The accuracy and applicability of the proposed displacement prediction equation can be enhanced by:
 - a. Incorporating a seismological estimator parameter that are regionally dependent.
 - b. Adding a parameter that reflects the different masonry-infill opening configuration.
 - c. Employing independent factors that reflect higher mode and p-delta effects depending on the number of floors.
4. As a compromise for the simplicity advantage, the HFD also adopts from the FBD method its limitation associated with the assumptions that the spectra for SDOF systems are valid for MDOF.
5. The author's recommendations for future study are
 - a. Extension of the HFD methodology to space frames, irregular frames and other RC structural systems such as shear wall buildings.
 - b. Including other damage and performance metrics in the HFD method for example, target yield mechanism, peak floor acceleration, and local curvature limits, for controlling structural and non-structural damage.
 - c. Developing more accurate story shear distribution relations for the different performance levels based on the results of THA, to be used in the HFD method.
 - d. Employing correction factors for the period of vibration of the structure (used for obtaining the spectral acceleration from the response spectrum) for performance levels associated with earthquakes of very high return period, in order to account for the considerable softening effects at this response level.
 - e. Converting the deterministic design format to a probabilistic one, for example designing with the aim that the odds of achieving a certain performance level can be reduced to an acceptable minimum (with the desired level of confidence). This probabilistic definition would be more rational given the uncertainties inherent to earthquake engineering and would follow the pathway of the next-generation performance-assessment framework.

REFERENCES

- Abd El Basset, Y. A. (2017). "Proposed Changes to Seismic Design Provisions of Framed Structures in the Egyptian Code for Design and Construction of Concrete Structures (ECP203-2007)." Master of Science Thesis. Faculty of Engineering Library, serial number XIIF/10646. Cairo University.
- Algan, B. B. (1982). "Drift and Damage Considerations in Earthquake Resistant Design of Reinforced Concrete Buildings." PhD thesis, University of Illinois, Urbana Champaign, USA.
- Akkar, S., Gulkan, P., and Yazgan, U. (2004). "A Simple Procedure to Compute the Interstory Drift for Frame Type Structures." *Proceedings: The 13th World Conference on Earthquake Engineering, August 1-6, Vancouver, B.C., Canada, Paper No. 2274*
- Aschheim, M. A. (2000). "The primacy of the yield displacement in seismic design." *In: Second US-Japan workshop on performance-based design of reinforced concrete buildings*, Sapporo, Japan, September 10-12.
- Aschheim, M. (1999). "Yield Point Spectra: A simple alternative to the Capacity Spectrum Method." *Report on SEAOC 1999 Convention, Reno, Nevada, USA.*
- Aschheim, M.A., and Black, E. F. (2000). "Yield point spectra for seismic design and rehabilitation." *Earthquake Spectra, EERI 2000*, 16(2), 317-35.
- Aslani, H., and Miranda, E. (2005). "Probabilistic earthquake loss estimation and loss disaggregation in buildings." *Report No. 157*, John A. Blume Earthquake Engineering Center, Stanford University, Stanford, USA.
- ATC. (1978). "Tentative provisions for the development of seismic regulations for buildings." *ATC-3-06*. Applied Technology Council, California, USA.
- ATC. (1996). "Seismic Evaluation and Retrofit of Concrete Buildings." *Report No. SSC96-01, ATC-40*, prepared by Applied Technology Council for California Seismic Safety Commission, Redwood City, California, USA.
- ATC. (2012a). "Seismic Performance Assessment Methodology for Buildings, Volume 1 – Methodology." *Report No. FEMA P58-1*, Federal Emergency Management Agency, Washington D.C., USA.
- ATC. (2012b). "Seismic Performance Assessment Methodology for Buildings, Volume 2 – Implementation Guide." *Report No. FEMA P-58-2*, Federal Emergency Management Agency, Washington D.C., USA.
- ATC. (2012c). "Seismic Performance Assessment Methodology for Buildings, Volume 3 – Supporting Electronic Materials." *Report No. FEMA P-58-3*, Federal Emergency Management Agency, Washington D.C., USA.
- ATC. (2016). "Guidelines for Nonlinear Structural Analysis for Design of Buildings: Part II – Reinforced Concrete Moment Frames." *ATC-114, draft report for Applied Technology Council Project*, Redwood City, California, USA.
- ATC. (2017). "Guidelines for Nonlinear Structural Analysis for Design of Buildings: Part III – Reinforced Concrete Moment Frames." *ATC-114, draft report for Applied Technology Council Project*, Redwood City, California, USA.
- Azak, T. E. (2013). "A Predictive Model for Maximum Interstory Drift Ratio (MIDR) and its Implementation in Probability-Based Design and Performance Assessment Procedures." PhD thesis, Civil Engineering, Middle East Technical University, Turkey.

References

- Azak T. E. and Akkar S. (2014). "A Predictive Model for Maximum Interstory Drift Ratio for Code Complying Low- and Mid-Rise Frame-Type Regular RC Buildings in Turkey." *Proceedings of the 2nd European Conference on Earthquake Engineering and Seismology*, Istanbul, Turkey.
- Bai, J-W., and Heuste, M. B. (2007) "Deterministic and Probabilistic Evaluation of Retrofit Alternatives for a Five-Story Flat-Slab RC Building." *MAE research center report*, Texas A&M University, USA.
- BSSC. (2009). "NEHRP recommended seismic provisions for new buildings and other structures." *Report FEMA-P750*, Building Seismic Safety Council, Washington D.C., USA.
- Bazeos, N. (2009). "Comparison of three seismic design methods for plane steel frames." *Soil Dynamics and Earthquake Engineering*, 29, 553– 562.
- Bazeos, N., and Beskos, D. E. (2003). "New seismic design method for building framed structures." In: *Atluri, S. N., Beskos, D.E., and Polyzos, D., (Eds.) Proceedings of international conference on computational and experimental engineering and sciences*, Corfu, Greece: Tech Science Press.
- Bazzurro, P., and Cornell, C. A. (1994). "Seismic hazard analysis for non-linear structures. I: Methodology." *ASCE Journal of Structural Engineering*, 120(11), 3320–3344.
- Bento, R. , Falcão, S., and Rodrigues, F. (2004). "Non-Linear Static Procedures in Performance-based Seismic Design." *13th World Conference on Earthquake Engineering*, Vancouver, B.C., Canada, Paper No. 2522 (August 1-6).
- Bertero, V. V. (1977). "Strength and deformation capacities of buildings under extreme environments." *Structural Engineering and Structural Mechanics*, Pister KS (ed.), Prentice Hall: Englewood Cliffs, NJ, 211– 215.
- Bertero, V., Bendimerad, M., and Shah, C. (1988). "Fundamental Period of Reinforced Concrete Moment Resisting Frame Structures." *Report no. 87, Stanford University*, Stanford, USA.
- Bommer, J., Elnashai, A. And Weir, A. G. (2000). "Compatible Acceleration and Displacement Spectra for Seismic Design Codes." *12th world Conference on Earthquake Engineering*, Auckland.
- Bradley, B. A., Dhakal, R. P., Mander, J. B., and Li, L. (2008). "Experimental multi-level seismic performance assessment of 3D RC frame designed for damage avoidance." *Earthquake Engineering and Structural Dynamics*, 37(1), 1-20.
- Broderick, B. M. (1994). "Seismic testing, analysis and design of composite frames." PhD thesis, Imperial College, London, UK.
- Broderick, B. M., and Elnashai, A. S. (1994). "Seismic resistance of composite beam-columns in multi-storey structures, Part 2: Analytical model and discussion of results." *Journal of Constructional Steel Research*, 30 (3), 231 -258.
- Broderick, B. M., Elnashai, A. S., and Izzudin, B. A. (1994). "Observations on the effect of numerical dissipation on the nonlinear dynamic response of structural systems." *Engineering Structures*, 16 (1), 51-62.
- Broderick, B.M. and Elnashai, A.S. (1995). "Proposal for behaviour factors for composite frames in Eurocode 8, European Seismic Design Practice: Research and Application." *Proceedings of the 5th SECED Conference*, Balkema, Rotterdam, pp. 333-340.
- Bursi, O.S. and Ballerini, M. (1996). "Behaviour of a steel-concrete composite substructure with full and partial shear connection." *Proceeding of the Eleventh World Conference on Earthquake Engineering*, Acapulco, Paper No. 771, 23-28.
- Calvi, G. M., Pampanin, S., Fajfar, P., and Dolsek, M. (2000). "New methods for assessment and design of structures in seismic zones: present state and research needs." *Engineering conference contributions*. Retrieved from

References

- https://ir.canterbury.ac.nz/bitstream/handle/10092/217/12587499_Main.pdf?sequence=1&isAllowed=y
- Carr, A. J. (2006). "Manual Ruauumoko." *Theory and User Guide to Associated Programs*. Department of Engineering, University of Canterbury, Christchurch, New Zealand.
- Casarotti C., and Pinho R. (2006). "Seismic response of continuous span bridges through fibre-based finite element analysis," *Journal of Earthquake Engineering and Engineering Vibration*, 5(1), 119-131.
- Chao S-H, Goel S. C. (2006a). "Performance-based design of eccentrically braced frames using target drift and yield mechanism." *AISC Engineering Journal*, Third quarter, 173–200.
- Chao S-H, Goel S. C. (2006b). "A seismic design method for steel concentric braced frames (CBF) for enhanced performance." *Proceedings of Fourth International Conference on Earthquake Engineering*, Taipei, Taiwan, 12–13 October, Paper No. 227.
- Chao, S.-H., Goel, S. C., and Lee, S.-S. (2007). "A Seismic Design Lateral Force Distribution Based on Inelastic State of Structures." *Earthquake Spectra*, Earthquake Engineering Research Institute, 23(3), August 2007, 547-569.
- Chao S-H, Goel S. C. (2008). "Performance-based plastic design of seismic resistant special truss moment frames." *AISC Engineering Journal*, Second quarter, 127–150.
- Chao S-H, Goel S. C., Lee S-S. (2007). "A seismic design lateral force distribution based on inelastic state of structures." *Earthquake Spectra*, 23(3), 547–569.
- Chopra, A. K. (2005). *Dynamics of Structures: Theory and Applications to Earthquake Engineering*, Second Edition, Prentice-Hall of India.
- Clough, R.W., and Penzien, J. (1993). *Dynamics of structures*, Mc Graw-Hill.
- Cornell, A. and Krawinkler, H. (2000). "Progress and Challenges in Seismic Performance Assessment." *PEER news*, April 2000.
- Cornell, C. A., M., Jalayer, F., Hamburger, R., and Foutch, D. A. (2002). "Probabilistic Basis for 2000 SAC Federal Emergency Management Agency Steel Moment Frame Guidelines." *Journal of Structural Engineering*, April 2002.
- CSI. (2013). *Analysis Reference Manual for SAP2000, ETABS, SAFE, CSI Bridge*. Computers and Structures, Berkeley, California.
- Dasgupta P., Goel S. C., Parra-Montesinos G. (2004). "Performance-based seismic design and behavior of a composite buckling restrained braced frame (BRBF)." *Proceedings of Thirteenth World Conference on Earthquake Engineering*, Vancouver, Canada, Paper No. 497.
- Dorra, E. (2011). "Greater Cairo Earthquake Loss Assessment and its Implications on the Egyptian Economy." Phd thesis, Imperial College, London, UK.
- ECP-201. (2012). "The Egyptian Code for calculation of Loads and forces on Structural and masonry works." Housing and Building National Research Center, Ministry of Housing, Building and Urban Planning, Cairo, Egypt.
- ECP-203. (2007) "The Egyptian Code of Practice No-203 for Design and Construction of Concrete Structures." Version 2013. Research Center for Housing and Construction, Cairo, Egypt.
- El Howary, H. A. (2009). "A Probabilistic Framework for Assessing Seismic Performance of Reinforced Concrete Moment Frame Buildings in Moderate Seismic Zones." Master of Science Thesis. Faculty of Engineering Library, serial number XIIF-8065. Cairo University.

References

- ElKassas, S. H. (2010). "Evaluation of Current Egyptian Seismic Code Approach to Estimation of Lateral Drift: Calibration of Displacement Amplification Factor for RC Ordinary Moment-Resisting Frame Buildings" Masters thesis, The American University in Cairo Press, Cairo, Egypt.
- ElKassas, S. H. and Haroun, M. A. (2012). "Evaluation of the Egyptian Seismic Code Approach to Estimation of Lateral Drift," *Proceedings of the 12th International Conference on Structures Under Shock and Impact*, WIT press, Chianciano Terme, Italy
- Elnashai, A. S. and Elghazouli, A. Y. (1993). "Performance of composite steel/concrete members under earthquake loading, Part I: Analytical model." *Earthquake Engineering and Structural Dynamics*, 22 (4): 15-345.
- Elnashai, A. S. and Izzuddin, B. A. (1993). "Modelling of Material Non-linearities in Steel Structures Subjected to Transient Dynamic Loading." *Earthquake Engineering and Structural Dynamics*, 22, 509-532.
- Elnashai, A. S., Mwafy, A. M., and Lee, D. (1999) "Collapse analysis of RC structures including shear, Structural Engineering in the 21st Century." *Proceedings of the 1999 Structures Congress*, New Orleans, Louisiana, American Society of Civil Engineers, Reston, Virginia, 195-198.
- ElNashai, A. S., Pinho, R., and Antoniou, S. (2000). "INDYAS – A Program for INelastic DYnamic Analysis of Structures." *Report No. ESEE 00-2*, Engineering Seismology and Earthquake Engineering.
- Elnashai, A.S and Mwafy, A.M. (2002), "Calibration of force reduction factors of RC Buildings." *Journal of Earthquake Engineering*, Imperial College Press, 6 (2), 239-273.
- Elnashai, A. S., Papanikolaou, V., and Lee D. H. (2003). "Zeus Non-linear: A system for inelastic analysis of structures." *User Manual*, version 1.8.7. Urbana-Champaign, IL, USA.
- El Tawil, S. and Deierlin, G. G. (1996) "Inelastic Dynamic Analysis of Mixed Steel-Concrete Space Frames." *Report No. 96* (5 May), School of Civil and Environmental Engineering, Cornell University, NY, USA.
- EN1998-1. (2004). "Eurocode 8 (EC8): Design of structures for earthquake resistance. Part 1: General rules, seismic actions and rules for buildings." *Doc CEN/TC250/SC8/N306*, European Committee for Standardization, Brussels, Belgium.
- Fajfar, P. (1999). "Capacity spectrum method based on inelastic demand spectra." *Earthquake Engineering and Structural Dynamics*, 28, 979-993.
- Fardis, M. (ed). (2010). *Advances in Performance-Based Earthquake Engineering*. Vol 13: Springer e-books.
- FEMA. (1997a). "NEHRP Guidelines for the Seismic Rehabilitation of Buildings." *Report FEMA-273*, prepared by the Applied Technology Council and the Building Seismic Safety Council, for the Federal Emergency Management Agency, Washington D.C., USA.
- FEMA. (1997b). "NEHRP Commentary on the Guidelines for the Seismic Rehabilitation of Buildings." *Report FEMA-274*, prepared by the Applied Technology Council and the Building Seismic Safety Council, for the Federal Emergency Management Agency, Washington D.C., USA.
- FEMA. (2000). "Pre-standard and Commentary for the Seismic Rehabilitation of Buildings." *Report FEMA-356*, prepared by the American Society of Civil Engineers for the Federal Emergency Management Agency, Washington D.C., USA.
- FEMA. (2001). "NEHRP recommended provisions for seismic regulations for new buildings and other structures." *Report FEMA-368*, Federal Emergency Management Agency, Washington D.C., USA.

References

- FEMA. (2005). "Improvement of Nonlinear Static Seismic Analysis Procedures." *Report FEMA-440*, prepared by the Applied Technology Council for the Federal Emergency Management Agency, Washington D.C., USA.
- FEMA. (2006). "Next-Generation Performance-Based Seismic Design Guidelines: Program Plan for New and Existing Buildings." *Report FEMA-445*, Washington D.C., USA.
- FEMA. (2017). "Recommended Simplified Provisions for Seismic Design Category B Buildings," *Report FEMA- P-1091*, Federal Emergency Management Agency under the National Earthquake Hazards Reduction Program (NEHRP), Washington D.C., USA.
- Franchin, P., Petrini, F., and Mollaioli, F. (2018). "Improved Risk-targeted Performance-based Seismic Design of Reinforced Concrete Frame Structures." *Earthquake Engineering and Structural Dynamics*, The Journal of the International Association for Earthquake Engineering, 47 (1), 49-67.
- Freeman, S. A. (1978). "Prediction of Response of Concrete Buildings to Severe Earthquake Motion." *Proceedings of Douglas McHenry International Symposium on Concrete and Concrete Structures*, Publication SP-55, American Concrete Institute, Detroit, Michigan, USA.
- Freeman, S. A. (1998). "The Capacity Spectrum Method as a Tool for Seismic Design." *Proceedings of the 11th European Conference on Earthquake Engineering*, Sept 6-11, Paris.
- Garg, R., Vemuri, J. and Subramaniam, K. (2019). "Correlating Peak Ground A/V Ratio with Ground Motion Frequency Content: Select Proceedings of SEC 2016." In book: *Recent Advances in Structural Engineering*, 2, 69-80. DOI: 10.1007/978-981-13-0365-4_6
- Gaetani d'Aragona, M., Polese, E., Cosenza, E., and Protta, A. (2018). "Simplified assessment of maximum interstory drift for RC buildings with irregular infills distribution along the height." *Bulletin of Earthquake Engineering*, September.
- Gasparini, D. A. and Vanmarcke, E. H. (1976). "SIMQKE a Program for Artificial Motion Generation: User's Manual and Documentation." Department of Civil Engineering, Massachusetts Institute of Technology, USA.
- Ghobarah, A. (2004). "On Drift limits associated with different damage levels" *International workshop on Performance based design: concepts and implementations*. Retrieved from https://www.researchgate.net/publication/272353679_On_drift_limits_associated_with_different_damage_levels
- Goel S. C., Chao S-H. (2008). "Performance-Based Plastic Design: Earthquake Resistant Steel Structures." International Code Council, Washington D.C., USA.
- Goel, S. C., Liao, W.-C., Mohammad, R. B., and Chao, S.-H. (2009a). "Performance-based plastic design (PBPD) method for earthquake-resistant structures: an overview." *The Structural Design of Tall and Special Buildings*, CTBUH.
- Goel, S. C., Liao, W.-C., Mohammad, R. B., and Leelataviwat, S. (2009b). "An Energy Spectrum Method for Seismic Evaluation of Structures." *Conference on improving the seismic performance of existing buildings and other structures, ATC & SEI Conference*, San Francisco, California, USA.
- Gulkan, P. and Sozen, M. A. (1999). "Procedure for determining seismic vulnerability of building structures." *ACI structural Journal*, 96(3), 336-342.
- Hamburger, R. (1998). "Performance Based Analysis and Design Procedure for Moment Resisting Steel Frames." *Background Document, SAC Steel Project*, September 10.
- Hamburger, R., Rojahn C., Moehle, J., Bachman, R., Comartin C., and Whittaker, A. (2004). "The ATC-58 Project: Development of Next-Generation Performance-Based Earthquake Engineering Design Criteria for Buildings." *Proceedings of the 13th World Conference on Earthquake Engineering*, Vancouver, B.C., Canada, August 1-6, Paper No. 1819.

References

- Hamburger, R. and Moehle, J. (2010). "Performance-Based Seismic Design of Tall Buildings in the Western United States." In: *Fardis, Michael N. (Ed). Advances in Performance-Based Earthquake Engineering*. Vol 13: Springer e-books, 125-135.
- Hamburger, R. (2011). "Introduction of Performance Criteria into Chapter 1 of ASCE 7-10." *2011 Structures Congress Proceedings, Section: Extreme Loads*, Las Vegas, Nevada, USA, April 14-16, 1432-1439.
- Hamburger, R. (2014). "FEMA P-58 Seismic Performance Assessment of Buildings." Tenth U.S. National Conference on Earthquake Engineering (10NCEE), *Frontiers of Earthquake Engineering*, Anchorage, Alaska, July 21-25.
- Hamburger, R. (2017). "ATC-58-2: Probabilistic Performance-based Seismic Assessment and Design Guidelines." *2017 SEAOC Convention Proceedings*, San Francisco, California, USA.
- Heidebrecht, A.C. and Stafford Smith, B. (1973). "Approximate analysis of tall wall-frame structures." *Journal of Structural Division*, ASCE, 99(2), 199-221.
- Heintz, J. A., Hamburger, R. O. and Mahoney, M. (2014). "FEMA P-58 Phase 2 – Development of Performance-Based Seismic Design Criteria." *Tenth U.S. National Conference on Earthquake Engineering Frontiers of Earthquake Engineering*, July 21-25, Anchorage, Alaska.
- Hellesland, J. and Scordelis A. (1981). "Analysis of RC bridge columns under imposed deformations." *IABSE Colloquium on advanced mechanics of reinforced concrete*, Delft, Holland, Final Report, 545-559.
- Housner, G. W. (1956). "Limit design of structures to resist earthquakes." *Proceedings of First World Conference on Earthquake Engineering*, Earthquake Engineering Research Institute, Berkeley, CA, USA, June (Part 5), 1–11.
- Housner, G. W. (1960). "The plastic failure of structures during earthquakes." *Proceedings of Second World Conference on Earthquake Engineering*, Tokyo, Japan, July 11–18, 997–1012.
- Iervolino, I., Maddaloni, G. and Cosenza, E. (2008). "Eurocode 8 Compliant Real Record Sets for Seismic Analysis of Structures." *Journal of Earthquake Engineering*, 12, 54–90, 2008 Copyright © A.S. DOI: 10.1080/13632460701457173
- Izzuddin, B. A. and Elnashai, A. S. (1989). "ADAPTIC – a program for adaptive large displacement elastoplastic dynamic analysis of steel, concrete and composite frames." *Research Report ESEE Report No. 89/7*, Imperial College, London, UK.
- Izzuddin, B. A. (1991). "Nonlinear dynamic analysis of framed structures." PhD thesis, Imperial College, University of London, UK.
- Izzuddin, B. A. and Elnashai, A. S. (1993). "Eulerian Formulation for large displacement analysis of space frames." *Journal of Engineering Mechanics Div.*, ASCE, Vol. 119(3), 549-569.
- Jeong, S-H. and Elnashai, A. S. (2004). "Analytical Assessment of an Irregular RC Full Scale 3D Test Structure." Report, Department of Civil and Environmental Engineering University of Illinois at Urbana-Champaign Urbana, Illinois, March.
- Jeong, S., and Elnashai, A. S. (2005). "Analytical Assessment of an Irregular RC Frame for Full-Scale 3D Pseudo-Dynamic Testing. Part I: Analytical Model Verification." *Journal of Earthquake Engineering*, 9(1), 95-128.
- Jiang, H., Lu, X. and Kubo, T. (2009). "Maximum Displacement Profiles of Reinforced Concrete Frames," *Journal of Asian Architecture and Building Engineering*, 8(1), May, 183-190.
- Kappos, A.J., Stylianidis, K.C. and Pitilakis, K. (1998). "Development of seismic risk scenarios based on a hybrid method of vulnerability assessment." *Journal of Natural Hazards*, 17(2), 177-192.

References

- Kappos, A. J. (1997). "A comparative assessment of RJC structures designed to the 1995 Eurocode 8 and the 1985 CEB seismic code." *The Structural Design of Tall Buildings*, 6 (1), 59-83.
- Karavasilis, T. L., Bazeos, N., and Beskos, D. E. (2006a). "Maximum displacement profiles for the performance-based seismic design of plane steel moment resisting frames." *Engineering Structures*, 28(1): 9-22.
- Karavasilis, T. L., Bazeos, N., and Beskos, D. E. (2006b). "A hybrid force/displacement seismic design method for plane steel frames." In: *Mazzolani, F. and Wada, A. (eds), Behavior of Steel Structures in Seismic Area, Proceedings of STESSA Conference*, Yokohama, Japan, Taylor & Francis, 39-44.
- Karavasilis, T. L., Bazeos, N., and Beskos, D. E. (2006c). "A hybrid force/displacement seismic design method for plane steel frames." *Proceedings of 1st European conference on earthquake engineering and seismology (1st ECEES)*, Geneva, Switzerland, 3-8 September, Paper No 1013.
- Karavasilis, T. L., Bazeos, N., and Beskos, D. E. (2007a). "Estimation of Seismic Drift and Ductility Demands in Planar Regular X-Braced Steel Frames." *Earthquake Engineering and Structural Dynamics*, 36(15), 2273-2289.
- Karavasilis, T. L., Bazeos, N., and Beskos, D. E. (2007b). "Behavior factor for performance-based seismic design of plane steel moment resisting frames." *Journal of Earthquake Engineering*, 11(4), 531-559.
- Karavasilis, T. L., Bazeos, N., and Beskos, D. E. (2008a). "A Hybrid Force/Displacement Seismic Design Method for Steel Building Frames." *The 14th world conference on Earthquake engineering*, October 12-17, Beijing, China.
- Karavasilis, T. L., Bazeos, N., and Beskos, D. E. (2008b). "Drift and ductility estimates in regular steel MRF subjected to ordinary ground motions: a design-oriented approach." *Earthquake Spectra*, 24(2), 431-51.
- Karavasilis, T. L., Bazeos, N., and Beskos, D. E. (2008c). "Seismic response of plane steel MRF with setbacks: estimation of inelastic deformation demands." *Journal of Constructional Steel Research*, 64(6), 644-654.
- Karavasilis, T. L., Bazeos, N., and Beskos, D. E. (2008d). "Estimation of seismic inelastic deformation demands in plane steel MRF with vertical mass irregularities." *Engineering Structures* 30(11), 3265-3275.
- Karavasilis, T. L., Bazeos, N., and Beskos, D. E. (2009). "Comparison of Two Currently used and One Proposed Seismic Design Methods for Steel Structures." In: *Pantelakis, S. and Rodopoulos, C. (Eds), Engineering Against Fracture: Proceedings of the 1st Conference* ©Springer Science + Business Media, B.V.
- Karavasilis T. L., Makris, N., Bazeos, N., and Beskos D. E. (2010). "Dimensional response analysis of multi-storey regular steel MRF subjected to pulse-like earthquake ground motions." *Journal of Structural Engineering (ASCE)*, 136 (8).
- Karavasilis T. L., Bazeos, N. and Beskos, D. E. (2010). "A new Seismic Design Method for Steel Structures." In: *Fardis, M.N. (Ed). Advances in Performance-Based Earthquake Engineering (Chapter 15)*. Vol 13: Springer e-books.
- Katsanos, E. I. and Vamvatsikos, D. (2017). "Yield frequency spectra and seismic design of code-compatible RC structures: an illustrative example." *Earthquake Engineering & Structural Dynamics*, 46(11), 727-1745.
- Kramer, S. L. (2011). "Performance-based design in geotechnical earthquake engineering practice." *Proceedings of the 5th international conference on earthquake geotechnical engineering on invited state-of-the-art paper*, Santiago, Chile.

References

- Kramer, S. L. (2014). "Performance-based design methodologies for geotechnical earthquake engineering." *Bulletin of Earthquake Engineering*, 12(3), 1049–1070.
- Krawinkler, H. and Miranda, E. (2004). "Performance-Based Earthquake Engineering." *In: Bertero V.V. and Bozorgnia, Y. (Eds). Earthquake Engineering from Engineering Seismology to Performance-based Engineering*, CRC Press, FL.
- Kutner, M., Nachtsheim, C., Neter, J. & Li, W. (2005). *Applied Linear Statistical Models*. 5th ed. McGraw-Hill. Page 289.
- Lee, D. (1999). "Inelastic seismic analysis and behavior of RC bridges", PhD thesis, Imperial College, University of London, UK.
- Lee, S-S and Goel, S. C. (2001). "Performance-Based design of steel moment frames using target drift and yield mechanism." *Research Report no. UMCEE 01-17*, Dept. of Civil and Environmental Engineering, University of Michigan, Ann Arbor, MI, USA.
- Leelataviwat, S., Goel, S. C., and Stojadinovic, B. (1999). "Toward performance-based seismic design of structures." *Earthquake Spectra*, 15(3), 435–461.
- Leelataviwat, S., Saewon, W., and Goel, S. C. (2007). "An energy-based method for seismic evaluation of structures." *Proceedings of Structural Engineers Association of California Convention, SEAOC 2007*, Lake Tahoe, CA, USA, 26–29 September, 21–31.
- Liao, W.-C. and Goel S. C. (2010a). "Performance-Based Plastic Design (PBPD) of Reinforced Concrete Special Moment Frame Structures." *The 3rd Congress of the International Federation for Structural Concrete (fib)*, Washington D.C., USA.
- Liao, W.-C. and Goel S. C. (2010b). "Performance-Based Plastic Design (PBPD) of Reinforced Concrete Special Moment Frame Structures." *9th US National and 10th Canadian Conference on Earthquake Engineering (9USN/10CCEE)*, Toronto, Canada.
- Liao, W.C., and Goel, S. C. (2014). "Performance-Based Seismic Design of RC SMF Using Target Drift and Yield Mechanism as Performance Criteria." *Advances in Structural Engineering*, 17(4), Multi-Science Publishing Co Ltd, 529-543.
- Lin, Y. Y. and Miranda, E. (2004). "Non-Iterative Capacity Spectrum Method Based on Equivalent Linearization for Estimating Inelastic Deformation Demands of Buildings." *Journal of Structural Mechanics and Earthquake Engineering*, JSCE, No. 733/I-69.
- Liu, L., Li, S., and Zhao, J. (2018). "A novel non-iterative direct displacement-based seismic design procedure for self-centering buckling-restrained braced frame structures." *Bulletin of Earthquake Engineering*, 16(11), 5591–5619.
- Loeding, S., Kowalsky, M. J. and Priestley, M. J. N. (1998). "Direct Displacement-based Design of Reinforced Concrete Building Frames." *Report No. SSRP-98/08*, University of California, San Diego, California, USA.
- Madas, P. J. and Elnashai, A. S., (1992). "A new passive confinement model for the analysis of concrete structures subjected to cyclic and transient dynamic loading." *Earthquake Engineering & Structural Dynamics*, 21(5), 409-431.
- Mahmoudi M. and Zaree, M. (2013). "Performance Based Design Using Force Reduction Factor and Displacement Amplification Factors for BFS." *Asian Journal of Civil Engineering*, (BHRC), 14(4), 577-586
- Mander, J. B., Priestley, M. J. N., and Park, R. (1988). "Theoretical Stress-Strain Model for Confined Concrete." *Journal of Structural Engineering*, ASCE, 114 (8),1804-1826.

References

- Mansour, A. M. (2015). "Evaluation of the Force Reduction Factor for Steel Eccentric Braced Frames." Master of Science Thesis. Faculty of Engineering Library, serial number XIIIIF/9935. Cairo University.
- Mari A., Scordelis, A. (1984). "Nonlinear geometric material and time dependent analysis of three dimensional reinforced and prestressed concrete frames." *SESM Report 82-12*, Department of Civil Engineering, University of California, Berkeley, USA.
- Martinez-Rueda, J. E. (1997). "Energy dissipation devices for seismic upgrading of RC structures." PhD thesis, Imperial College, University of London, UK.
- Martinez-Rueda, J. E. and Elnashai, A. S. (1997). "Confined concrete model under cyclic load", *Materials and Structures*, 30 (3), 139-147.
- MATLAB. (2009). *The Language of Technical Computing*, The MathWorks, Inc. USA.
- Mehanny, S. S. and Deierlein, G. G. (2000). "Modeling and assessment of seismic performance of composite frames with reinforced concrete columns and steel beams." *Report No. 136, The John A. Blume Earthquake Engineering Center*, Stanford University, Stanford, USA.
- Miranda, E. and Akkar, S. D. (2006). "Generalized Interstory Drift Spectrum." *Journal of Structural Engineering*, ASCE, June, 840-852.
- Miranda, E., and Aslani, H. (2003). "Probabilistic response assessment for building specific loss estimation." *Rep. No. 2003-03*, PEER, Pacific Earthquake Engineering Research Center.
- Miranda, E. (1992). "Nonlinear response spectra for earthquake resistant design." *Proceedings of the Tenth World Conference on Earthquake Engineering*, Balkema, Rotterdam, 5835-5840.
- Moehle, J. P. (1984). "Strong Monitor Drift Estimates for R/C Structures." *Journal of Structural Engineering*, 110(9), 1988-2001.
- Moehle, J. P. (2003). "A framework for performance-based earthquake engineering." *Proceedings of the Tenth U.S.-Japan Workshop on Improvement of Building Seismic Design and Construction Practices*, Report ATC-15-9, Applied Technology Council, Redwood City, CA, USA.
- Moehle, J. P. and Deierlein, G. G. (2003). "A Framework Methodology for Performance-based Earthquake Engineering." *Proceedings of the 13th World Conference on Earthquake Engineering*, Paper 679.
- Mohammadi, R. K. and El Naggar, M. H. (2004). "Modifications on Equivalent Lateral Force Method." *13th World Conference on Earthquake Engineering*, Vancouver, B.C., Canada, August 1-6, Paper No. 928
- Morillas, L., Benavent-Climent, A., and Escolanomargarit, D. (2014). "Seismic Performance of Common Reinforced Concrete Moment Resisting Frame Structures." *Second European Conference on Earthquake Engineering and Seismology*, Istanbul, Aug 25-29.
- Mwafy, A. M. (2001). "Seismic performance of code designed RC buildings." PhD thesis, Department of Civil and Environmental Engineering, Imperial College, London, UK.
- Nassar A. A., and Krawinkler H. (1991). "Seismic demands for SDOF and MDOF systems." *Report No. 95*, The John A. Blume Earthquake Engineering Center, Stanford University, Stanford, USA.
- Neuenhofer A., Filippou F. C. (1997). "Evaluation of nonlinear frame finite-element models." *Journal of Structural Engineering*, 123(7), 958-966.
- Newmark, N. M. and Hall, W. J. (1973). "Procedures and criteria for earthquake resistant design." *Building Science Series No. 46*, National Bureau of Standards, U.S. Dept. of Commerce, Washington D.C., USA.

References

- Newmark, N. M. and Hall, W. J. (1982). *Earthquake Spectra and Design*. Earthquake Engineering Research Institute, Berkeley, California.
- NZS. (1995). "Concrete Structures Standard - Part 1: The Design of Concrete Structures; Part 2: Commentary on the Design of Concrete Structures." *Standards (NZS 3101)-New Zealand*, Wellington, New Zealand.
- OpenSees Development Team. (2006). "OpenSees: Open System for Earthquake Engineering Simulation Manual, OpenSees, version: 2.0.0." Pacific Earthquake Engineering Research Center, University of California, Berkeley, California, USA.
- Osteraas, J. D. and Krawinkler, H. (1990). "Strength and ductility considerations in seismic design." Report No. 90, John A. Blume Earthquake Engineering Center, Department of Civil Engineering, Stanford University, Stanford, USA.
- Pantelakis, S. and Rodopoulos, C. (Eds). (2009). *Engineering Against Fracture: Proceedings of the 1st Conference* ©Springer Science + Business Media B.V.
- Pauley, T. and Priestley, M. J. N. (1992). *Seismic Design of Reinforced Concrete and Masonry Buildings*. John Wiley, New York.
- Piana, C., Qiana, J., Muhoa, E. V., and Beskos, D. E. (2018). "A hybrid force/displacement seismic design method for reinforced concrete moment resisting frames." *Soil Dynamics and Earthquake Engineering*, in press, available online Sept. 2018. Retrieved from <https://doi.org/10.1016/j.soildyn.2018.09.002>
- Pinho, R., (2000). "Selective repair and strengthening of RC buildings." PhD thesis, Imperial College, University of London, London, UK.
- Priestley, M. J. N. and Kowalsky, M. J. (1998). "Aspects of drift and ductility capacity of rectangular cantilever structural walls." *Bulletin of the New Zealand National Society for Earthquake Engineering*, NZNSEE, 31(2), 73–85.
- Priestley, M. J. N. and Kowalsky, M. J. (2000). "Direct Displacement-Based Design of Concrete Buildings." *Bulletin of the New Zealand National Society for Earthquake Engineering*, 33(4), December (ISSN 0110-0718), 421-444
- Psycharis, I. N., Papastamatiou, D. Y., and Alexandris, A. P. (2000). "Parametric investigation of the stability of classical columns under harmonic and earthquake excitations." *Earthquake Engineering and Structural Dynamics*, 29(8), 1093–1109.
- Rai, D., (2000). "Future Trends in Earthquake-resistant Design of Structures." *Current Science*, 79(9), (10 November)
- Ramadan, M. M. (2016). "Assessment of Seismic Response Reduction Factor of Multistory Reinforced Concrete Framed Structures using Nonlinear Dynamic Analysis." Master of Science Thesis. Faculty of Engineering Library, serial number XIIF/10191. Cairo University.
- Rossetto, T. (2002). "Prediction of deformation capacity of non-seismically designed reinforced concrete members." *Proceedings of the 7th U.S. National Conference on Earthquake Engineering: Urban Earthquake Risk*, Earthquake Engineering Research Institute, Oakland, California, USA. CD-ROM.
- SAC. (2000). "Recommended Seismic Design Criteria for New Steel Moment-Frame Buildings." report no FEMA-350, developed by the SAC Joint Venture for the Federal Emergency Management Agency, Washington D.C., USA.
- Salari, M. R., Spacone, E., Shing, P. B., and Frangopol, D. M. C. (1998). "Nonlinear analysis of composite beams with deformable shear connectors." *Journal of Structural Engineering*, 124(10), 1148–1158.

References

- Spacone E., Ciampi V., and Filippou F.C. (1996) "Mixed formulation of nonlinear beam finite element." *Computers & Structures*, 58(1), 71-83.
- SEAOC. (1959). "Recommended lateral force requirements and commentary, First Edition." Seismology Committee, Structural Engineers Association of California, Sacramento, California, USA
- SEAOC. (1980). "Recommended lateral force requirements and commentary, Fourth Edition Revised." Seismology Committee, Structural Engineers Association of California, Sacramento, California, USA.
- SEAOC. (1995). "Vision 2000: Performance-Based Seismic Engineering of Buildings." Structural Engineers Association of California, Sacramento, California, USA.
- SEAOC. (1999). "Blue book or Recommended Lateral Force Requirements and Commentary (7th Edition)." Seismology Committee, Structural Engineers Association of California, Sacramento, California, USA.
- SEI. (2010). "ASCE 7-10 Minimum Design Loads for Buildings and Other Structures." American Society of Civil Engineers, Reston, VA, USA.
- SEI. (2006). "ASCE 41 Standard for Seismic Rehabilitation of Existing Buildings." American Society of Civil Engineers, Structural Engineering Institute, Reston, VA, USA.
- Seismosoft. (2008). *Seismosignal v 3.2.0*, www.seismosoft.com.
- Seismosoft. (2013). "SeismoStruct – A Computer Program for Static and Dynamic Nonlinear Analysis of Framed Structures." *Manual*. www.seismosoft.com.
- Shome, N., Cornell, C. A., Bazzurro, P., and Carballo, J. E. (1998). "Earthquakes, records, and nonlinear responses." *Earthquake Spectra*, 14(3), 469-500.
- Silva, W.P. and Silva, C.M.D.P.S. (2011). "LAB Fit Curve Fitting Software (Nonlinear Regression and Treatment of Data Program)." V 7.2.48. www.labfit.net
- Skalomenos, K. A., Hatzigeorgiou, G. D., and Beskos, D. E. (2015). "Application of the hybrid force/displacement (HFD) seismic design method to composite steel/concrete plane frames." *Journal of Constructional Steel Research*, 115, 179-190.
- Smyrou, E., Priestley, M. J. N., and Carr, A. J. (2012). "Modelling of elastic damping in nonlinear time-history analyses of cantilever RC walls." *Bulletin of Earthquake Engineering*, 9, 1559 – 1578.
- Stamatopoulos, H. and Bazeos N. (2011). "Seismic inelastic response and ductility estimation of steel planar chevron-braced frames." In: Boudouvis AG, Stavroulakis GE, Eds. Proceedings of 7th GRACM conference on computational mechanics, Athens, Greece, 30 June-2 July.
- Tzimas, A. S., Karavasilis, T. L., Bazeos, N., and Beskos, D. E. (2013). "A Hybrid force/displacement seismic design method for steel building frames." *Engineering Structures*, 56, 1452-1463.
- Tzimas, A. S., Karavasilis, T. L., Bazeos, N., Beskos, D. E. (2017). "Extension of the hybrid force/displacement (HFD) seismic design method to 3D steel moment-resisting frame buildings." *Engineering Structures*, 147, 486-504.
- Vamvatsikos, D. and Aschheim, M. A. (2016). "Performance-based seismic design via yield frequency spectra." *Earthquake Engineering & Structural Dynamics*, 45(11), 1759–1778.
- Varughese, J. A., Menon, D. and Prasad, A. M., (2012) "Simplified Procedure for Displacement-based Design of Stepped Buildings." *15th World conference on Earthquake Engineering (WCEE)*, Lisboa, Portugal.
- Veletsos, A. S. and Newmark, N. M. (1960) "Effect of inelastic behavior on the response of simple systems to earthquake motions." *Proceedings of the World Conference on Earthquake Engineering*, Japan, 2, 895–912.

References

- Whittaker, A., Deierlein, G., Hooper, J. and Merovich, A. (2004). "Engineering Demand Parameters for Structural Framing Systems." *Report number: ATC-58-2-2.2*, Applied Technology Council, USA.
- Yang, T. Y., Moehle, J. P., Stodjadinovic, B. and Der Kiureghian, A. (2006). "An Application of the PEER Performance-based Earthquake Engineering Methodology." *Proceedings of the 8th U.S. National Conference on Earthquake Engineering*, Paper No.1448.
- Zotos, P. C. and Bazeos, N. (2009). "Estimation of seismic response in planar x-braced multi-storey steel frames." *Proceedings of 2nd international conference on computational methods in structural dynamics and earthquake engineering*, Island of Rhodes, Greece, 22–24 June, Paper CD364.

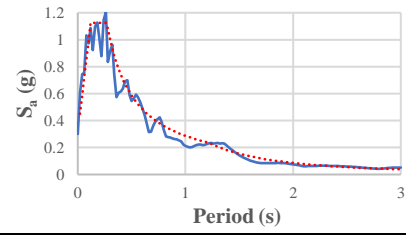
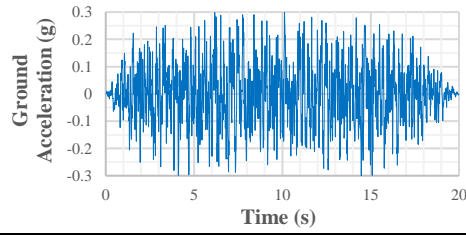
APPENDIX A

Earthquake
Reference

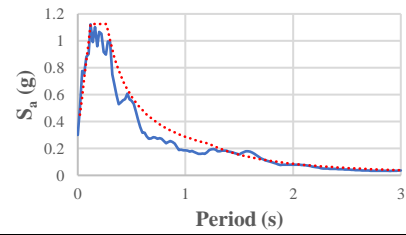
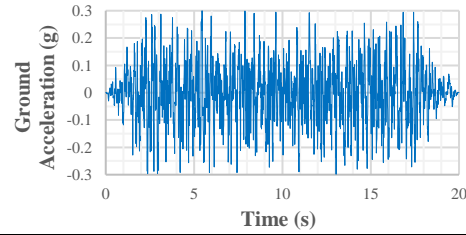
(a) Accelerogram

(b) 5% damped Spectrum

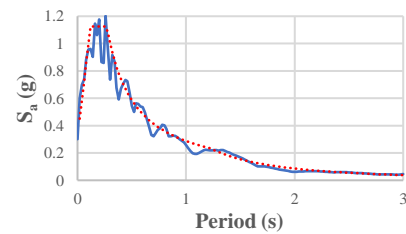
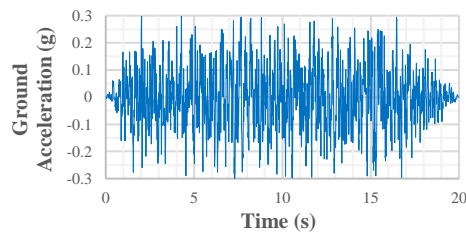
EQ1



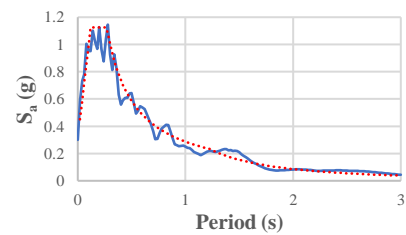
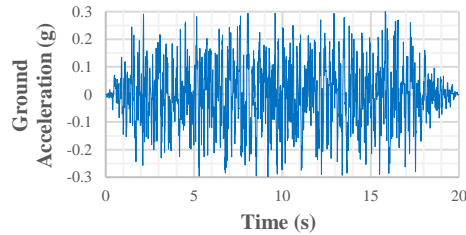
EQ2



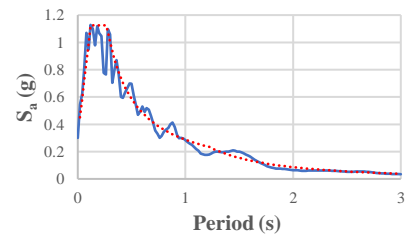
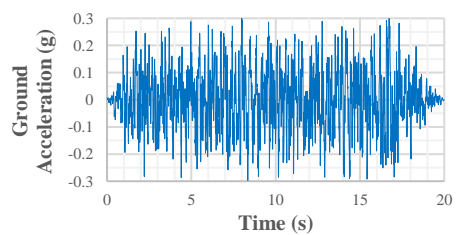
EQ3



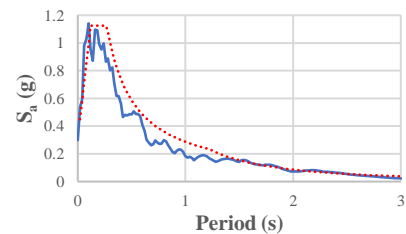
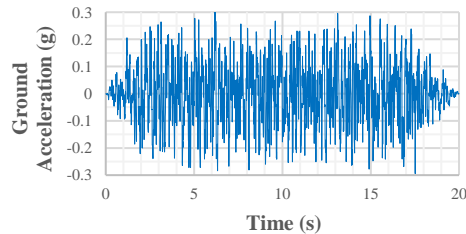
EQ4



EQ5



EQ6



EQ7

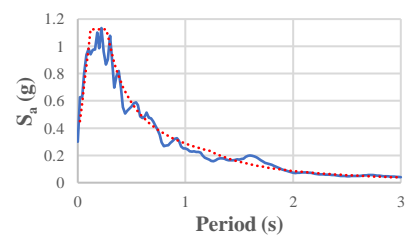
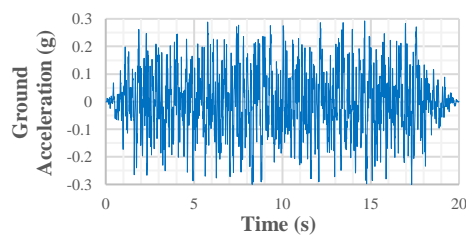


Figure A-1: Artificial ground motion records accelerograms and pseudo-acceleration spectra

APPENDIX B

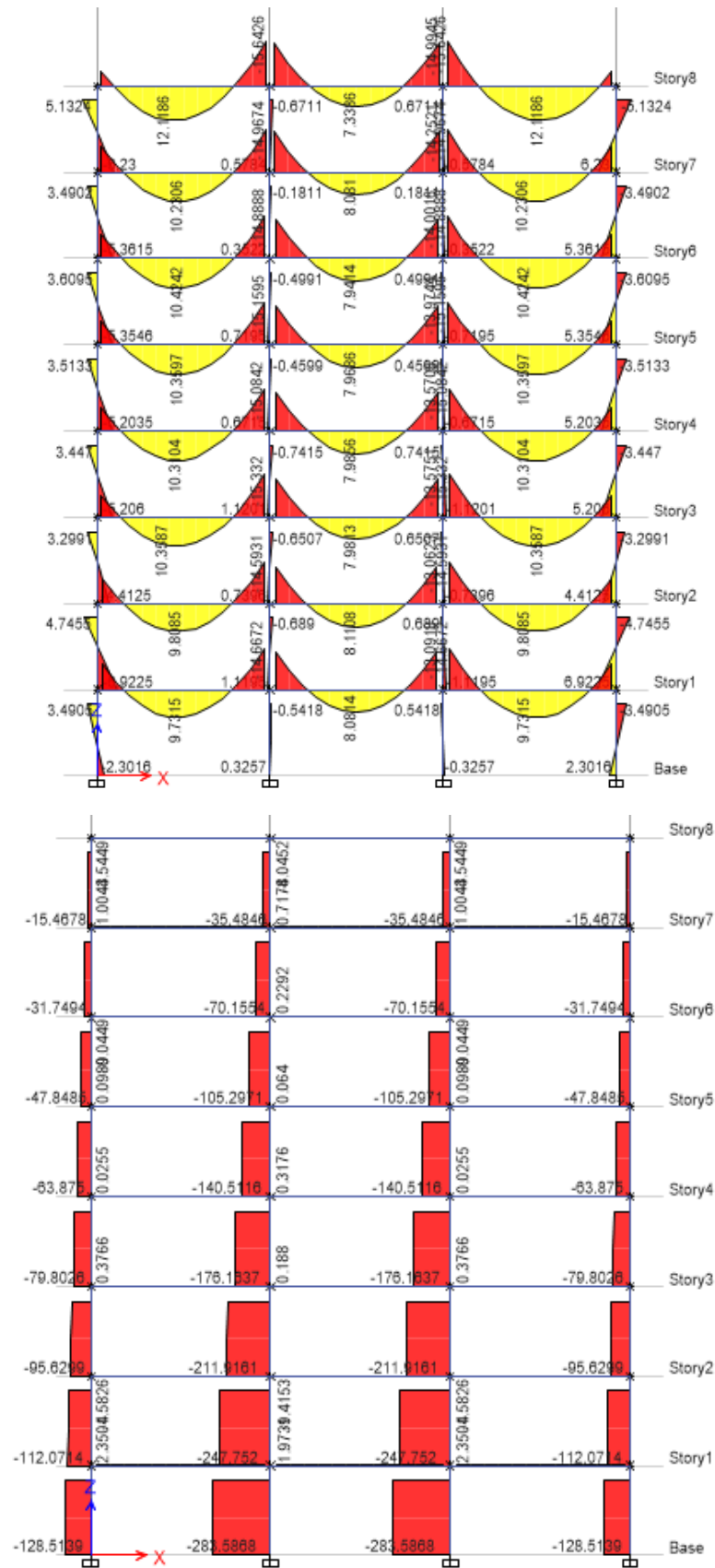


Figure B-1 Bending moment diagram (up) and axial force diagram (down) for the case study frame under the gravity load combination (Etabs output)

APPENDIX C

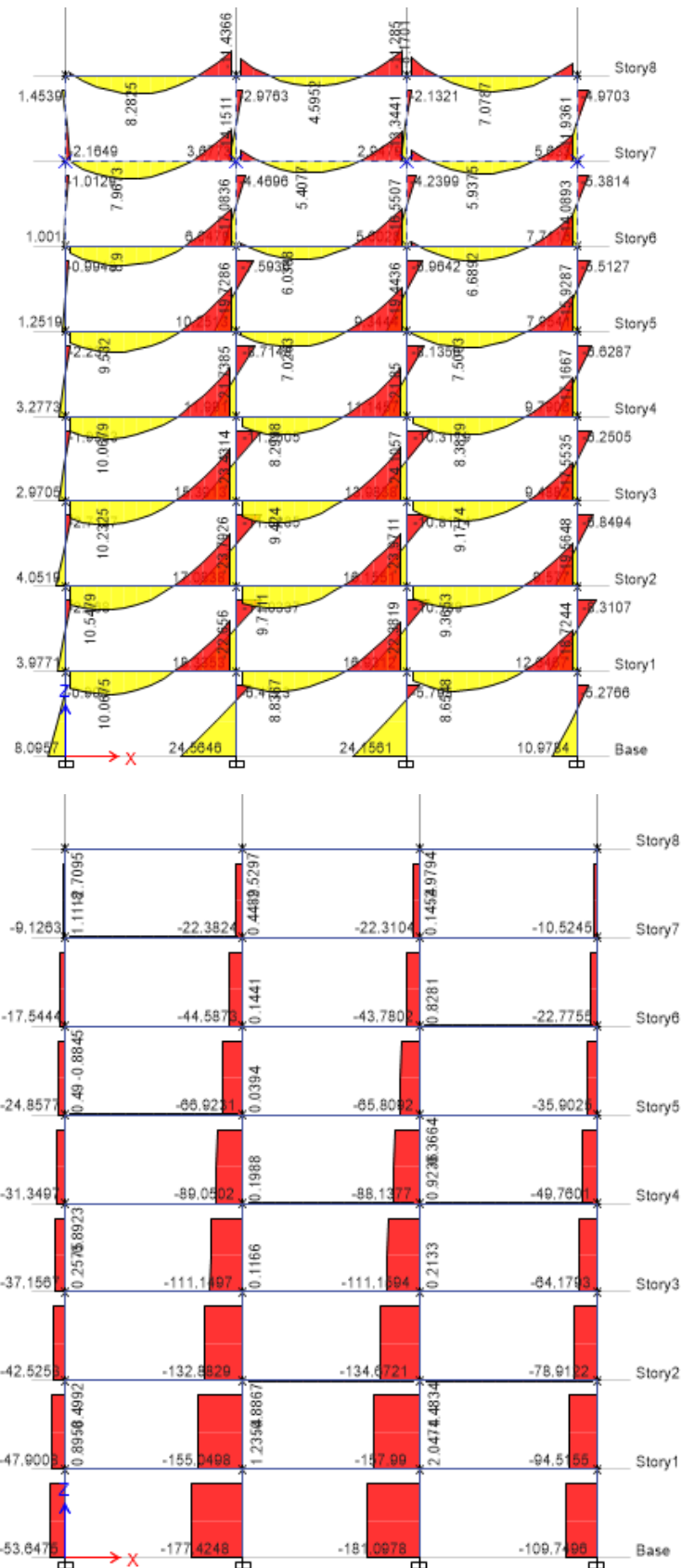


Figure C-1 Bending moment diagram (up) and axial force diagram (down) for the case study BL-frame for the strength design stage, iteration 1 (Etabs output)

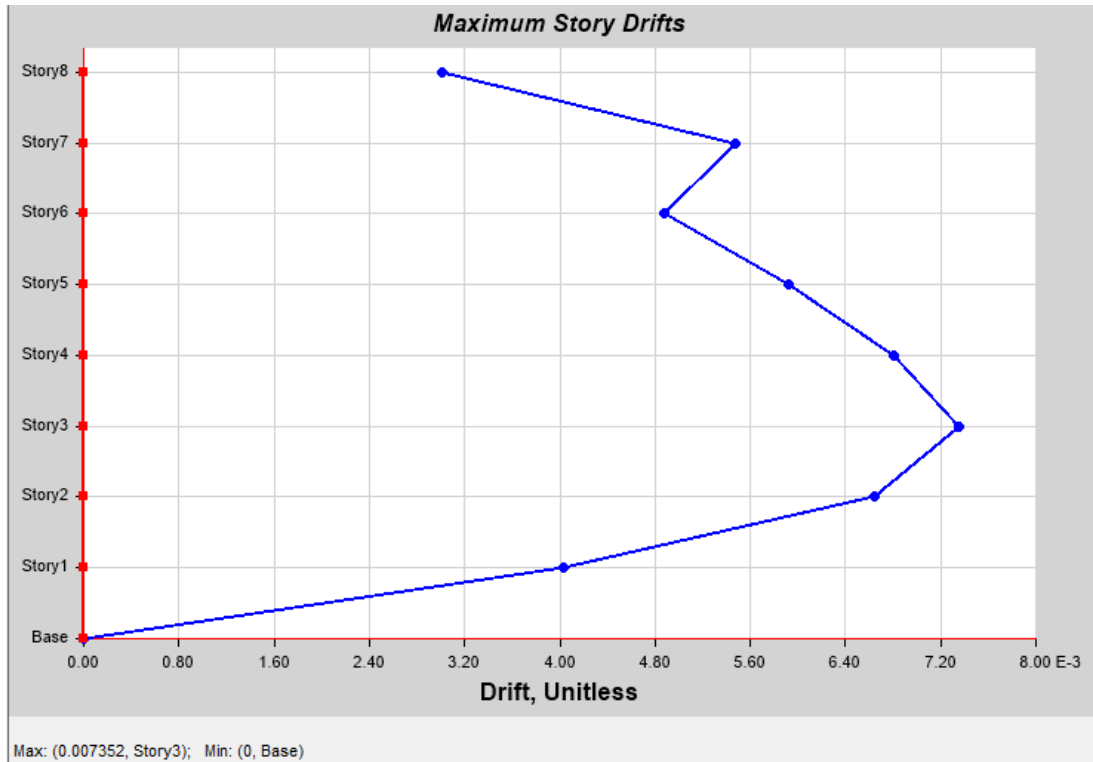


Figure C-2 Inter-story drift diagram for the case study BL-frame after the strength design stage, iteration 1 (Etabs output)

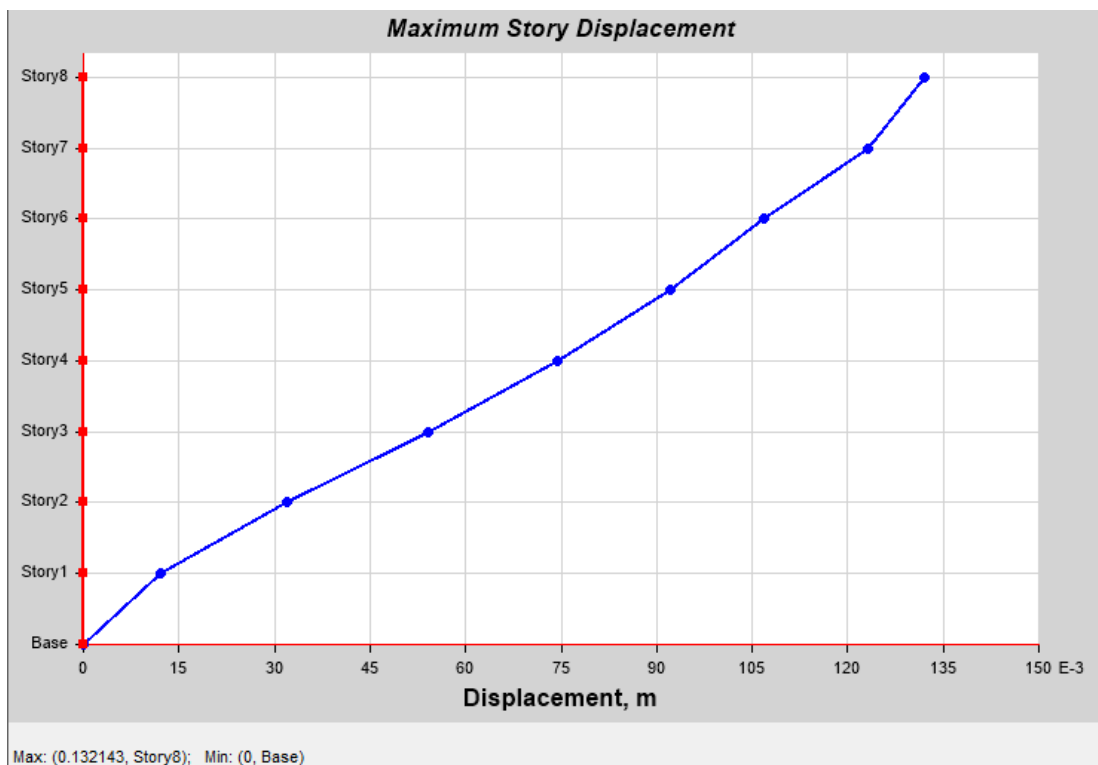


Figure C-3 Displacement profile for the case study BL-frame after the strength design stage, iteration 1 (Etabs output)

APPENDIX D

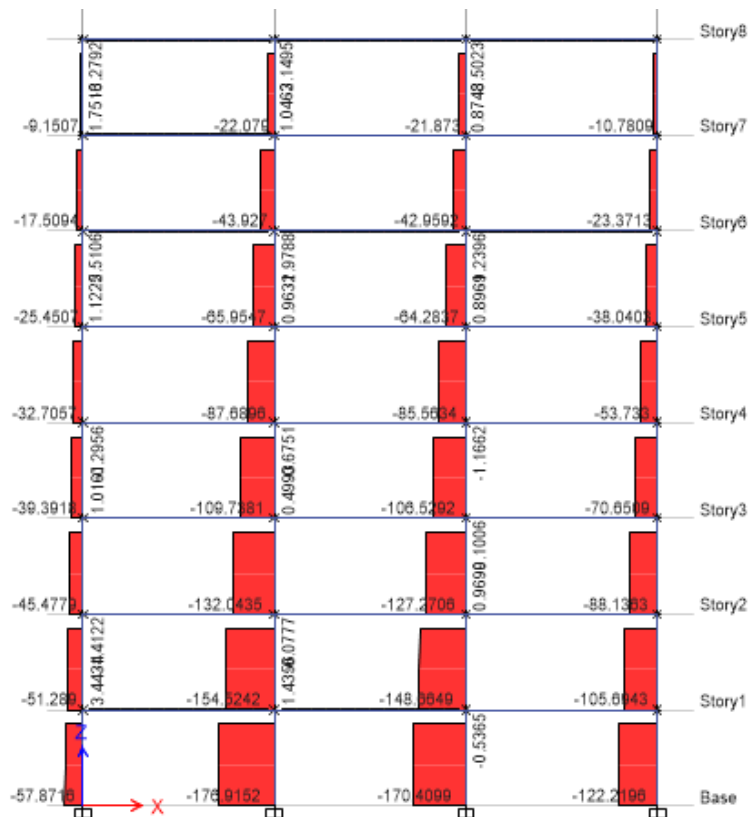
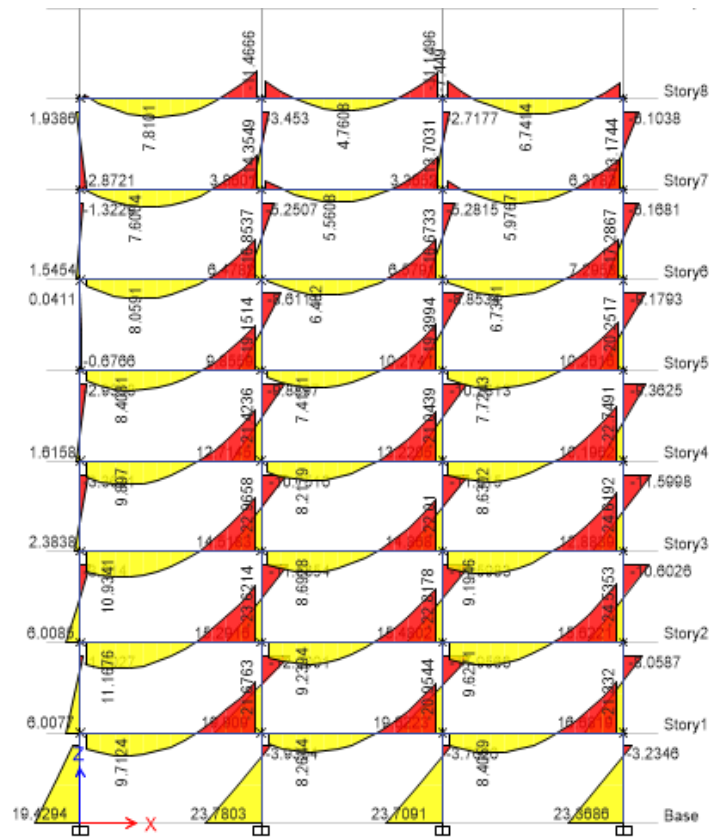


Figure D-1 Bending moment diagram (up) and axial force diagram (down) for the case study BL-frame final design (Etabs output)

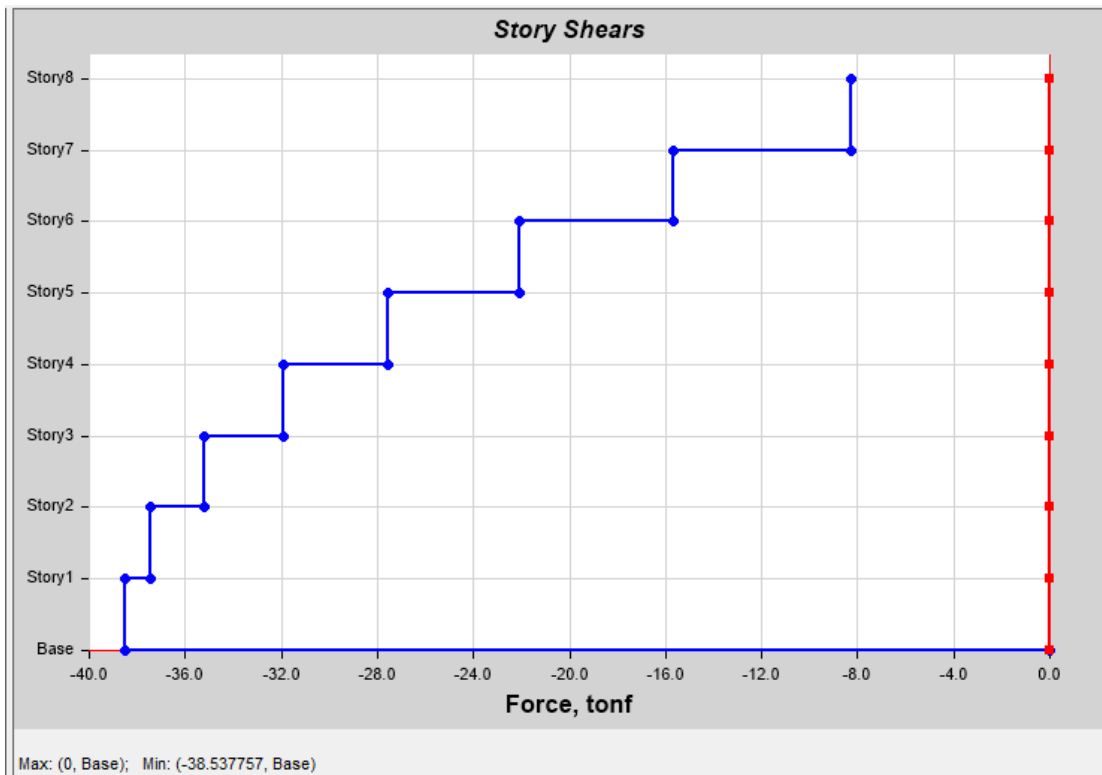


Figure D-2 Story shear diagram for the case study BL-frame final design (Etabs output)

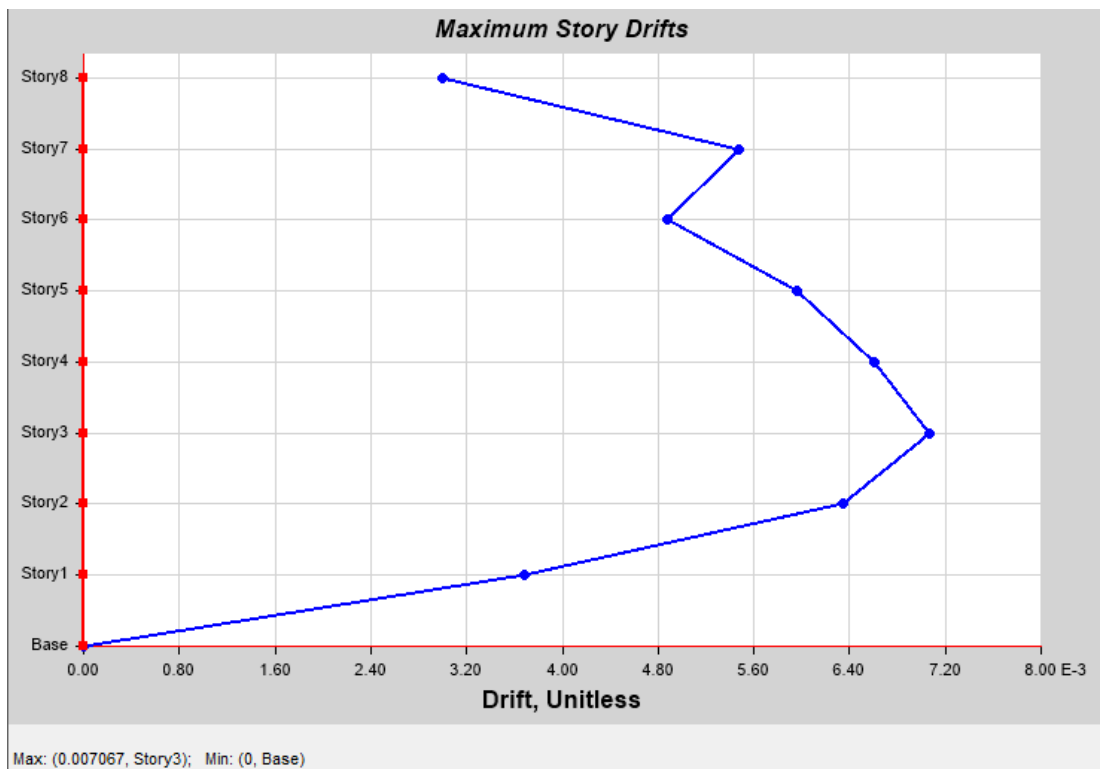


Figure D-3 Inter-story drift diagram for the case study BL-frame final design (Etabs output)

APPENDIX D

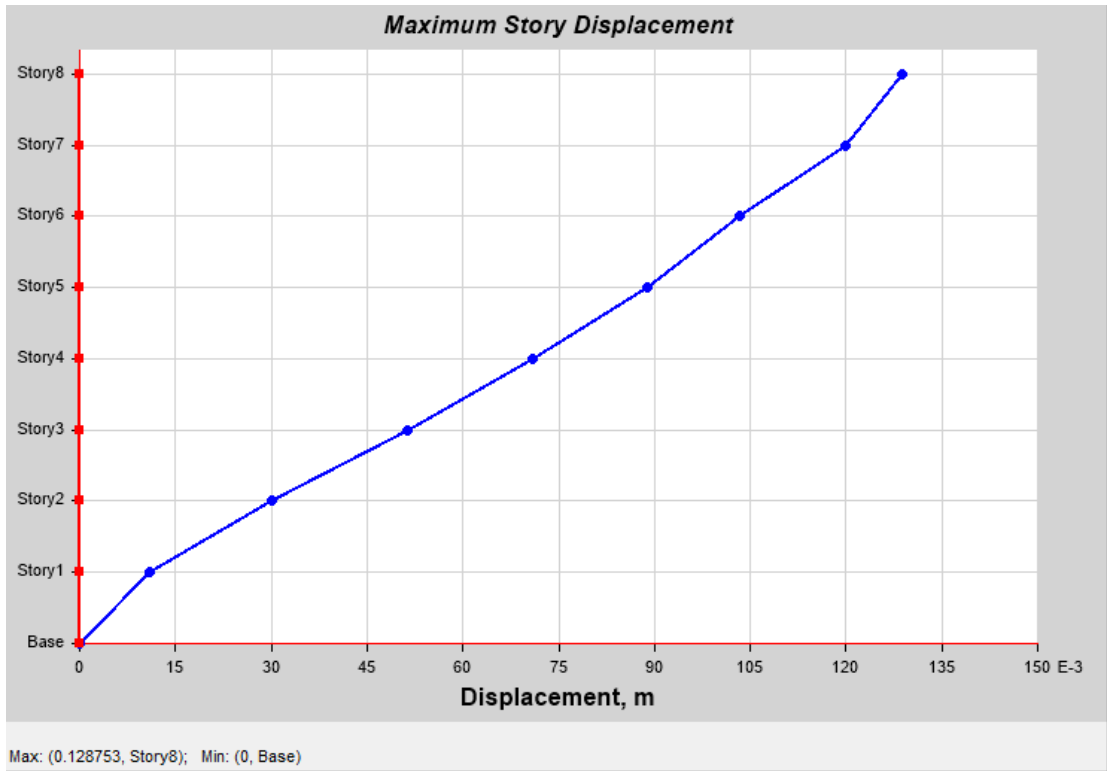


Figure D-4 Displacement profile for the case study BL-frame final design (Etabs output)

APPENDIX E

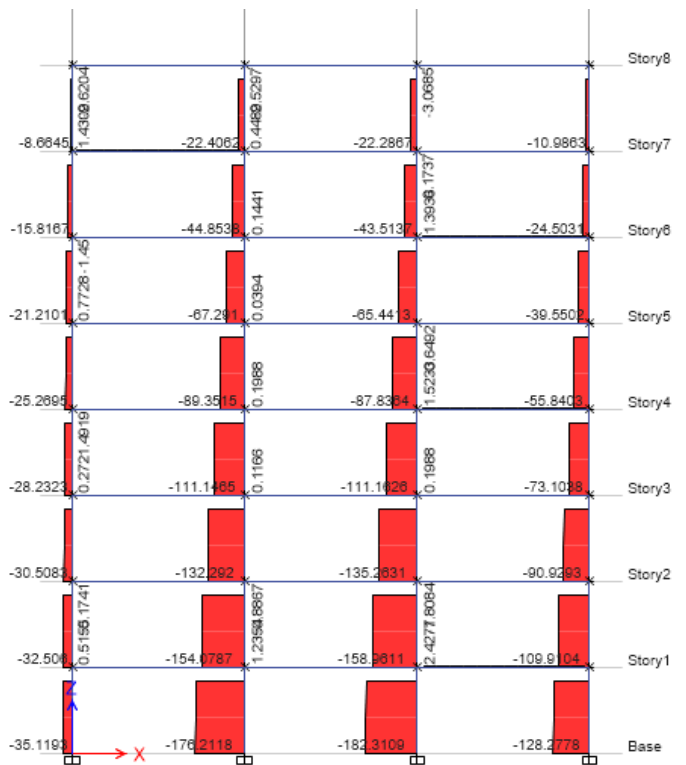
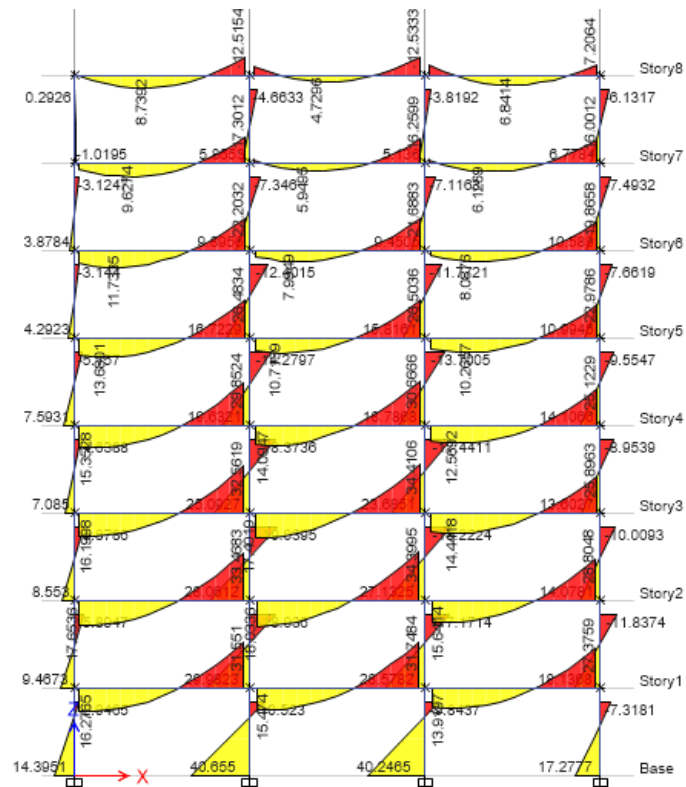


Figure E-1 Bending moment diagram (up) and axial force diagram (down) for the case study MD-frame, with the FOE seismic loading (Etabs output)

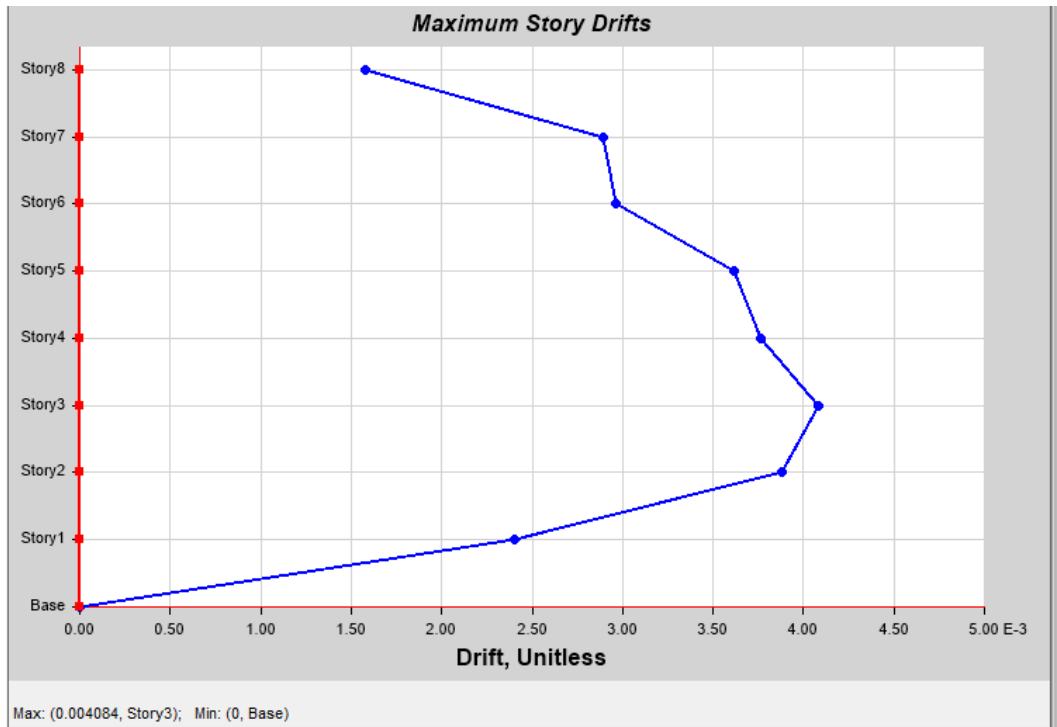


Figure E-2 Inter-story drift diagram for the case study MD-frame with the FOE seismic loading (Etabs output)

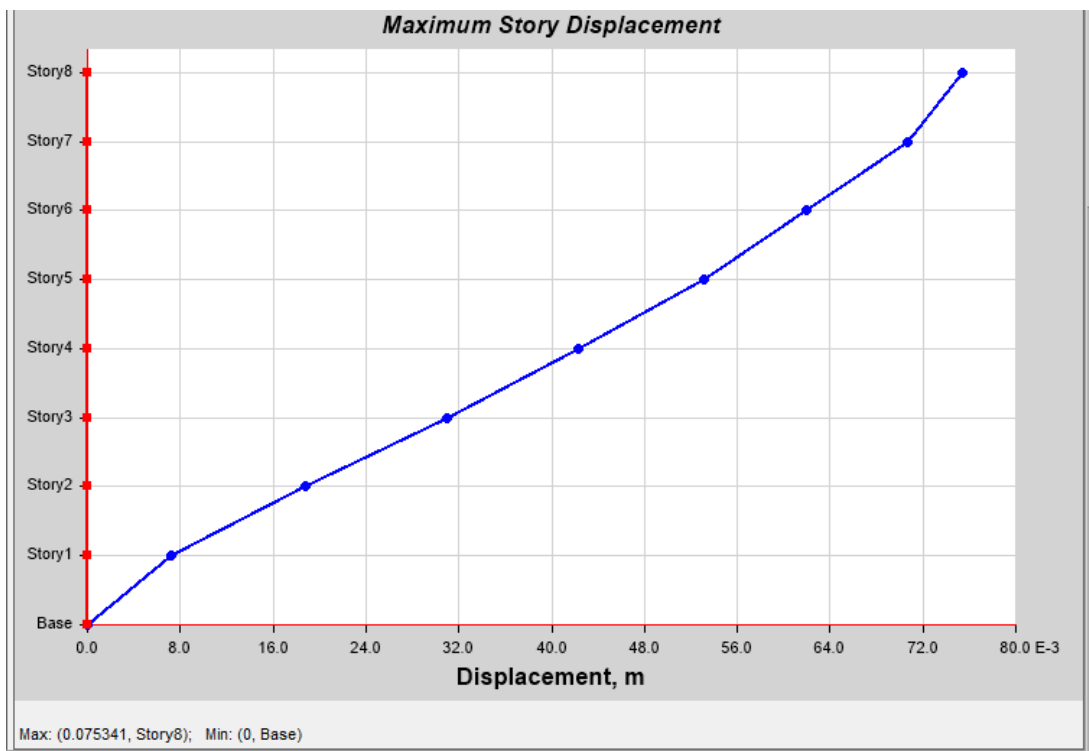


Figure E-3 Displacement profile for the case study MD-frame with the FOE seismic loading (Etabs output)

APPENDIX F

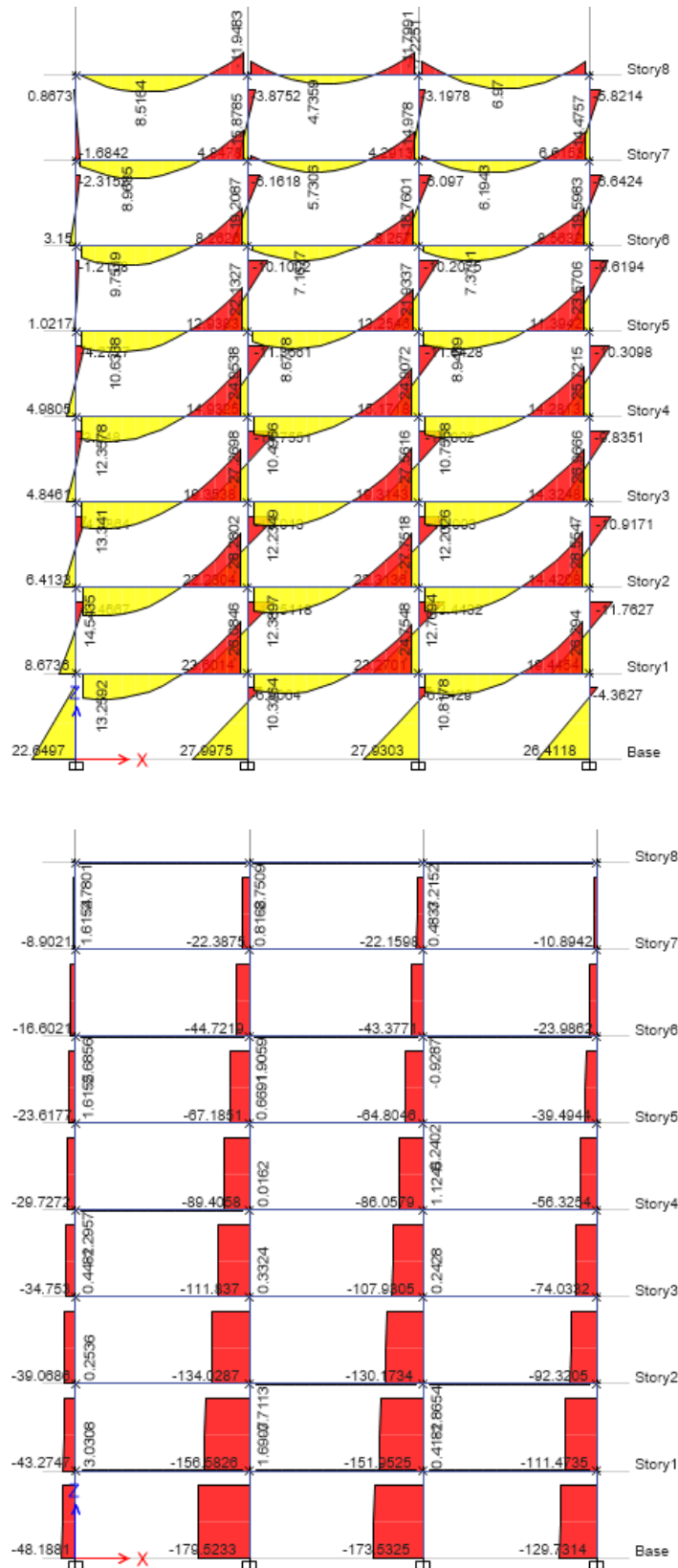


Figure F-1 Bending moment diagram (up) and axial force diagram (down) for the case study MD-frame, final design (Etabs output)

APPENDIX F

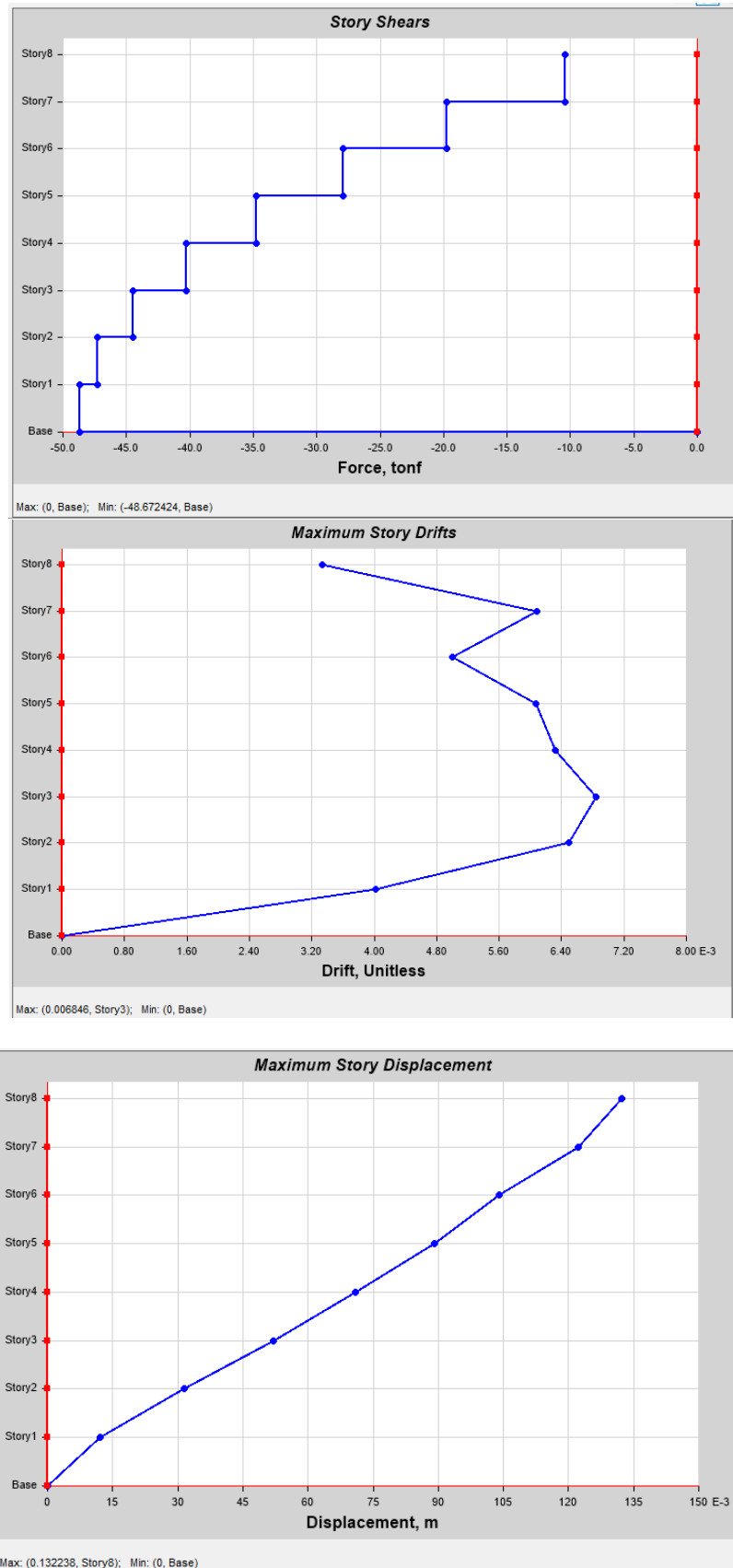


Figure F-2 Story shear, drift and displacement for the case study MD-frame final design (including CP performance level) (Etabs output)

APPENDIX F

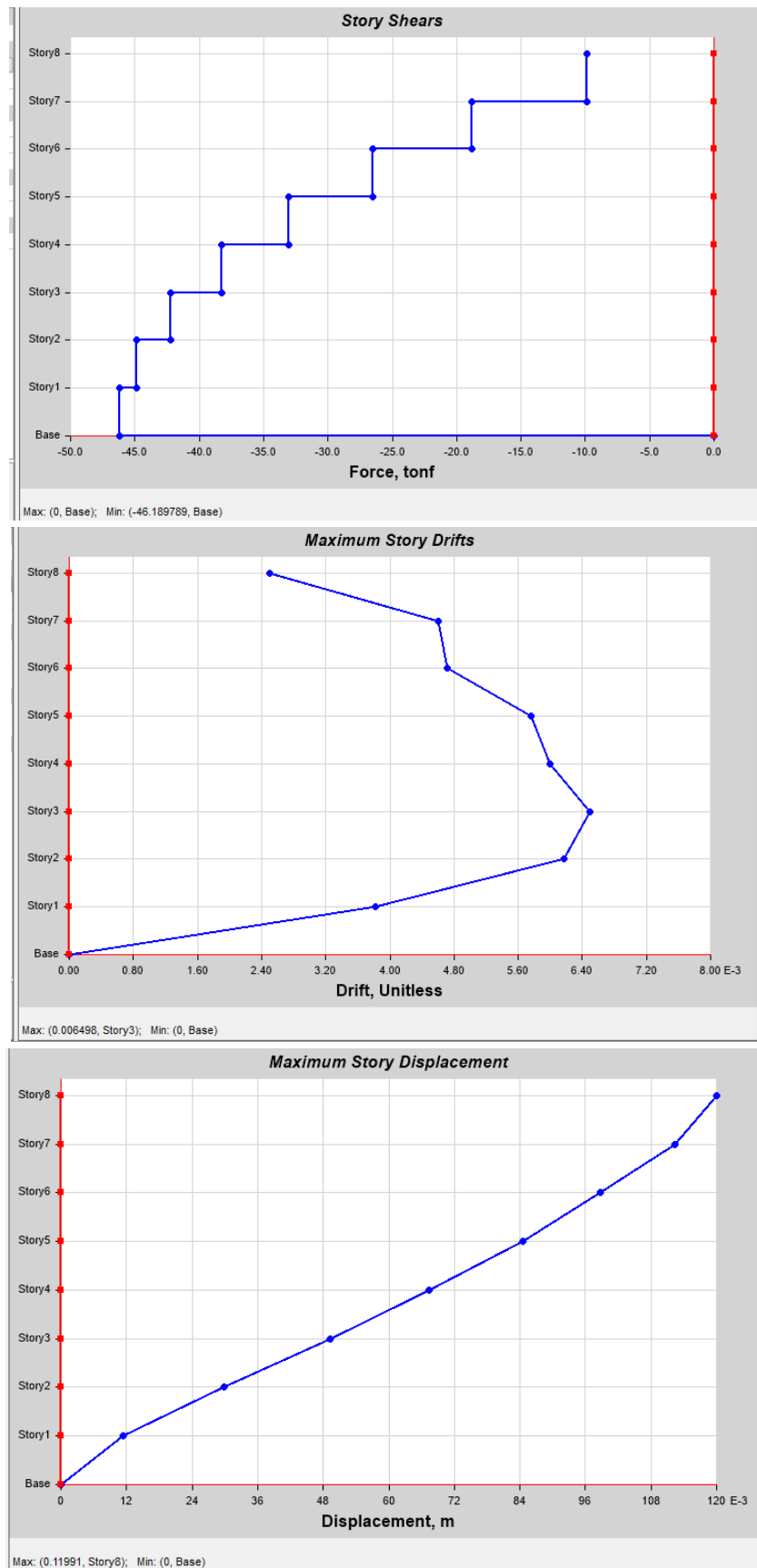


Figure F-3 Story shear, drift and displacement for the case study MD-frame final design (excluding CP performance level) (Etabs output)